TIDAL FACIES, STRATIGRAPHIC ARCHITECTURE, AND ALONG-STRIKE VARIABILITY OF A HIGH ENERGY, TRANSGRESSIVE SHORELINE, LATE CRETACEOUS, KAIPAROWITS PLATEAU, SOUTHERN UTAH

by

Patrick Ryan Dooling

A thesis submitted to the faculty of
The University of Utah
in partial fulfillment of the requirements for the degree of

Master of Science

in

Geology

Department of Geology and Geophysics

The University of Utah

May 2013

The University of Utah Graduate School

STATEMENT OF THESIS APPROVAL

The thesis of **Patrick Ryan Dooling**

has been approved by the following supervisory committee members:

Cari Johnson	, Chair	**11/16/12** Date Approved
Lisa Stright	, Member	**11/26/12** Date Approved
Lauren Birgenheier	, Member	**11/27/12** Date Approved

and by **D. Kip Solomon** , Chair of

the Department of **Geology and Geophysics**

and by Donna M. White, Interim Dean of The Graduate School.

ABSTRACT

The John Henry Member of the Straight Cliffs Formation contains regressive and transgressive marginal marine strata deposited along the shoreline of the Late Cretaceous Western Interior Seaway. Four main facies associations – wave-dominated facies, coastal plain sandstones and mudstones, sandstone-rich tidal deposits, and carbonaceous lagoonal mudstones – reflect deposition in regressive shorefaces and transgressive tide-dominated barrier island systems. Regressive-Transgressive (R-T) cycles are defined by two main transgressive surfaces, the first (wave ravinement) marking the maximum transgression and beginning of regression, and the second (tidal ravinement) recording the onset of transgression. Wave ravinement surfaces are underlain by tidal and coastal plain deposits and overlain by distal to proximal lower shoreface deposits, forming the base of the regressive interval. The shoreface deposits thin at the base onto the wave ravinement surface and are eroded at the top by tidal ravinement, which marks the onset of the transgressive portion of the cycle. Transgressive deposits are either sandstone or mudstone dominated and thicken landward to form successions more than 20 m thick. R-T cycles stack progradationally in the lower John Henry Member and exhibit net retrogradational stacking through the middle and upper John Henry Member.

The John Henry Member at Left Hand Collet Canyon contains two distinct tidal facies associations: mudstone rich units and sandstone rich deposits. Mudstone dominated facies reflect deposition in a microtidal, wave-dominated lagoon. Sandstone rich deposits reflect erosion and deposition in a mesotidal barrier island system with frequent migratory inlets and efficient longshore transport. Along-strike correlations, ~20 km to the southeast to Rogers Canyon, show variations in the upper John Henry Member. This interval at Left Hand Collet is characterized by tidal ravinement into proximal lower to middle shoreface and sandstone dominated tidal deposition during transgression. At Rogers Canyon, it is dominated by lower and upper shoreface deposits with little tidal ravinement. These variations are attributed to increased sediment supply via longshore drift from a delta to the north of Left Hand Collet as well as a more embayed coastal morphology. An accretionary shoreline trajectory with high rates of sediment supply is necessary to preserve transgressive deposits, while high basinal energy at the onset of transgression is required to erode the shoreface. Finally, transgressions form significant landward thickening, sandstone rich facies with discernible trends that may be useful in reservoir characterization and modeling studies.

TABLE OF CONTENTS

ACKNOWLEDGEMENTS

I am extremely grateful for all the people who have helped me through my research and through the past two years. I would like to thank my advisor, Cari Johnson, for all of her guidance and assistance in my research. Thanks to Lauren Birgenheier and Lisa Stright for agreeing to be on my thesis committee and providing useful insight. Thanks to Tony Ekdale for assistance in identifying trace fossils and all the wisdom he has imparted on me during my studies. Thanks to Jessica Allen for help in the formative stages of this project and introducing me to the Straight Cliffs Formation in the field. Thanks to Anton Wroblewski and Brian Bracken for beneficial feedback. I am indebted to Luke Pettinga for all of his help with field work. Thanks to Alex Turner, Brenton Chentnik, Julia Mulhern, and Heather Judd for additional field assistance, as well as Gordon Chapdelaine, Leah Toms, Morgan Rosenberg, and Paul Thomas for their attempted assistance, only to be thwarted by vehicle problems. Additional thanks to Brendan Horton and Jim Lehane for their presence in the office. This project would not have been possible without the financial support given to the Rocks to Models (R2M) Consortium at the University of Utah by Chevron, ConocoPhillips, Hess, Shell, and Statoil. Thanks to the Bureau of Land Management and Grand Staircase-Escalante National Monument (GSENM) for permitting the field work on their land. Last but never least, I am forever grateful for the endless and unwavering support of my family.

INTRODUCTION

Transgressive sedimentary deposits accumulate as sea level rises and the shoreline migrates landward. The expression and preservation of transgressions in the rock record is highly variable and depends on many controlling factors including sediment supply, accommodation space and subsidence, local bathymetry, local basinal energy, and shoreline trajectory/shelf gradient (Cattaneo and Steel, 2003; Helland-Hansen and Gjelberg, 1994; Steel et al., 2012). However, transgressive deposits are often overlooked in comparison to their regressive counterparts, which typically form more significant reservoirs (Reynolds, 1999). In classic sequence stratigraphic models, the transgression is often marked by erosion or a thin marine lag that separates regressive parasequences (Van Wagoner et al., 1988; Kamola and Van Wagoner, 1995). Nevertheless, it is possible to deposit and preserve significant facies during transgressions (Cattaneo and Steel, 2003) and recognizing variations in these deposits is critical to understanding the evolution of the shoreline.

Transgressions increase the effects of tides on coastlines and recent studies highlight tidal effects and transgressions in marginal marine environments, specifically in the Western Interior Seaway (Bullimore et al., 2008; Dashtgard et al., 2010; Plink-Bjorklund, 2011; Steel et al., 2012). As sea level rises during transgressions, the shelf width increases and may fall into resonance with the tidal wavelength of the seaway (Longhitano et al., 2012). Tide-influenced successions are also found in conjunction with more localized embayments associated with estuaries and lagoons on transgressive coasts (Devine, 1991; Boyd, 2010). Sea level rise through these restricted or protected embayments increases the tidal prism, or volume of water in the inlet, resulting in higher tidal energies (Steel et al., 2012; Longhitano et al., 2012).

Recent studies suggest tide-influenced deposits are common during transgressive intervals of higher order (fourth-sixth order) cycles in the Upper Cretaceous marginal marine strata throughout the Western Interior Basin (Devine, 1991; Olsen et al., 1999, Ambrose and Ayers, 2007; Sixsmith et al., 2008; Allen and Johnson, 2011; Kieft et al., 2011). They are commonly associated with wave-dominated shoreface packages, and have stratigraphic architectures reflecting deposition during distinct regressive and transgressive intervals (Ambrose and Ayers, 2007; Sixsmith et al., 2008; Allen and Johnson, 2011; Kieft et al., 2011). Wave-dominated shorefaces are deposited during regressions, while tide-dominated back-barrier deposits and tidal inlets are more common during transgressions (Hendricks, 1994; Horn et al., 2001). Transgressive surfaces – flooding surfaces, wave-ravinement surfaces, and tidal ravinement surfaces – are key to recognizing regressive-transgressive cycles (Cattaneo and Steel, 2003).

Distinct transgressive deposits are abundant in the Coniacian-Santonian John Henry Member of the Straight Cliffs Formation in the Kaiparowits Plateau in southern Utah. Allen and Johnson (2010; 2011) found evidence of transgressive lagoonal fill in the Rogers Canyon area of the Kaiparowits Plateau (Figure 1). The present study, 20-30 km to north of Rogers Canyon, examines the along-strike expression of transgressive deposits and regressive-transgressive cycles (Figure 2).

The goal of this study is to examine along-strike changes in shoreface deposits and explore the possible mechanisms for process changes along the shoreline. This research also looks at the interplay between subsidence and sediment supply in marginal marine environments and the controls on preservation of transgressive deposits. Further, a facies model is developed for high energy, high sediment supply transgressive shorelines, with modern analogs playing key roles in and draw comparisons with modern analogs. These results help characterize the reservoir potential of these tidal deposits and discern predictable trends in transgressive reservoirs.

Figure 1 - Location map of the Straight Cliffs Formation in the Kaiparowits Plateau, southern Utah, USA. The study area of interest is Left Hand Collet along Fifty Mile Mountain. To the southeast at Rogers Canyon, marginal marine shoreface, lagoonal, and coastal plain deposits are common (Peterson, 1969b; Allen, 2009). The strike of the paleoshoreline of the Western Interior Seaway is northwest-southeast in this area, slightly oblique to the trend of Fifty Mile Mountain (see inset). Nonmarine fluvial deposits are exposed at southwest regions of the Kaiparowits Plateau around Rock House Cove and Bull Canyon. Fluvial and paralic deposits are exposed at Kelly Grade. Previous study locations are highlighted. Light gray = extent of the Kaiparowits Plateau.

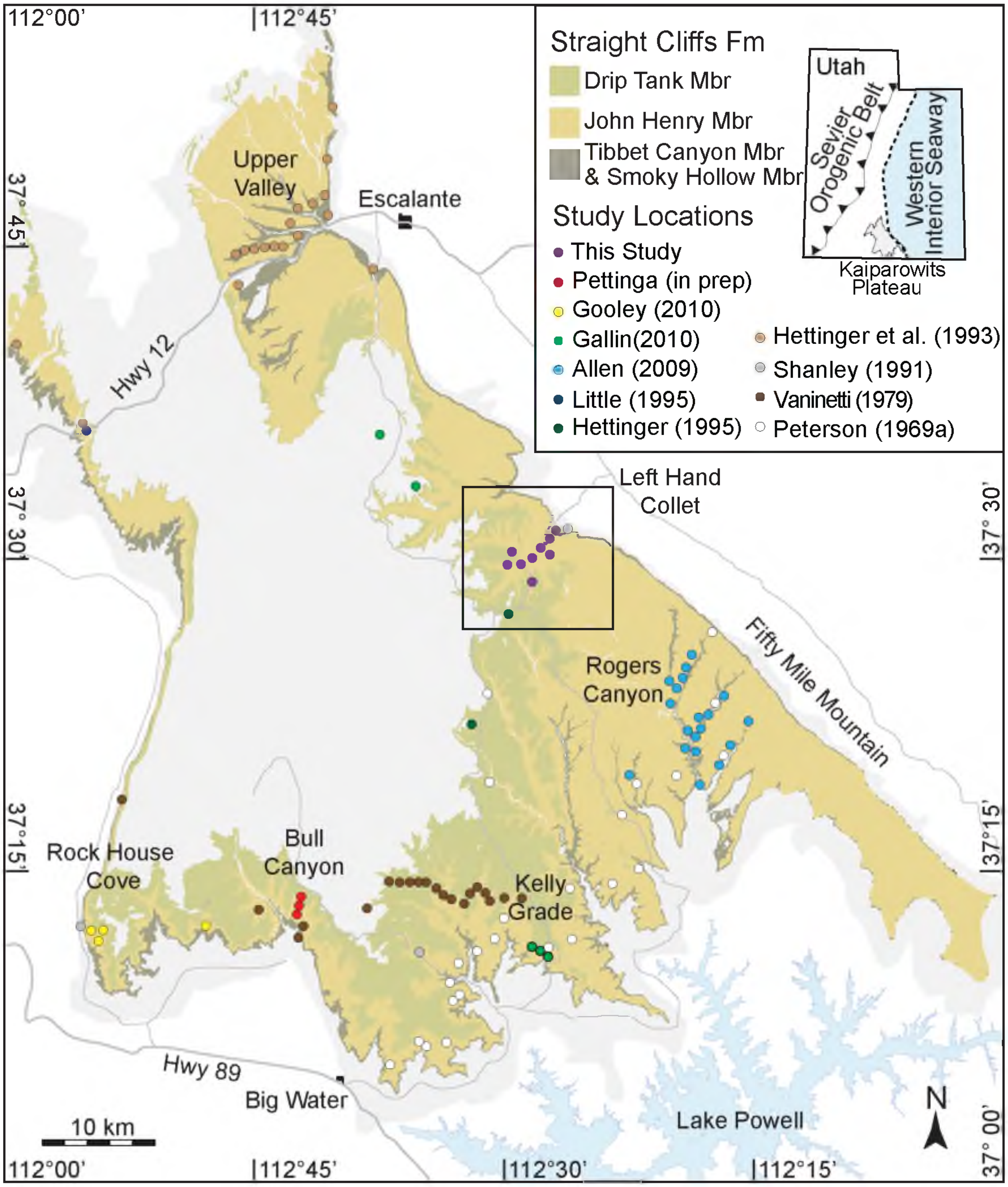

Straight Cliffs Fm
Drip Tank Mbr
John Henry Mbr
Tibbet Canyon Mbr & Smoky Hollow Mbr
Study Locations
This Study
Pettinga (in prep)
Gooley (2010)
Gallin(2010)
Allen (2009)
Little (1995)
Hettinger (1995)
Hettinger et al. (1993)
Shanley (1991)
Vaninetti (1979)
Peterson (1969a)
Utah
Sevier Orogenic Belt
Western Interior Seaway
Kaiparowits Plateau
112°00'
112°45'
112°30'
112°15'
37°45'
37°30'
37°15'
37°00'
Upper Valley
Escalante
Hwy 12
Left Hand Collet
Rogers Canyon
Fifty Mile Mountain
Rock House Cove
Bull Canyon
Kelly Grade
Hwy 89
Big Water
Lake Powell
10 km
N

Figure 2 – Google Earth image of Left Hand Collet Canyon showing sections measured in this study (purple circles) and core described by Hettinger (1995) (green circle). Inset shows the location with respect to the Kaiparowits Plateau (Figure 1). The Tibbet Canyon and Smoky Hollow Members of the Straight Cliffs Formation are exposed at the mouth of the canyon. The gray and white stars denote the pinchout of the C and F shoreface, respectively. Dashed black line = Left Hand Collet Canyon Road; WC = Willard Canyon; Red star on the inset = town of Escalante; White arrow = paleolandward

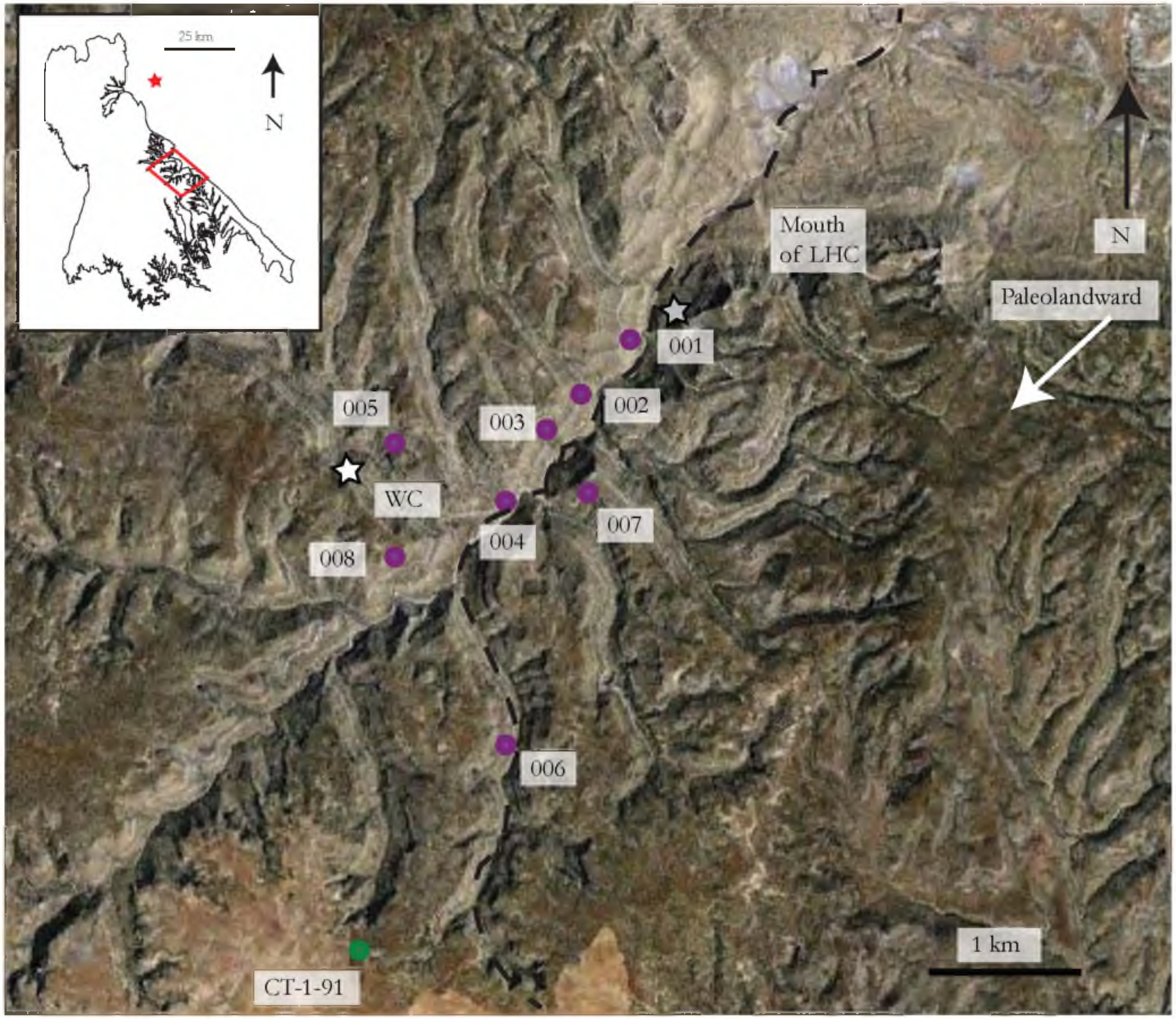
25 km
N
Mouth of LHC
N
Paleolandward
001
002
003
005
WC
004
007
008
006
1 km
CT-1-91

GEOLOGIC SETTING

The Straight Cliffs Formation comprises roughly 250 m of siliciclastic sandstone and mudstones. The John Henry Member has been the focus of recent studies (Shanley and McCabe 1991; Allen, 2009; Gallin, 2010; Gooley, 2010), in part because it records the nonmarine to marine transition in the Sevier foreland and Western Interior Seaway. Peterson (1969) conducted a lithostratigraphic study of the John Henry Member across the Kaiparowits Plateau and found seven shoreface sandstone packages (named A-G) in the northeast (Figure 3). To the southwest, the John Henry Member is composed of nonmarine fluvial facies. In the central regions of the Kaiparowits Plateau, the John Henry Member contains paralic coastal plain and coal-bearing strata (Figure 1) (Peterson, 1969a; Vaninetti, 1979; Gallin et al., 2010). The John Henry Member thickens irregularly from ~200 m in the southwest to 330 m to northeast (Peterson, 1969b).

The Kaiparowits Plateau contains an estimated 62 billion short tons of coal resources in the ground (Hettinger et al., 1996). Four coal zones are present in the John Henry Member including the lower, Christensen, Rees, and Alvey coal zones (Figure 3). Lithostratigraphically, the Alvey coal zone lies above the "G" shoreface, forming the top of the John Henry Member in the marginal marine (Figure 3) (Peterson, 1969b). McCabe and Shanley (1992) interpreted these coals to develop in steep-sided raised mires less than four km from the shoreline, with landward extents up to 26 km from the shoreline. Moreover, these mires are thought to control stacking patterns of shoreface and fluvial successions, as growth and compaction of mires may impact the relationship between accommodation and sediment supply.

Shanley and McCabe (1991) conducted the first sequence stratigraphic study in the John Henry Member. An unconformity and possible sequence boundary at the top of the "A" sandstone is evidenced by fluvial incision into a shoreface and subsequent estuarine valley fill during transgression at Left Hand Collet (Shanley and McCabe, 1991; Hettinger et al., 1993) (Figure 4D). Above the "A" sequence boundary, shorefaces are aggradationally stacked and pinch out into coal-bearing strata.

Allen and Johnson (2010 and 2011) revisited the marginal marine John Henry Member at Rogers Canyon (Figure 1) and found multiple retrogradationally stacked parasequences. The middle to upper John Henry Member (Figure 3) contains landward stepping shorelines deposited in an overall retrogradational-aggradational succession (Figure 3). Back-barrier lagoonal fill, washover fans, and flood-tidal deltas are interpreted to be deposited during transgressions. Regressive wave-dominated shorefaces erode into older transgressive deposits and are overlain by younger transgressive strata. The overall stacking patterns suggest deposition in Transgressive-Regressive (T-R) cycles.

Figure 3 – Stratigraphic column of the Straight Cliffs Formation including lithostratigraphic and sequence stratigraphic interpretations (Peterson, 1969b; Shanley and McCabe, 1995). Peterson (1969b) separated the strata into seven shoreface sandstones and three coal zones. Relative sea level curve based on the Rogers Canyon area (Allen and Johnson, 2010) and reinterpreted in this study according to the original lithostratigraphic study (see discussion). The strata are here simplified into the lower, middle, and upper John Henry Member based on interpreted facies distributions and relative sea level fluctuations. Ages based on timescale of Gradstein et al. (2012).

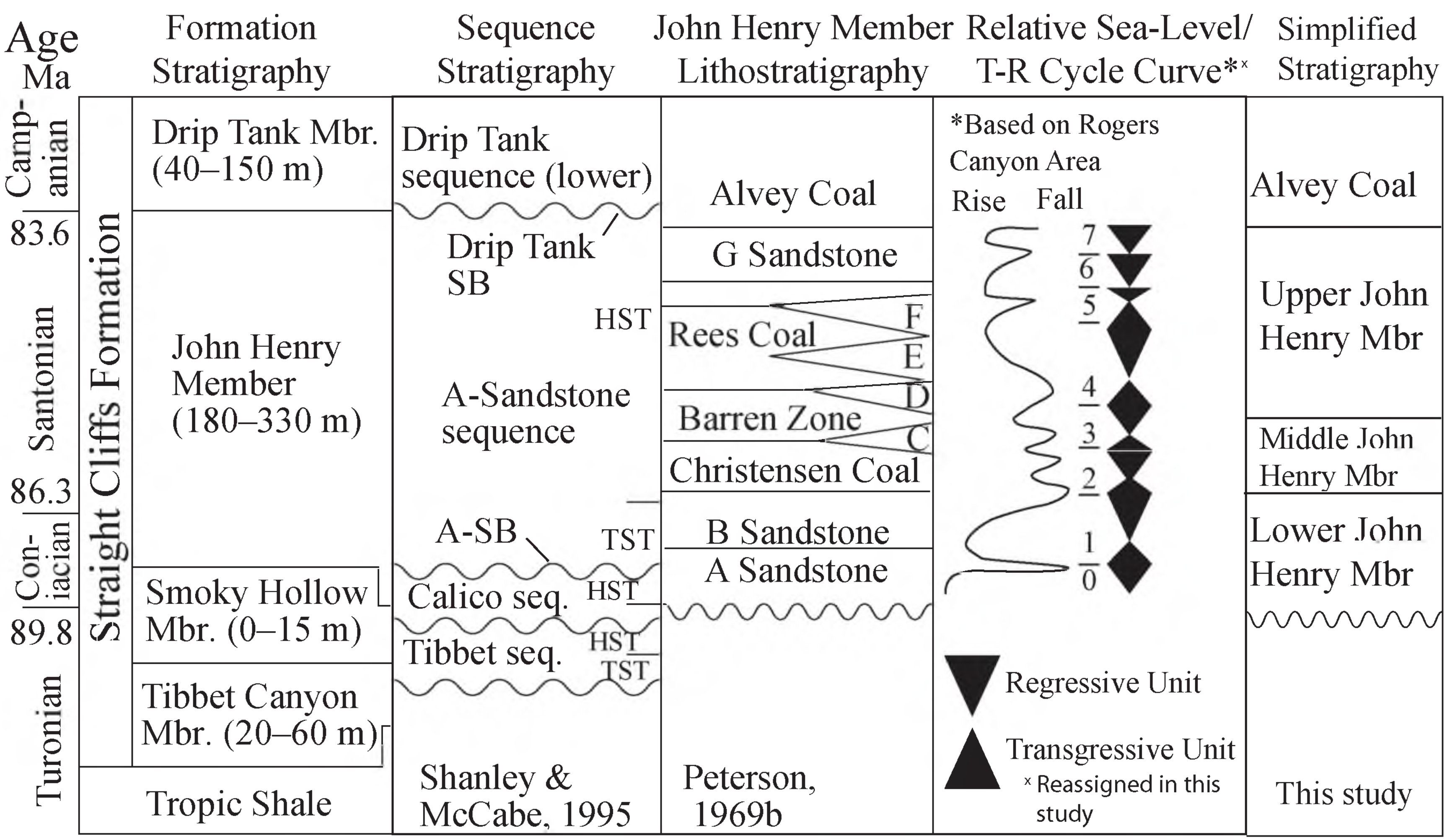
Age Ma
Formation Stratigraphy
Sequence Stratigraphy
John Henry Member Lithostratigraphy
Relative Sea-Level/ T-R Cycle Curve*ˣ
Simplified Stratigraphy
Camp-anian
83.6
Santonian
86.3
Con-iacian
89.8
Turonian
Straight Cliffs Formation
Drip Tank Mbr. (40–150 m)
John Henry Member (180–330 m)
Smoky Hollow Mbr. (0–15 m)
Tibbet Canyon Mbr. (20–60 m)
Tropic Shale
Drip Tank sequence (lower)
Drip Tank SB
HST
A-Sandstone sequence
A-SB
TST
Calico seq.
HST
Tibbet seq.
HST
TST
Shanley & McCabe, 1995
Alvey Coal
G Sandstone
Rees Coal
F
E
D
Barren Zone
C
Christensen Coal
B Sandstone
A Sandstone
Peterson, 1969b
*Based on Rogers Canyon Area
Rise
Fall
7
6
5
4
3
2
1
0
Regressive Unit
Transgressive Unit
ˣ Reassigned in this study
Alvey Coal
Upper John Henry Mbr
Middle John Henry Mbr
Lower John Henry Mbr
This study

Figure 4 – Wave-dominated shoreface facies association. A) Hummocky cross-stratification common in facies association 1; B) Trace fossil assemblage including *Thalassinoides*, *Planolites*, and *Chondrites* assigned to the *Cruziana* ichnofacies; C) Swaley cross-stratification common in proximal lower to middle shoreface (Jacob staff intervals = 10 cm); D) A-B interval of the John Henry Member, showing fluvial incision into the second parasequence of the A shoreface. Fluvial channels are generally limited to the lower John Henry Member. Black line = Flooding surface; Red line = Regressive surface of nonmarine erosion.

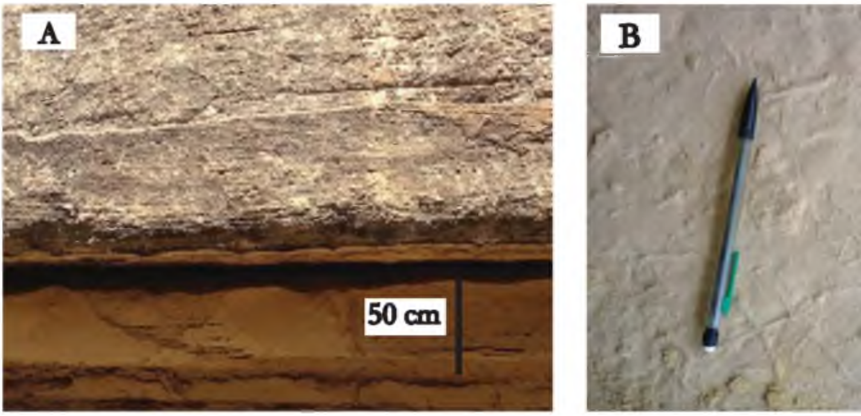
A
B
50 cm

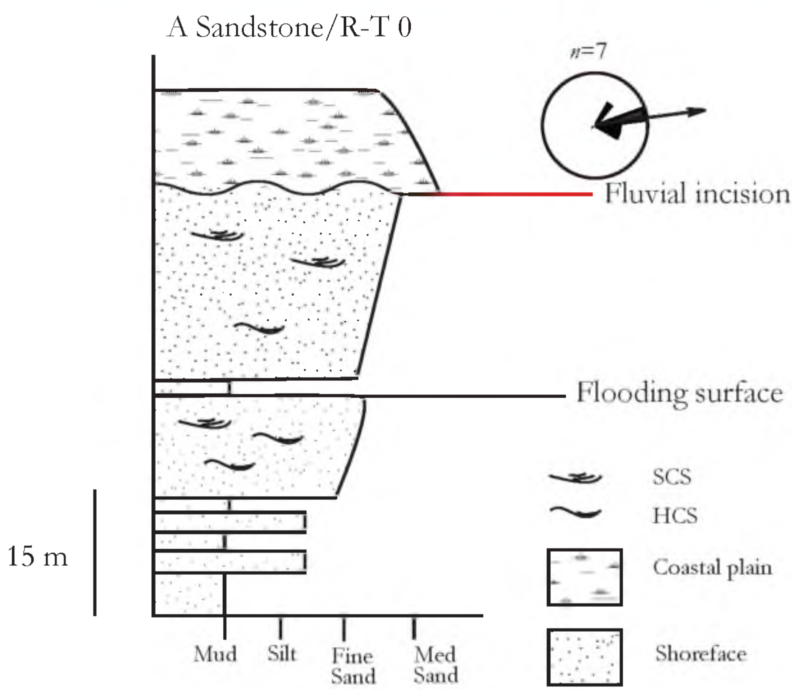
A Sandstone/R-T 0
n=7
Fluvial incision
Flooding surface
SCS
HCS
Coastal plain
Shoreface
15 m
Mud
Silt
Fine Sand
Med Sand


C

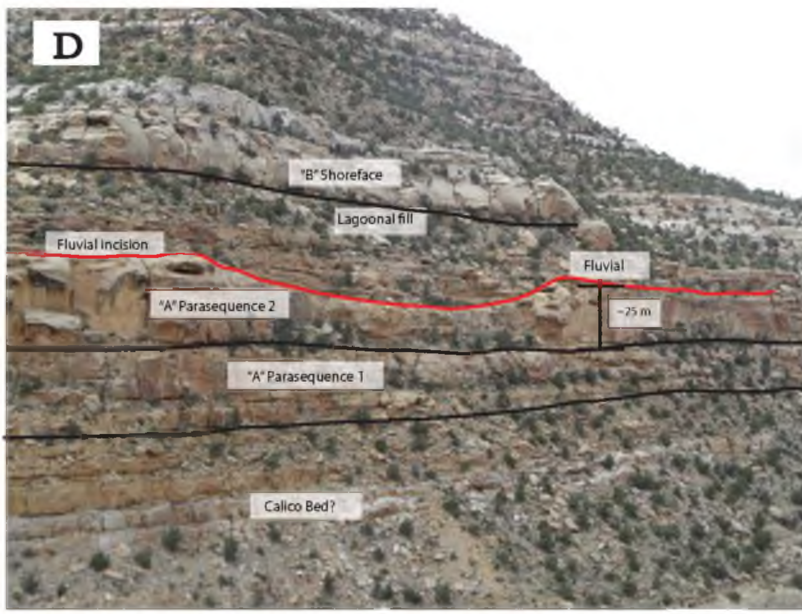
D
"B" Shoreface
Lagoonal fill
Fluvial incision
Fluvial
"A" Parasequence 2
~25 m
"A" Parasequence 1
Calico Bed?

METHODS AND DATASET

The dataset collected at Left Hand Collet includes eight measured vertical sections comprising over 1500 m of section over ~30 km^2 (Figure 2). Five sections have been measured roughly along depositional dip in the northeast-southwest trending main canyon and three measured in branching strike canyons trending northwest-southeast. The lower portions of the section at Left Hand Collet are not exposed up-dip due to cover. Measured sections record details of grain size, sorting, sedimentary structures, fossil content, trace fossils and bioturbation index, bed thickness and geometry, and contacts between beds. Seven hundred paleocurrent measurements were collected throughout the area to determine paleoflow directions. Six Gigapan photomosaics have been taken to capture high-resolution imagery and correlate between sections.

RESULTS

Nine lithofacies are identified in the John Henry Member at Left Hand Collet based on lithology, primary sedimentary structures, trace and body fossil content, and overall geometry (Table 1). Lithofacies and their interpreted depositional environments are grouped into four main facies associations (FAs): wave-dominated shorefaces (FA1), lagoonal facies (FA2), tide-dominated deposits (FA3), and coastal plain units (FA4). These associations reflect the dominant process controlling deposition: wave/storm activity, tidal energy, or rivers. The facies represent a mixed wave and tide-dominated environment with minor fluvial input. Furthermore, the facies associations are interpreted to reflect sea level fluctuations, with wave-dominated shorefaces representing regressive shorelines (e.g., parasequences, Van Wagoner et al., 1988), and tidal and lagoonal facies commonly deposited and preserved during transgression.

Facies Association 1 - Wave-dominated shorefaces

Wave and storm dominated facies are extensive throughout the marginal marine deposits of the Straight Cliffs Formation and are prominent cliff-forming units. At Left Hand Collet, there are seven wave-dominated shorefaces with similar internal facies associations, termed A-G according to the lithologic study of Peterson (1969), and ranging from 6-25 m thick. Deposits of FA1 are typically overlain and eroded into by deposits of facies association 3.

Facies 1.1 – Interbedded mudstones and siltstones

Description. Interbedded mudstones, siltstones, and fine grained sandstones comprise facies 1.1. Thicknesses of mudstone and sandstone beds are around 5-10 cm and 50 cm, respectively, stacking to form sheets up to 5 m thick. This unit displays considerable coarsening upward trends in grain size from mudstone to sand-dominated. Sandstones contain abundant hummocky cross-stratification (Figure 4A). Shell fragments are rare, though trace fossils including *Ophiomorpha, Thalassinoides, Chondrites,* and *Zoophycos* are common (Figure 4B).

Interpretation. Facies 1.1 records mudstone deposition from suspension in the distal lower shoreface, at or below fair weather wave base and hummocky cross-stratified sandstones reworked in storm events above storm-wave base. This facies records the most distal facies deposited on the shelf. Coarsening-upward trends in grain size and decreasing mudstone content reflect shoaling-upward conditions.

Facies 1.2 – Hummocky-Swaley Cross-Stratified Sandstones

Description. Facies 1.2 contains very fine- to fine grained sandstones with hummocky cross-stratification (HCS) passing upwards into swaley cross-stratification (SCS) (Figure 4C). This unit is one of the thickest and most regionally extensive observed, with deposition in tabular sheets between 5 and 25 m thick ranging for 10s of kms along Fifty Mile Mountain. Shell fragments including *Inoceramus* are common, along with occasional *Chondrites, Ophiomorpha, Planolites,* and *Thalassinoides* burrows (Figure 4). Pebble and sharks teeth lags are common in this facies in the lower portions of the John Henry Member ("A" sandstone).

Interpretation. The abundance of hummocky and swaley cross-stratification in facies 1.2 implies deposition by storm events near fair-weather wave base (Duke, 1985). Biological content is dominated by the *Cruziana* ichnofacies and is consistent with a shoreface interpretation (Pemberton et al., 1992). Coarsening-upwards trends in grain-size and the transition from HCS to SCS represents shallowing waters from proximal lower to middle shoreface. Overall thickness of tabular units may reflect a high sediment supply and/or high accommodation setting. The abundance of storm wave generated structures (HCS-SCS) implies deposition in wave-dominated shorefaces.

Facies Association 2 – Coastal Plain

2.1 – Fining-upwards trough cross-stratified sandstones

Description. Facies 2.1 consists of fining-upward medium to fine-grained sandstones with gravel lags, some shell hash, plant material and wood fragments. East-directed trough cross-stratification is prevalent throughout this facies. This facies is strongly channelized with internal scour surfaces, although these deposits are not necessarily confined to discrete channels. Individual channels range from 0.5 to 3 m and stack to form complexes up to 10 m thick. In the John Henry Member at Left Hand Collet, this facies is limited to the top of the "A" sandstone, where channels incise roughly 2-5 m into facies 1.2 (Figure 4D). This contact is flat and sharp based in places where fluvial deposits lie directly on top lower shoreface deposits. There are fluvial successions in the Drip Tank Member of the Straight Cliffs Formation at the top of Left Hand Collet above the Alvey coal zone.

Facies 2.2 – Rooted carbonaceous mudstones

Description. This facies contains abundant root and terrestrial material in carbonaceous mudstones. It is found in thin, ~50 cm intervals adjacent to facies 2.1. Bioturbation is nonexistent.

Interpretation of Facies Association 2

Facies 2.1 and 2.2 are consistent with deposition in a coastal plain. Facies 2.1 is interpreted as fluvial channel deposits. These channels commonly erode into lower shoreface in the 'A' interval of the lower John Henry Member (Figure 4D). Flow was directed roughly perpendicular to the shoreline (Figure 4), with abundant scour and accretion surfaces. The lack of tidal indicators, bioturbation, along with the abundance of terrestrial matter is consistent with this interpretation. Facies 2.2, mudstones and siltstones with abundant terrigenous material and occasional coal beds, is considered to represent interdistributary fill.

Genetic Stratigraphy of Regressive Deposits

Facies associations 1 and 2 record deposition in regressive shorelines. Wave-dominated shoreface facies represent deposition between storm-weather and fair-weather wave base (Leckie and Walker, 1982; Walker and Plint, 1992; Dumas and Arnott, 2006). The shorefaces commonly overlie lagoonal, tidal, or coastal plain facies; therefore, the base of facies association 1 is a marine flooding surface or wave ravinement surface (Swift, 1968) (Figure 5; Table 2). A wave ravinement surface, which records the maximum transgression, is characterized by a firmground *Glossifungites* ichnofacies or pebble lag at the top of an underlying coal-bearing coastal plain or back-barrier facies (Figure 6) (Helland-Hansen and Martinsen, 1996). This placement of deeper facies on top of shallower facies reflects final erosion of the coastline by wave action in shoreface retreat (Cattaneo and Steel, 2003) and the beginning of regressive deposition. Facies 1.1 and 1.2 represent shoaling-upwards parasequences (Van Wagoner et al., 1988; Walker and Plint, 1992), although there are little to no upper shoreface or foreshore facies present. Rather, the tops of parasequences are commonly marked by a tidal ravinement surface, which scours into the shoreface and is overlain by tidal and lagoonal facies as described below. Parasequences can also be capped by a regressive surface of erosion and coastal plain deposition (Figure 4). Coastal plain facies assemblages erosionally overlie lower shoreface facies and are capped by a process change surface and tide-influenced lagoonal mudstones. This juxtaposition marks the onset of fluvial influence in the system and is interpreted to represent subaerial exposure and the regressive maximum at the tops of progradational parasequences (Van Wagoner et al., 1988).

Facies Association 3– Tide-dominated facies

Overall, facies 3.1-3.3 contain indicators of periodic variations in flow velocity, as well as opposing current directions common in tide-dominated environments. Key tidal indicators include single or paired mud or organic drapes, mud rip-ups, flaser or wavy bedding, herringbone cross-laminations, bidirectional paleoflow directions, sigmoidal foresets, and reactivation surfaces (Nio and Yang, 1991). Trace and body fossil content, though variable, is consistent with a tidal and back-barrier interpretation. Facies 3.1 and 3.3 are dominantly fine to medium sandstone rich, while facies 3.2 contains abundant inclined heterolithic stratification.

3.1- Channelized, bidirectional cross-bedded sandstones

Description. The base of facies 3.1 is an erosive surface with up to 1 m of relief (Figure 6). Clay rip-ups, double mud drapes, shell hash, and wavy and flaser bedding are most prominent at the base of these units (Figure 7A, B). The facies typically coarsens upward into medium-grained sandstones with abundant reactivation surfaces, wave-ripples, tabular and herringbone cross-stratification, draped cross-sets, and occasional soft-sediment deformation (Figure 7C-G). This unit contains sparse bioturbation and variable fossil content. Trace fossils include *Teredolites* borings in wood (Figure 7I), and rare *Skolithos* and

Thalassinoides. Shell hash containing oyster and inocermid fragments are common, and leaf fossils and plant material occur along with the large wood lags (Figure 7H).

Sandstones are channelized but amalgamate to form sheet-like geometries (Figure 8). At channel edges, articulated 15 cm *Ostrea* shells are found in lags up to 50 cm thick (Figure 7). Thicknesses of individual channels range from 1-5 m, with amalgamation into larger sheets up to 15 m thick. Internal scour surfaces within facies 3.1 cut as deep as 9 m (Figure 8). Widths of individual channel belts are on the order of 500 m, while amalgamated sheets can have widths over 5 km. Paleocurrents transition from primarily southward migrating cross-laminations at the base to strongly bidirectional herringbone cross-stratification to landward dipping planar laminations at the top (Figure 9). Bidirectional paleocurrents are variable through time and space, but generally range from east-west or northeast-southwest (Figure 9).

Facies 3.1 contains significant variability along depositional dip (Figure 10). To the northeast, this unit thins considerably and corresponds to <50 cm mudstone beds full of terrestrial plant material and wood fragments. Moving up-dip to the southwest, sandstones of this facies occasionally contain rare swaley cross-stratification or east-directed tabular cross-sets, although sandstones occur in discrete channels. Further up-dip, bidirectional tabular and herringbone cross-stratification are the dominant sedimentary structures in thicker (up to 5 m) individual channels. Finally, facies 3.1 pinches out landward into paralic coal bearing strata and lagoonal mudstones of facies 4.1. These changes occur gradationally along the 5 km transect.

<u>Interpretation.</u> This facies is interpreted as tidal inlet channel fill. Bases reflect tidal erosion into shoreface deposits (Figure 6) (facies 1.2), and primary sedimentary structures suggest bidirectional flow common in tide-dominated environments (Figure 9). Southward

accretion at the base of the channels is consistent with migration of a tidal inlet with longshore currents (Ericksen and Slingerland, 1990; Sanders and Kumar, 1975, Fitzgerald et al., 2012). Periodic variations in flow velocity caused by the tidal fluctuations are preserved in mud draping and rip-up clasts (Nio and Yang, 1991). Trace and body fossil content are consistent with this interpretation (Pemberton et al., 1992). The erosive nature of this facies, lack of wave- or storm-dominated structures, and abundant tidal indicators likely indicate a high energy tide-dominated environment.

Tidal channels correlate basinward with thin mudstones that lie between proximal lower/middle shoreface facies (Figure 10, R-T 3). These mudstones, rich in terrestrial plant matter, coaly clasts, and woody debris, may be fluid-muds (Ichaso and Dalrymple, 2009; Longhitano et al., 2012) deposited at the mouth of an ebb-tidal delta or in a wave-dominated delta front. Slightly up-dip, this correlates to heterolithic mudstones and sandstones with ebb-directed cross-sets and occasional storm-generated structures, possibly indicative of deposition in front of the barrier island in an ebb-tidal delta (Figures 6 and 11). Ebb-tidal deposits are noted as far 5-7 km from the barrier island from modern inlets (Frey and Howard, 1986). Further landward, thick channelized sandstones with herringbone cross-stratification reflect deposition near the throat of the main channel belt (Figures 7 and 11). The bases of these channels contain a shell lag or southward oriented tabular cross-sets (Figure 6 and 9). Flood-tidal currents bring sand into the lagoon, while ebb-currents drain the back-barrier platform. Landward, these inlets pinch out into either lagoonal mudstones or interfinger with paralic coal bearing strata (Figure 10, R-T 5). Overall, the cross-section and relationship with facies associations 1 and 4 suggests that these channels cut through a barrier island system and are therefore interpreted as tidal inlet deposits (Figure 12).

3.2 – Inclined Heterolithic Strata

Description. This facies consists of inclined heterolithic fine-grained sandstones and clay and silty mudstones with extensive bioturbation (Figure 13A). Sandstone bodies have an overall sigmoidal shape with some trough cross-stratification (Figure 13B), wavy and flaser bedding, and mud draping on sigmoidal cross-sets. Bioturbation is extensive in both mudstones and sandstones (BI=4/5) and primary sedimentary structures are typically reworked by biological activity (Figure 13C). Trace fossils include sand-filled *Thalassinoides, Planolites, Berguaria, Gastrochaenolites,* and *Rosselia (*Figure 13D-F). Furthermore, the tops of these facies contain a gravel lag or firmground represented by the *Glossifungites* ichnofacies, which is overlain by facies 1.1 or 1.2 (Figures 6 and 13G, H).

Thickness of individual sandstone and mudstone beds range from 5-90 cm which stack to form bedsets between 8-10 m with lateral extents around 200-300 m. Facies 3.2 is typically found directly adjacent to or overlying facies 3.1. Inclined heterolithic strata occasionally lie atop an erosional surface into facies 3.2 with up to 10 m of relief (Figures 6 and 10).

Interpretation. Facies 3.2 contains several records of periodic variations in flow velocities and marine bioturbation indicative of a tide-dominated environment. Interbedded sandstones and mudstones, mud-draping on cross-sets, and sigmoidal tidal bundles are consistent with this interpretation (Nio and Yang, 1991). The extensive bioturbation suggests an open marine influence, but the relatively high mud content suggests deposition in a protected back-barrier lagoonal setting. Furthermore, the deposition of barforms, and lateral transition into facies 3.1 suggests that these were bars attached to tidal channels. The gravel or firmground lag at the top of facies 3.2, combined with the overlying distal lower shoreface deposits of facies 1.1, suggests that a flooding surface or wave ravinement surface occurs at the tops of these facies (Figure 6).

3.3 – Non channelized, bidirectional cross-bedded sandstones

Description. Facies 3.3 is composed of fine to medium grained sandstones with an overall tabular shape and no internal channelization. Importantly, this facies does not have an erosive base. In the "B" interval, it sits conformably above facies 1.2 and pinches out along dip into and is overlain by mudstones of facies 4.1 (Figure 14D). In the "G" interval, this facies lies conformably above facies 3.1 (Figures 10 and 14B). Thicknesses generally range from 10-16 m. Along-dip extents of these sheets are up to 4 km or greater. This facies displays a convex-upward, mounded geometry at its strike and dip pinch-outs with slight erosion (Figure 14).

Primary sedimentary structures include bidirectional tabular and herringbone cross-stratification with some planar laminations, most commonly near the top (Figures 9 and 14A). Some mud draping and clay rip-ups are found near the base. Bioturbation is sparse except for the upper ~50 cm of these beds (Figure 14C). Shell fragments are rare. No clear vertical trend in grain size is observed in this facies. While both facies 3.1 and 3.3 are tabular fine to medium grained sandstones with bidirectional flow indicators, this facies is distinguishable from facies 3.1 due to its conformable base and lack of channelization.

Interpretation. This facies is interpreted to reflect migration of dunes and barforms in a sandy back barrier setting (Figure 12). Bidirectional paleocurrents and herringbone cross-stratification suggest a strong tidal influence. Sand is carried landward via tidal inlets, forming dunes and bars that are reworked by tidal processes. During sea level rise and shoreface retreat, tidal inlet deposits will migrate with the longshore current and back-step through the lagoon (Sanders and Kumar, 1975). This dynamic, continuous movement and reworking of sands by tidal currents produces a sheet-like geometry and is documented in modern and ancient high energy tidal environments (Sixsmith et al., 2008).

Facies Association 4.1 - Low-Energy Lagoonal Facies

Carbonaceous mudstones and parallel laminated mudstones and siltstones are prevalent in the John Henry Member. These successions can be up to 40 m thick in the paleolandward regions of Left Hand Collet (Figure 15A). Successions are generally capped by a coal or a shell lag and overlain by facies association 1 (Figure 6).

Facies 4.1 – Carbonaceous Mudstones

Description. Facies 4.1 consists of fine-grained carbonaceous mudstones with coal seams between 5 and 40 cm thick. Oyster, pelycypod, gastropod, and *inoceramus* shells are pervasive throughout this unit, although bioturbation is not common (Figure 15B-D). Shells are typically fragmented, though some articulated fossils are present. At times, oyster shells are concentrated in lags about 75 cm thick (Figure 15D). Woody debris and plant material are common.

Interpretation. Facies association 4 is consistent with sedimentation in a restricted lagoon behind a barrier island system (Figure 12). The abundance of fine-grained material suggests a low-energy setting with deposition due to suspension settling. Shell material indicates a marine influence and brackish water conditions at times. Coal beds indicate the presence of emergent peat swamps near landward regions of the lagoon. A lagoonal mudstone interpretation is preferred over bayfill or estuarine environments due to the brackish water conditions, little evidence of freshwater input and the presence of facies 4.2 (below) implying a barrier island system (Davis and Hayes, 1984). A bay is typically used to define a body of water surrounded by land on three sides and a more open connection to the ocean (Davis, 1994).

Facies 4.2 – Planar laminated sandstones

Description. Thin, 0.5-2 m planar laminated, very fine-grained sandstones occur within mudstones of facies 4.1 (Figure 15E). Bases of sandstones in facies 4.2 are slightly erosive with trough cross-stratification and planar laminations dipping gently towards the land (Figure 15E, F). Tops of these beds are extensively bioturbated with a restricted *Skolithos* ichnofacies (Figure 15B, G). Cerithid gastropod shells are found on the tops of these sandstones, along with oyster and large inoceramid fragments (Figure 15D). These sandstones tend to be very discrete with lateral extents on the order of 100 m.

Interpretation. Facies 4.2 records deposition of discrete washover fans on the landward sides of barrier islands during storm events (Figure 12). Planar laminations record the influx of marine sediments landward across a barrier island into the lagoon. This influx of sediments and nutrients from the open marine leads to colonization and reworking by fauna. Once influx of sediment ceases, biological activity becomes the dominant process of sediment reworking (Zonneveld et al., 2001; Allen and Johnson, 2010).

Genetic Stratigraphy of Transgressive Deposits

Facies associations 3 and 4 record deposition during sea level rise. A tidal ravinement surface which erodes into the lower-middle shoreface is found at the base of tidal inlets (Figures 5 and 6; Table 2). This surface marks a process change from a wave-dominated to a tide-influenced coastline and corresponds to the "A1" surface of Allen and Johnson (2011) in Rogers Canyon. Tidal ravinement surfaces form via channel thalweg scouring during migration of tidal channels in a transgression (Swift, 1968). Tidal ravinement surfaces are diachronous, but extend more than 5 km along-dip and all along strike in the study area. Tidal incision into lower shoreface can be as deep as 10 m; this amount of incision requires high local energy to form (Helland-Hansen and Martinsen, 1996). Behind shoreface pinchouts, these are conformable surfaces separating two tidal units, with an implied regression between (Figure 5) (A2 surface of Allen and Johnson, (2011)).

Tidal inlets and overlying bars and tidal sheets reflect deposition behind a barrier island (Figure 12). These sand-rich units interfinger with fine-grained mudstones of facies 4.1 landward (Figure 10; R-T cycle 5). Lagoonal facies associations are found above and paleolandward of shoreface pinchouts and associated erosive tidal channel fills. At the tops of tidal or lagoonal facies, a transgressive lag representing a wave ravinement surface is common (Figure 6). Wave-dominated shorefaces overlie tide-dominated back-barrier deposits, indicating a deepening of relative sea level.

Recent work has shown the prominence of tidal accumulations during the transgressive interval of regressive-transgressive fourth-order sequences across the Western Interior Seaway (Devine, 1991; Mellere and Steel, 1995b; Seidler and Steel, 2001; Kieft et al., 2011; Allen and Johnson, 2011; Steel et al., 2012). These tidal deposits range from thin lags on transgressive ravinement surfaces (Hwang and Heller, 2002) to 15 m thick successions of lagoonal and tidal inlet facies (Bullimore et al., 2008).

The tide-influenced strata of the John Henry Member at Left Hand Collet are interpreted to occur during transgressive phases of 4^{th} order cycles rather than at the tops of regressive intervals (Allen and Johnson, 2011). Tidal ravinement reflects the regressive-transgressive turn-around as described by Devine (1991). Transgressive deposits are preserved above the tidal ravinement surface but below the wave ravinement surface (cf. T-B scenario of Cattaneo and Steel, 2003). The overall retrogradational stacking patterns of the middle parasequences in the John Henry Member reflect the punctuated landward movement of the shoreline (Figure 3) (Allen and Johnson, 2011). Moreover, tidal deposits are common during sea level rise, as increased tidal prism and tidal resonance coupled with reduced wave power due to the frictional attenuation of wave energy lead to tidal influence (Ainsworth et al., 2011; Longhitano et al., 2012). During transgressions, flood-tidal currents push reworked shelf deposits landward into protected embayments, creating sand-dominated back-barrier deposits observed at Left Hand Collet.

Alternatively, shoreface successions could represent a wave-dominated delta front with tide-influenced channels incising and reworking the sediment as the delta progrades (*sensu* Bhattacharya and Giosan, 2003). However, this interpretation is not preferred for several reasons. The John Henry Member shows a retrogradational stacking pattern implying deposition by a transgressing sea, which is not conducive to deltaic deposition. Moreover, based on field observations in this study and core studies to the west by Hettinger (2000) and Gallin (2010), there is no clear fluvial connection between the marginal marine sediments and the coastal plain, which would be necessary to feed the delta system. Barrier island and lagoonal systems are common in modern transgressive systems with a low topographic gradient and ample sediment supply (Cattaneo and Steel, 2003; Boyd, 2010). During falling sea level, the size, and number of inlets is reduced due to the decreased tidal prism (Stutz and Pilkey, 2011). Regressive barrier islands do occur in modern coastlines, but their preservation potential is low as the basinward movement of the shoreline fills in and erodes the barrier island complex. In contrast, if the shoreline trajectory is sufficiently steep during transgressions, it is possible to preserve transgressive deposits (see discussion below) (Helland-Hansen and Gjelberg, 1994; Cattaneo and Steel 2003).

Regressive-Transgressive Cycle Architecture and Evolution

The overall geometries and architectures observed at Left Hand Collet reflect deposition in distinct regressive and transgressive cycles (Table 3) (Curray, 1964, Swift, 1968; Devine, 1991; Olsen et al., 1999; Cattaneo and Steel, 2003; Sixsmith et al., 2008; Kieft et al., 2011; Allen and Johnson, 2011) which are separated by two main types of transgressive surfaces: A surfaces, found at the base of transgressive intervals, and B surfaces, found at the base of regressive intervals (Table 2). Each cycle includes a regressive and a transgressive unit that form sigmoidal-shaped wedges (Figures 5 and 16). Regressive wedges thin landward onto the basal wave ravinement surface and thin at the upper boundary due to tidal ravinement (i.e. Figure 16, R-T 4 and 5). Transgressive wedges thicken up depositional dip as the shoreline migrates landward (Folkestad and Satur, 2008).

These cycles are defined as regressive-transgressive cycles bound by maximum transgressive surfaces (Figure 5) (Galloway, 1989; Kieft et al., 2011). Conventional transgressive-regressive stratigraphy bases cycles on the bottom of the transgressive interval (Embry and Johannessen, 1993). However, tidal ravinement surfaces mark the base of transgressions with varying amounts of ravinement (~20 cm to 10 m) in the John Henry Member at Left Hand Collet. These surfaces are highly diachronous and thus not an effective marker surface to base cycles. Maximum transgressive surfaces (i.e., wave ravinement or flooding surfaces) tend to have less erosion (less than 10 cm) at Left Hand Collet and may provide more effective correlating surfaces. Thus, the maximum transgressive surface marks the base and top of an R-T cycle (Kieft et al., 2011). However, complications arise when shorefaces (and therefore wave ravinement surfaces) pinchout, as in the C and F intervals. In this case the regression is inferred and only the transgressive portion of the cycle is preserved (Figure 16, R-T 5).

Overall, the stacking patterns of cycles at Left Hand Collet can be differentiated into three sections based on overall shoreline migration and pinchouts (Figure 3): thick, progradational packages at the base (R-T 0-2; "A-C" sandstones), retrogradationally stacking strata in the middle (R-T 2-4; "C-E" sandstones), and slight progradation followed by retrogradation (R-T 4-6; "F-G" sandstones) at the top of the John Henry Member. R-T cycles are summarized in Table 3. The overall stratigraphic evolution of the John Henry Member in Left Hand Collet is described below.

R-T cycle 0 ("A" sandstone of Peterson, 1969a) contains two parasequences and is the thickest cycle observed at ~75 m (Figure 4). A flooding surface separates the underlying coastal plain facies of the Smoky Hollow Member of the Straight Cliffs Formation from the first shoreface of the John Henry Member. There are two regressive, 20-25 m thick parasequences within R-T cycle 0 separated by a flooding surface. The second parasequence contains an upper erosional surface with ~3 m of relief, capped by channelized and non-channelized coastal plain facies (Figure 16). Above the coastal plain facies, a transgressive surface marks the onset of sea level rise and deposition of ~15 m of transgressive, lagoonal fill and tidally-influenced barforms. A flooding surfaced marked by a pebble lag at the top of the transgressive interval separates the tidal facies from overlying distal lower shoreface (facies 1.1).

R-T cycle 1 ("B" sandstone) is marked by a basal flooding surface and a 30 m upward shoaling parasequence from facies 1.1 to 1.2. Basinward, the regressive shoreface is capped by a nonerosive transgressive surface with a slight mudstone break and a 10 m tidal sheet which pinches out into lagoonal mudstones and coals (Figure 14). The tidal sheet shows bidirectional, NW-SE paleocurrents (Figure 9) parallel to the overall strike of the shoreline, indicating deposition in back-barrier system migrating with long-shore drift. Up-dip from the tidal sheet pinchout, a tRs incises up to 10 m into the shoreface and is overlain by inclined heterolithic strata, lagoonal mudstones, and coals (Figure 11A). In Left Hand Collet, a transgressive surface separates coals from R-T cycle 1 from lagoonal mudstones of R-T cycle 2 (Figure 16).

The shoreface pinchout ("C" sandstone) in R-T cycle 2 is the most basinward of all R-T cycles at Left Hand Collet (Figure 17B). A regressive shoreface is bound by a flooding surface at the base and a transgressive surface at the top. Landward, within 1 km of the mouth of Left Hand Collet, this shoreface pinches out into lagoonal mudstones and coal mires of the Christensen coal zone (Figures 15 and 16). This slope-forming interval consists of ~40 m of lagoonal mudstones and coals, while the shoreface observed at Left Hand Collet was only ~10 m thick. Based on studies in the John Henry Member to the south, there are up to four additional shorefaces that pinch out into this thick succession of mudstones that are not observed at Left Hand Collet (Figure 6 of Allen and Johnson, 2011). Thus, the Christensen coal zone is likely an amalgamation of lagoonal deposits from up to four R-T cycles, with only the transgressive interval preserved. However, at Left Hand Collet, only one shoreface is present.

Above the Christensen coal zone, the two overlying cycles (R-T 3-4) are retrogradationally stacked with respect to R-T 2 (Figures 16 and 17). R-T cycle 3 is underlain by a wave ravinement surface below facies 1.2. The shoreface facies are capped by a tidal ravinement surface (Figures 6F and 11B). Landward, the regressive wedge thins as the shoreface is incised and overlain by a landward thickening, 15 m interval with amalgamated tidal channels and attached barforms (Figures 8 and 13). At the base of the transgressive section, paleocurrents show a south to southeast movement of tidal inlets, consistent with migration of inlets with longshore transport (*sensu* Kumar and Sanders, 1974) (Figure 9). In amalgamated tidal channels above, paleocurrents trend NE-SW perpendicular to the orientation of the shoreline (Figure 9), which is consistent with orientations of tidal inlets cutting through barrier islands. This package is truncated by a wave ravinement surface, marked by a slight erosive surface and a firmground lag with a *Glossifungites* ichnofacies (Figure 6).

R-T cycle 4 includes a basal wRs and regressive sandstones of facies association 1.2. This shoreface is truncated by a tRs. Basinward, the regressive shoreface is overlain by a thin 2 m section of interbedded mudstones and thin tidal sandstones with abundant clay rip-ups (Figure 7). Landward, tidal inlets and lagoonal facies dominate this transgressive succession, with tidal channels containing southward migrating bars downlapping onto a tRs (Figure 8). Paleocurrent directions indicate predominantly east-directed flow (Figure 9). Tidal channels are found adjacent to lagoonal mudstones (Figure 8). Basinward, this cycle is capped by a wRs. Landward, a surface separates transgressive deposits in R-T cycle 4 with lagoonal mudstones and tidal channels forming behind the pinchout of the regressive shoreface of R-T cycle 5 (Figure 16).

R-T cycle 5 ("F" sandstone) steps basinward with respect to the inferred pinchout of the shoreface of the underlying cycle (Figure 10). The regressive shoreface is underlain by a wRs; however, this shoreface pinches out 4-5 km into Left Hand Collet into lagoonal mudstones and coastal plain coals of the Rees coal zone (Figures 2 and 17). Small tidal channels within the lagoon have a dominant east direction, with a subordinate westward current (Figure 9). This shoreface pinchout (Figure 2) has an east-west orientation, oblique to the NW-SE trend observed in other shorefaces of the John Henry Member. A process change surface separates the regressive shoreface from the overlying transgressive tidal sheet. The tidal sheet also pinches out into lagoonal mudstones (Figure 10). At the shoreface pinchout, the wRs, which separates cycle 5 from cycle 4 below, becomes a conformable surface which separates the two transgressive intervals (Figure 16). Cycle 5 is capped by a wave ravinement surface on top of a coal bed.

R-T cycle 6 ("G" sandstone) is bounded at the base by a wRs and contains regressive shoreface deposits of facies 1.1 and 1.2 (Figure 5). Tidal ravinement into the shoreface is extensive throughout Left Hand Collet. Basinward, a tRs is overlain by thin, amalgamated channels and inclined heterolithic strata (Figure 11C). Landward, tidal channels at the base of the transgressive interval transition upwards into a thick, 15 m tabular tidal sheet (Figure 11D). Paleocurrents in the tidal channels have a bidirectional east-west orientation, while the tidal sheet above has a dominant northeast trend with a strong subordinate southwest direction (Figure 9). The tidal sheet is extensive for several kilometers to the north and west, but is eroded into by tidal channels to the south. The Alvey coal zone is exposed above R-T 6, as well as a thick fluvial succession that likely belongs to the Drip Tank Member of the Straight Cliffs Formation.

Figure 5 – Schematic illustration of the two main types of transgressive surfaces that separate regressive and transgressive intervals: surfaces that mark the maximum transgression (B1/wRs and B2/flooding surface) and surfaces that mark the onset of transgression (A1, A2, A3/tRs) (Allen and Johnson, 2011). "A" surfaces separate underlying wave-dominated shoreface from overlying tidal deposits, marking a process change and the onset of transgression. A1 – conformable surface at the top of regressive units and base of transgressive units, marking process change. A2 – surface between two transgressive units with inferred regressive intervals pinching out paleoseaward. A3 – tidal ravinement surface marked by significant incision into the underlying shoreface facies. "B" surfaces separate underlying transgressive facies from overlying regressive facies. B1 – wave ravinement surface separating underlying back-barrier facies from overlying shoreface facies, with minor erosional relief. B2 – flooding surface between two regressive parasequences. See Table 2 and Allen and Johnson (2011) for a full summary of bounding surfaces.

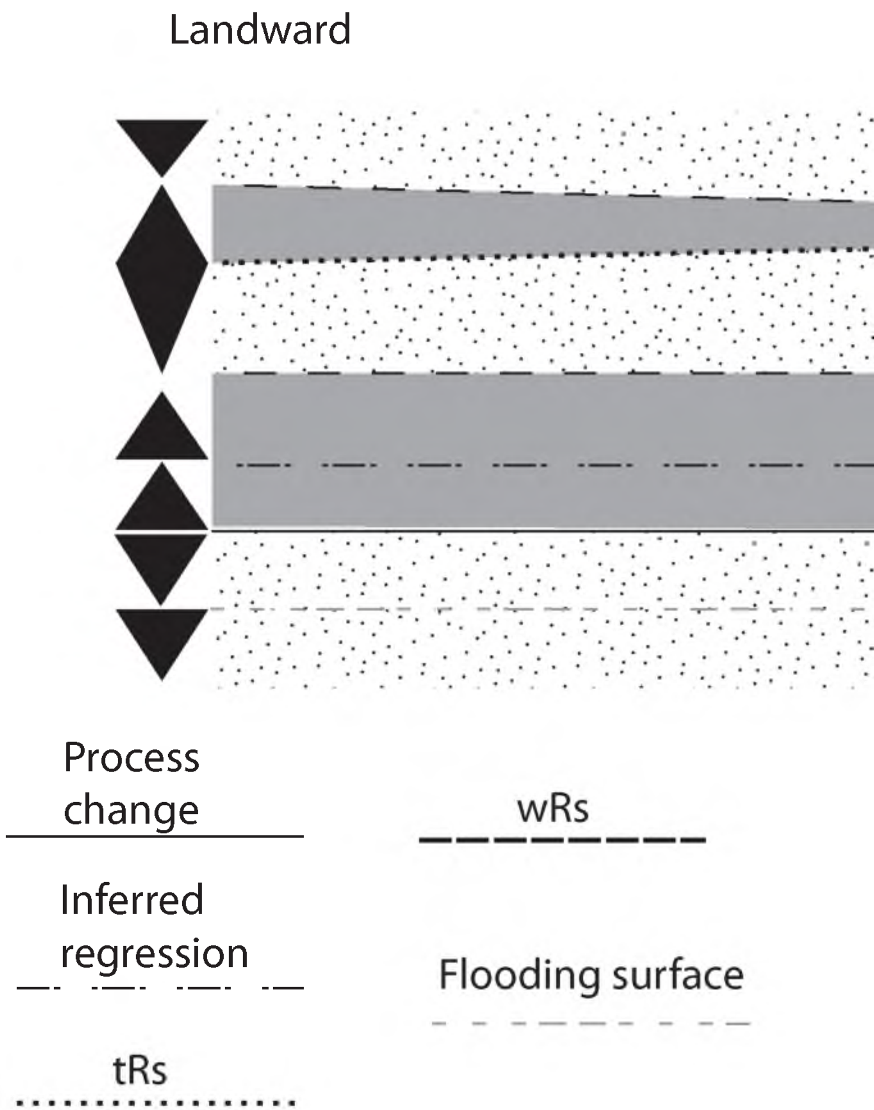

Landward
Process change
wRs
Inferred regression
Flooding surface
tRs

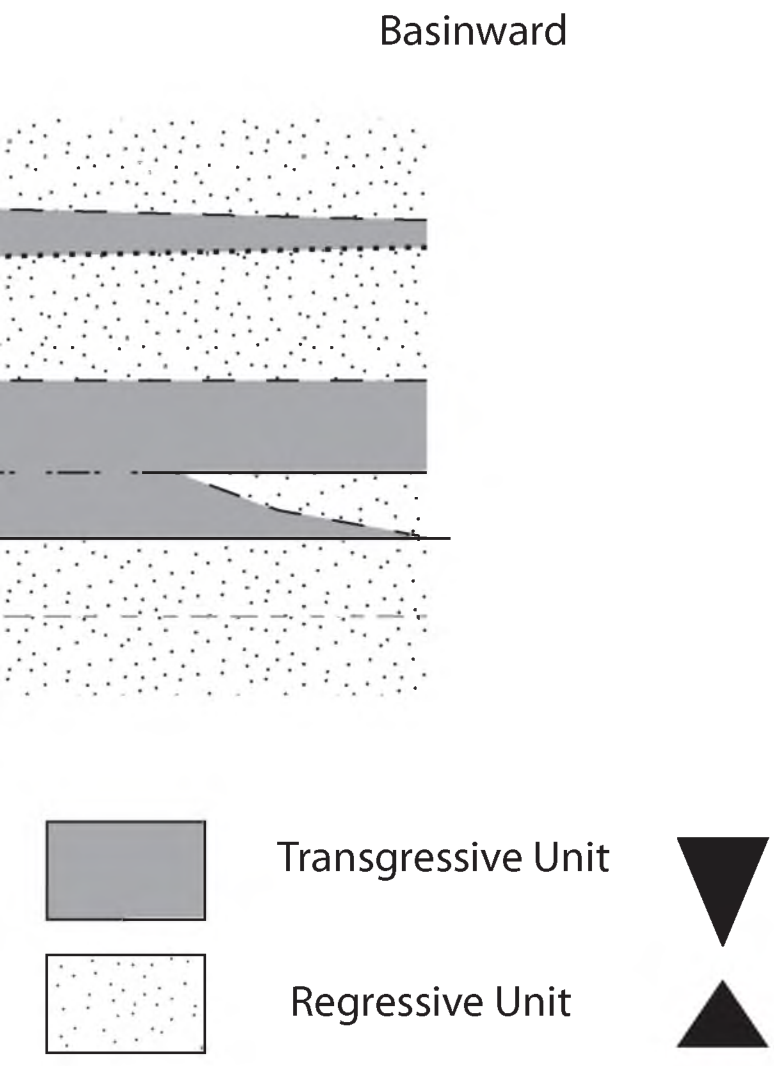
Basinward
Transgressive Unit
Regressive Unit

Figure 6 – Bounding surfaces of R-T cycles in the John Henry Member at Left Hand Collet. A-C are maximum transgressive surfaces: A) and B) are wave ravinement surfaces, while C) is a flooding surface between two shorefaces. A) Wave ravinement surface characterized by a pebble lag at the contact between coal-bearing lagoonal fill below and distal lower shoreface above; B) Wave ravinement surface overlying a coal bed with *Thalassinoides* burrows filled with sand from the overlying G shoreface. Photos D), E), and F) are tidal ravinement surfaces and are characterized by erosion into shoreface deposits and a change from wave to tide-dominated environments. D) 10 m of tidal incision overlain by inclined heterolithic strata in the B interval; E) Shell lag with ~20 cm of erosion at the base of a tidal channel in the D interval; F) Southward directed tabular cross sets downlapping onto a tidal ravinement surface incising into the D shoreface.

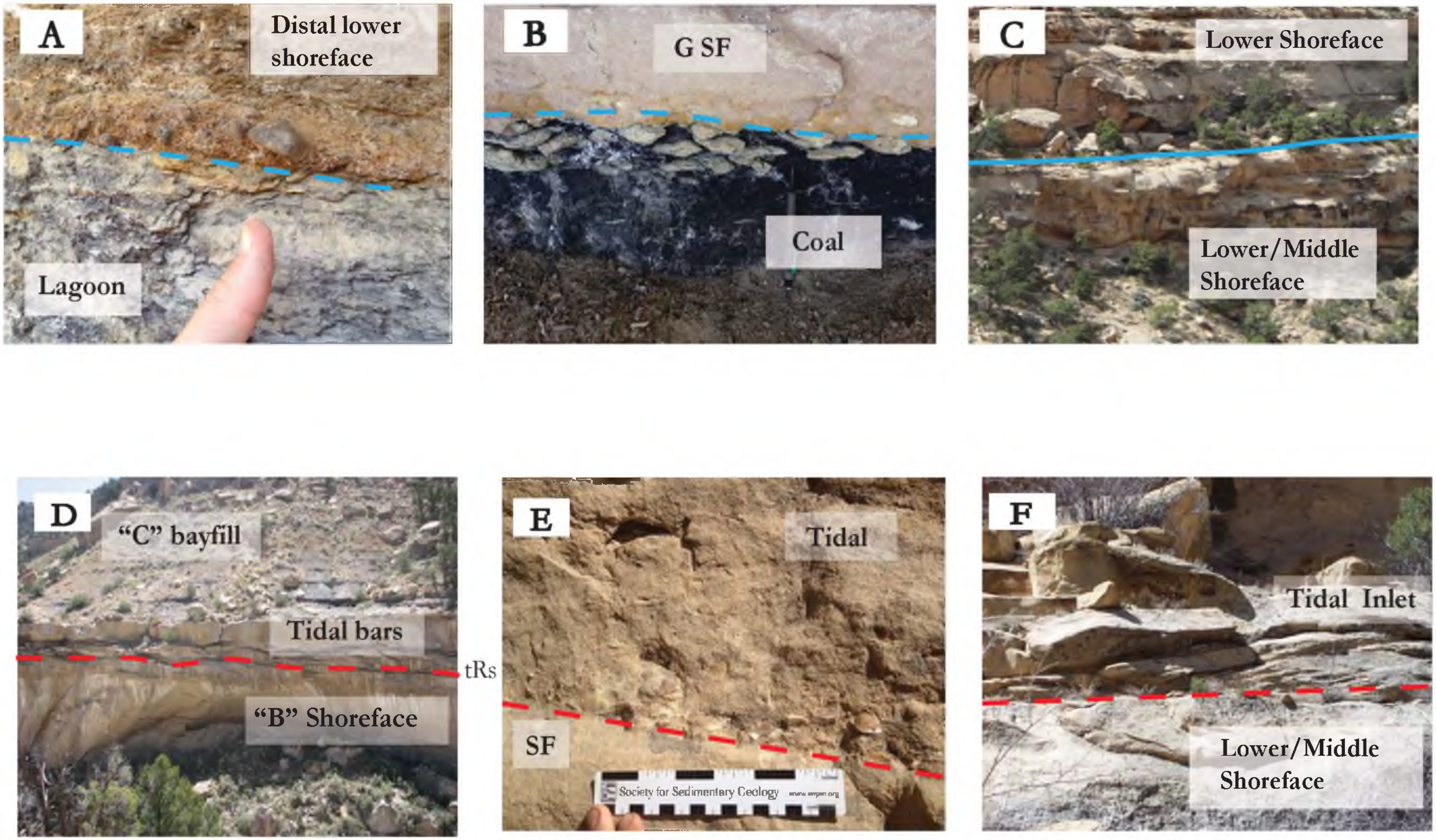
A
Distal lower shoreface
Lagoon
B
G SF
Coal
C
Lower Shoreface
Lower/Middle Shoreface
D
"C" bayfill
Tidal bars
tRs
"B" Shoreface
E
Tidal
SF
Society for Sedimentary Geology
F
Tidal Inlet
Lower/Middle Shoreface

Table 1

Summary of Facies Associations in the John Henry Member at Left Hand Collet

	Lithofacies	Description	Geometry	Fossil Content	Depositional Environment
		Facies Association 1: Wave-dominated shorefaces			
1.1	Interbedded mudstones and HCS sandstones	Upward coarsening fine-grained sands and silts with interbedded carbonaceous mudstones. Hummocky cross-stratification is common in sand interbeds.	10-50 cm beds amalgamate to form sheets up to 5 m	BI = 0-2; *Ophiomorpha*, *Thalassinoides*, *Chondrites*, rare *Zoophycos*	Offshore transition to storm-dominated distal lower shoreface
1.2	Hummocky-swaley cross-stratified sandstones	Upward coarsening fine-grained sands with abundant hummocky cross-stratification transitioning upward to swaley cross-stratification.	Sands form tabular sheets between 5-25 m thick with lateral extents of 10's of km's along strike	BI = 1-2; *Ophiomorpha* and *Thalassinoides*; *Inoceramus* shell fragments are common	Storm and wave-dominated lower to middle shoreface
		Facies Association 2: Coastal Plain			
2.1	TCS channelized sandstones	Fining-upwards medium grained sandstones with unidirectional east directed trough cross-stratification (TCS)	Channels amalgamate to form channel belts up to 10 m thick	BI = 0; Occasional wood fragments	Fluvial channels
2.2	Rooted carbonaceous shales	Carbonaceous to non-carbonaceous shales with occasional coal beds and coaly clasts	Thin beds ~50 cm thick	BI = 0; Root marks are common throughout this facies	Interdistributary deposits

Table 1(continued)

	Lithofacies	Description	Thickness	Fossil Content	Depositional Environment
		Facies Association 3: Tide Dominated Facies			
3.1	Channelized, bidirectional sandstones	Bases of sandstones have an erosive scour with up to 1 m of relief and abundant clay rip-ups and double mud drapes. Fine to medium-grained sandstones have bidirectional current indicators, herringbone cross-stratification, and abundant reactivation surfaces	Individual beds range from 1-5 m and stack to form sheets up to 20 m thick. Internal scour surfaces up to 9 m thick separate individual channels	BI = 0-2; Bioturbation is variable; wood lags with abundant *Teredolites* borings are common	Tidal inlet fill
3.2	Inclined heterolithic strata	Interbedded sigmoidal shaped sands and mudstones. Mud-draping on cross-sets and some trough cross-stratification is found, though bioturbation is extensive and reworks the majority of the sediment	Beds range from 5-90 cm thick and stack to form bedsets between 8-10 m	BI=5; *Thalassinoides*, *Planolites*, *Berguaria*, *Gastrochaenolites*, and *Rosselia*	Back-barrier tidal barforms
3.3	Non-channelized, bidirectional sandstones	Fine to medium grained sands with trough and herringbone cross-stratification. There is no erosive base or internal channelization to this facies	Tabular sandstones up to 16 m thick	BI = 0-1; Few shell fragments, leaf fossils	Tidal sheets
		Facies Association 4: Lagoonal Facies			
4.1	Carbonaceous shales	Parallel laminated carbonaceous shales with thin coal seams	Coal range from 5-40 cm thick; Shales stack up to 40 m thick	Fragmented oyster, pelcypod, gastropod, and *inoceramus* shells	Lagoonal Shales
4.2	Planar laminated sandstones	Very fine to fine-grained sandstones with slightly erosive bases. Trough cross-stratifications transition to planar laminations dipping gently towards the land	Sand beds are generally less than 1 m thick with lateral extents around 100 m	BI = 2-3; *Skolithos* ichnofacies; gastropods, oysters, & inoceramids	Washover fans

Table 2

Major surfaces in the John Henry Member at Left Hand Collet.

Surface	Description	Key Characteristics	Erosional?
	A Surfaces: Separate underlying regressive facies from overlying transgressive facies		
Transgressive surface	Conformable surface at the top of regressive units and the base of transgressive units where no erosion is noted; process change from wave to tide-dominated	Regressive units below, transgressive above	Conformable
Process change	Surface between two transgressive units, with inferred regressive intervals pinching out paleoseaward	Occasional coals or shell lags	Conformable
Tidal ravinement surface	Erosional surface marks a process change from a wave to tide-dominated coastline; Separates underlying shoreface from overlying tidal channel facies; Marks turn-around from regression to transgression	Tidal incision into shoreface	Yes – up to 10 m of relief
	B Surfaces: Separate underlying transgressive facies from overlying regressive facies		
Wave ravinement surface	Separates underlying back-barrier or coastal plain facies from overlying shorefaces;	Firmground marked by *Glossifungites* ichnofacies or pebble lag	Yes – minor relief on the order of 10 cm.
Flooding surface	Surface between two regressive parasequences; record slight deepening of facies	Occasional shell lags	No

Figure 7 – Facies 3.1 Channelized bidirectional sandstones; A) Clay rip-ups at the base of a tidal channel; B) Double mud drapes; C) Reactivation surfaces in a fine grained, tabular and trough cross-stratified sandstone D) Wave ripples at the top of an amalgamated tidal sandstone bed; E and F) Herringbone cross-stratification in fine to medium grained sandstones (Jacob staff interval = 10 cm); G) Double mud drapes on sigmoidal cross-sets in tidal channels; H) Wood lag along scour surface at the base of a tidal channel; I) *Teredolites* borings.

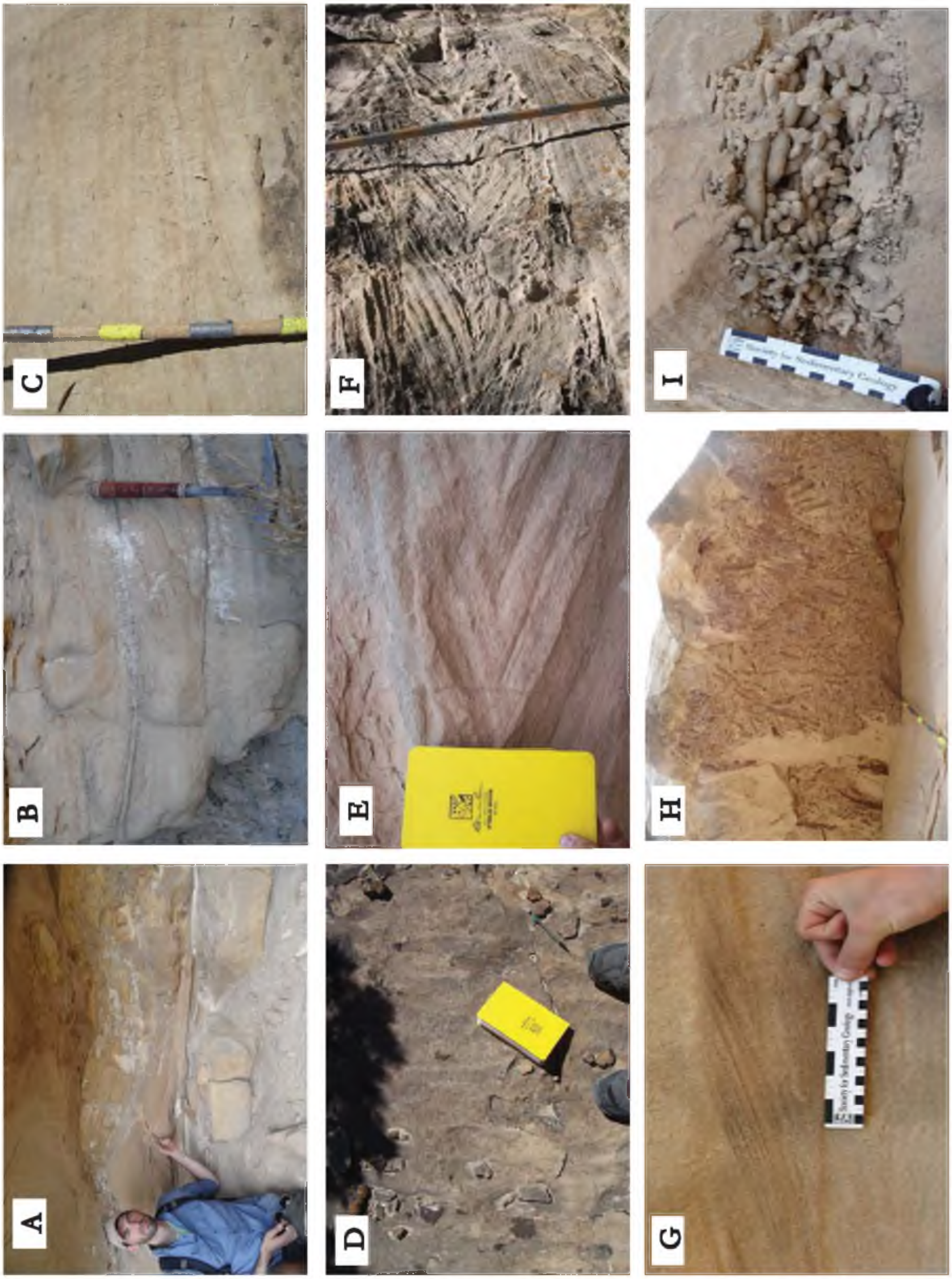
A
B
C
D
E
F
G
H
I
Society for Sedimentary Geology

Figure 8 – Tidal channel and inlet fill geometries; A)Nine meter channel incision into another tidal channel; B) Amalgamated tidal inlet fill, with the base of the outcrop exhibiting south-directed paleocurrents and the upper half of the outcrop containing paleocurrents directed to the north; C) Tidal ravinement surface at the base of a tidal channel. Arrows mark southward accretion of bars onto the ravinement surface. The covered slope to the side of the channel contains lagoonal mudstones.


A
2 m
B
1 m
C
1 m

Figure 9 - Schematic partial measured sections through tidal sections in the upper John Henry Member at Left Hand Collet. Tidal facies are variable, but tend to be either erosionally based channel deposits into shorefaces or lagoonal mudstones (F interval), or sharp-based tidal sheets (B interval). Paleocurrents measured from trough, tabular, and herringbone cross-stratification show bidirectional flow throughout the tidal facies. Bases of tidal inlets tend to have south directed currents above the tRs, consistent with migration of inlets with longshore drift (D and E intervals). The gray shading represents carbonaceous mudstones.

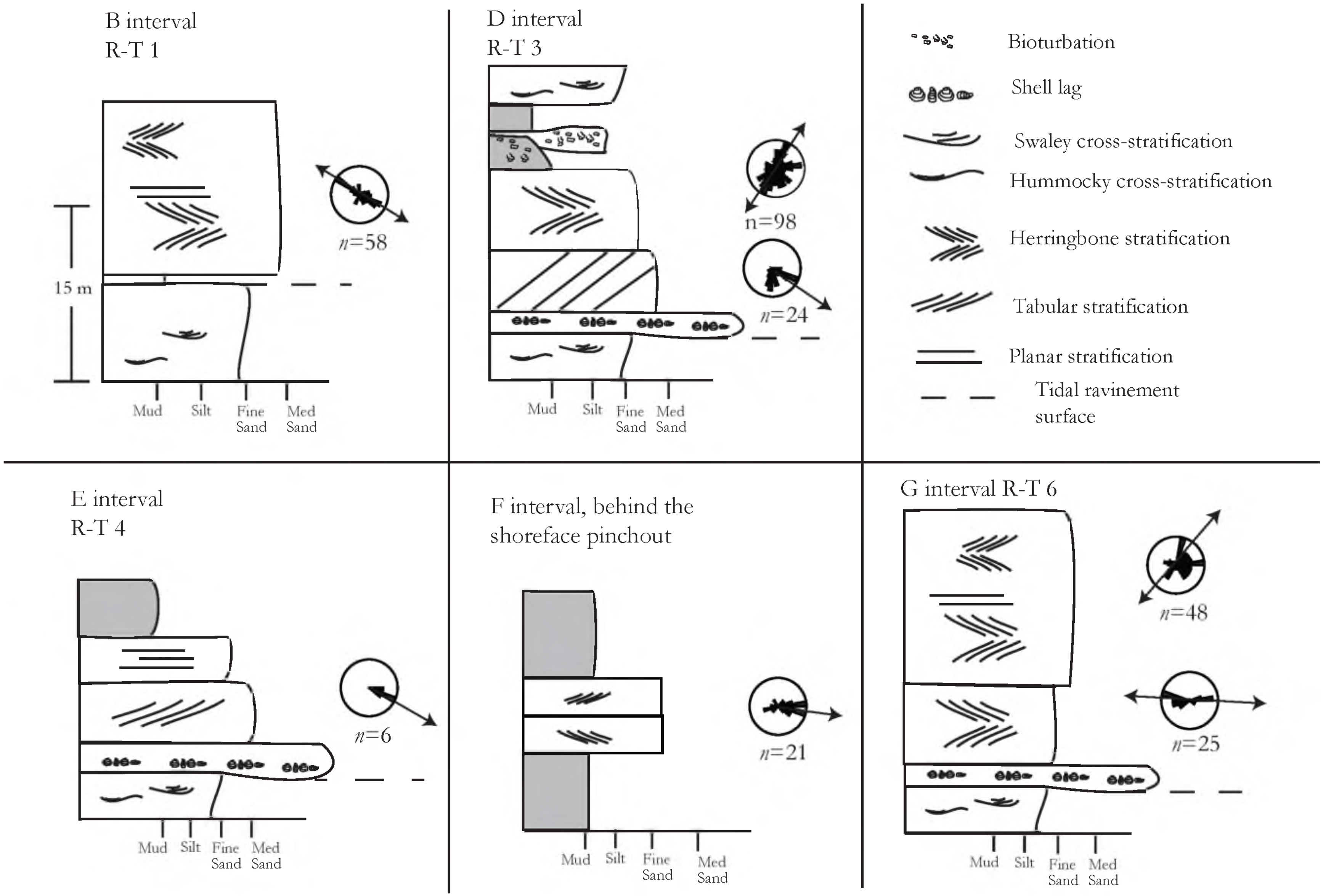
B interval
R-T 1
15 m
n=58
Mud
Silt
Fine Sand
Med Sand
D interval
R-T 3
n=98
n=24
Mud
Silt
Fine Sand
Med Sand
Bioturbation
Shell lag
Swaley cross-stratification
Hummocky cross-stratification
Herringbone stratification
Tabular stratification
Planar stratification
Tidal ravinement surface
E interval
R-T 4
n=6
Mud
Silt
Fine Sand
Med Sand
F interval, behind the shoreface pinchout
n=21
Mud
Silt
Fine Sand
Med Sand
G interval R-T 6
n=48
n=25
Mud
Silt
Fine Sand
Med Sand

Figure 10 – Schematic upper John Henry Member cross section highlighting R-T cycles, bounding surfaces, and relationships of facies associations. Locations of measured sections are shown on Figure 2.

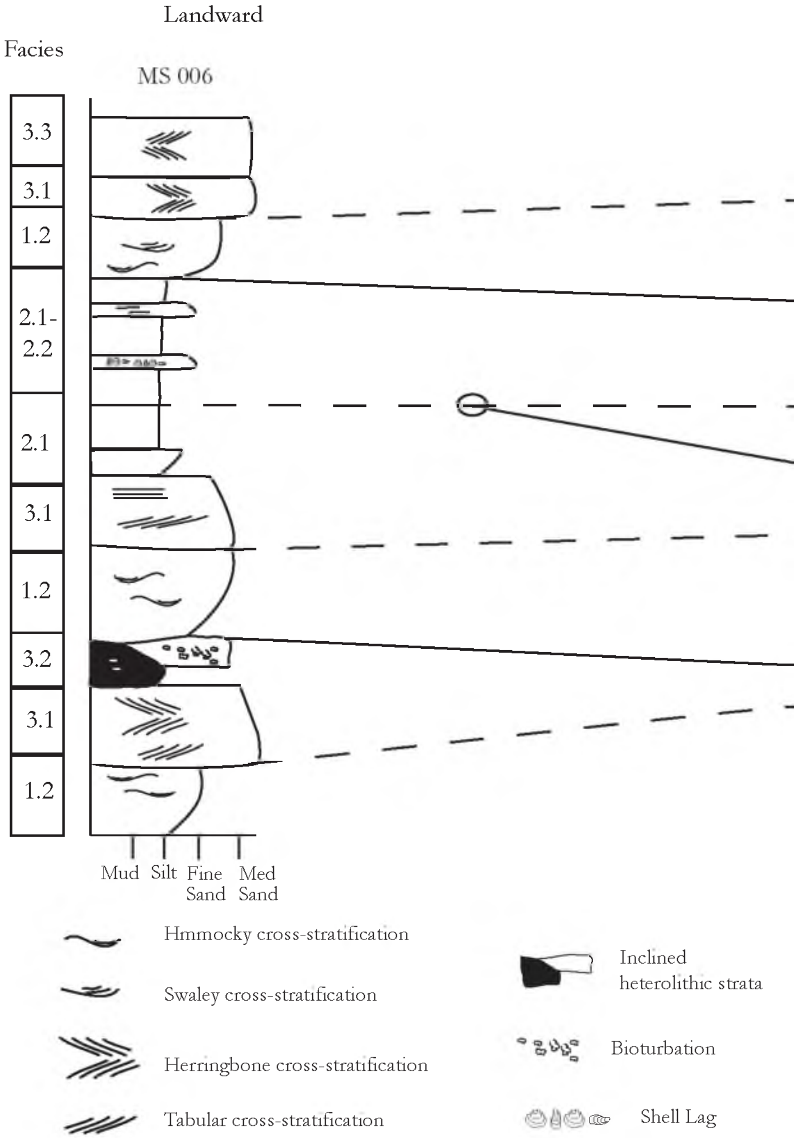
Landward
Facies
MS 006
3.3
3.1
1.2
2.1-
2.2
2.1
3.1
1.2
3.2
3.1
1.2
Mud
Silt
Fine Sand
Med Sand
Hmmocky cross-stratification
Swaley cross-stratification
Herringbone cross-stratification
Tabular cross-stratification
Inclined heterolithic strata
Bioturbation
Shell Lag

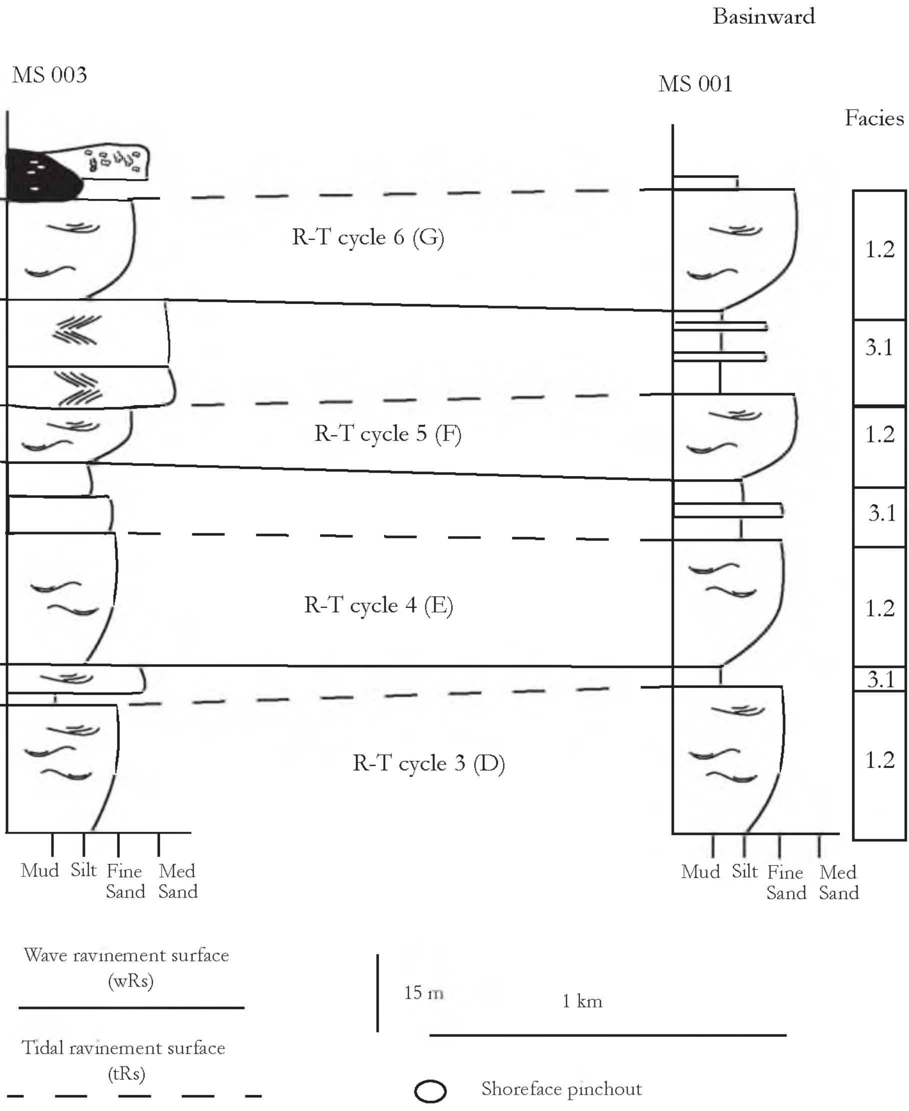
Basinward
MS 003
MS 001
Facies
R-T cycle 6 (G)
R-T cycle 5 (F)
R-T cycle 4 (E)
R-T cycle 3 (D)
1.2
3.1
1.2
3.1
1.2
3.1
1.2
Mud Silt Fine Sand Med Sand
Mud Silt Fine Sand Med Sand
Wave ravinement surface (wRs)
Tidal ravinement surface (tRs)
15 m
1 km
Shoreface pinchout

Figure 11 – Evidence for tidal ravinement into shorefaces throughout the John Henry Member at Left Hand Collet. A) Tidal ravinement into the B sandstone, overlain by inclined heterolithic strata (MS 004); B) Tidal ravinement into the D shoreface, overlain by tidal channel fill with a heterolithic base (MS 003); C) Near the mouth of the canyon in the most basinward section measured (MS 001), the G shoreface is truncated by a tidal ravinement surface and overlain by heterolithic tidal channel fill; D) Up-dip (MS 006), the G shoreface is eroded more heavily by sandstone-dominated channel fill. The tidal inlet fill is overlain by a 15 m thick tidal sheet without an erosional base.

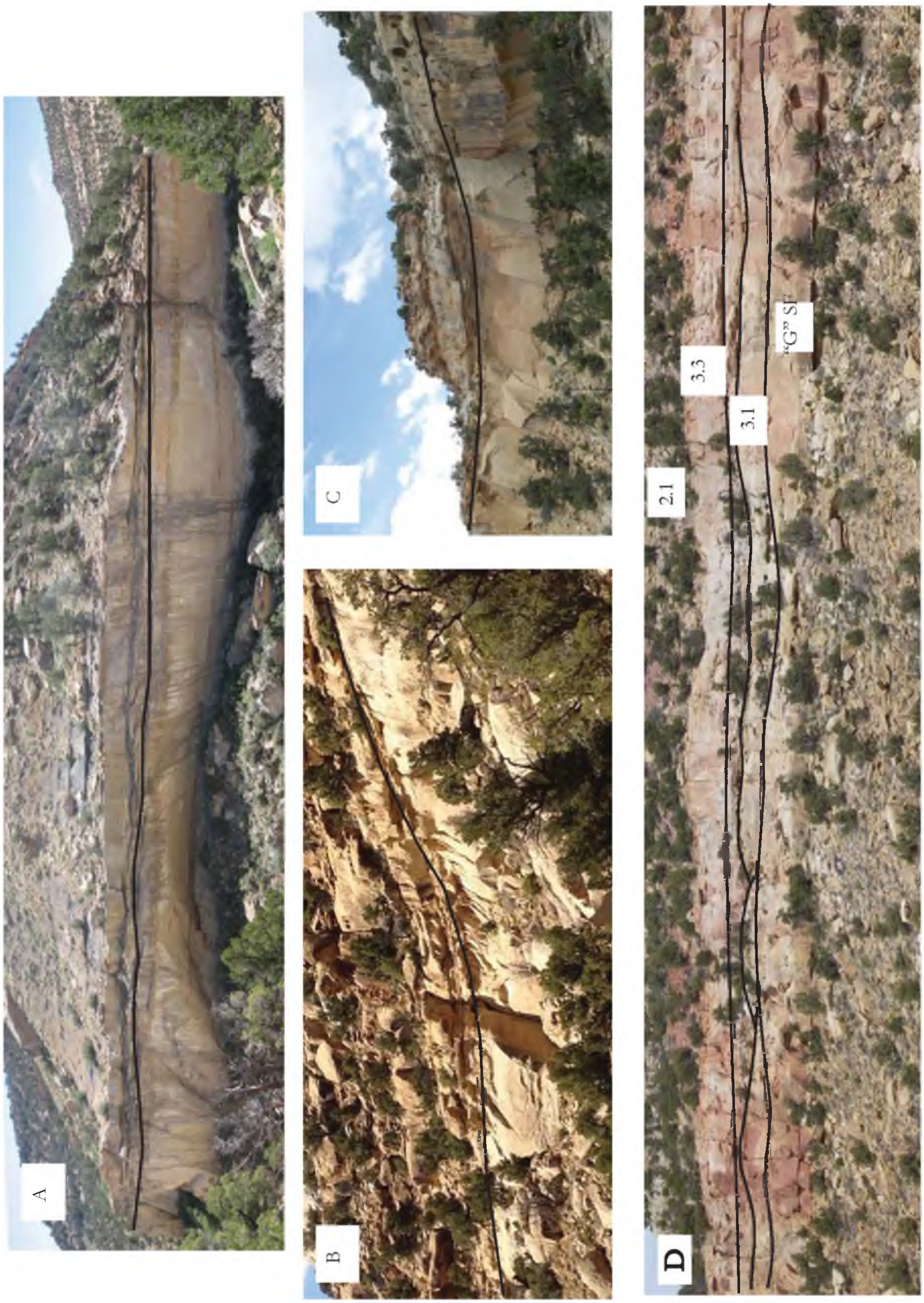
A
B
C
D
2.1
3.3
3.1

Figure 12 – Schematic illustration of barrier island lithofacies of the John Henry Member at Left Hand Collet. Tidal inlets connect the open seaway with the lagoon behind the barrier island. Flood currents bring sediment and nutrients into the lagoon, while ebb-currents shed sediment basinward. Tidal inlets migrate southward with longshore currents, creating an amalgamated succession of tidal inlet fill. Sand brought into the lagoon by flood currents and longshore transport is reworked into tidal sheetforms. Washover fans form during storm events when waves breach the barrier island.

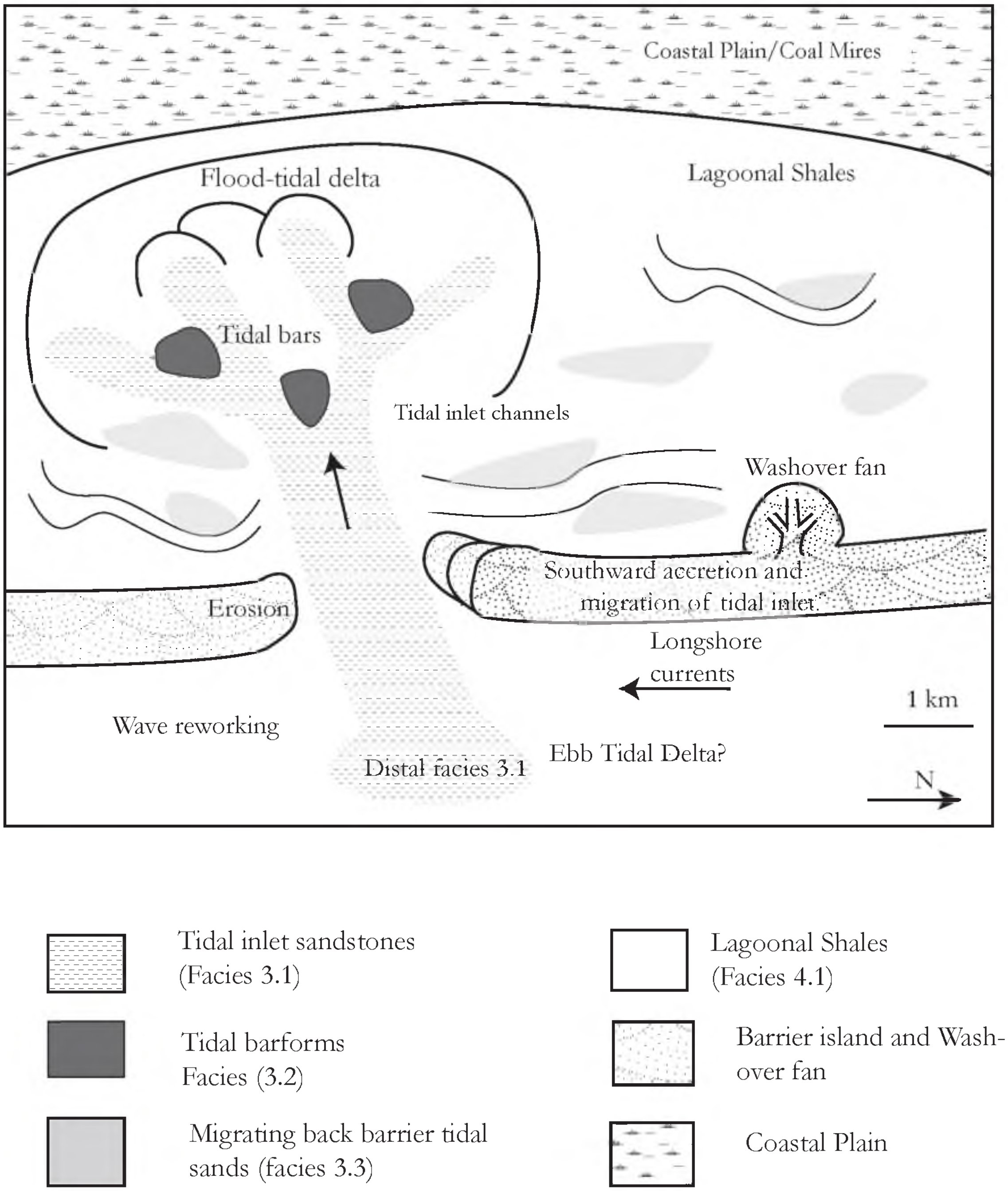
Coastal Plain/Coal Mires
Flood-tidal delta
Lagoonal Shales
Tidal bars
Tidal inlet channels
Washover fan
Southward accretion and migration of tidal inlet.
Erosion
Longshore currents
1 km
Wave reworking
Distal facies 3.1
Ebb Tidal Delta?
N
Tidal inlet sandstones (Facies 3.1)
Lagoonal Shales (Facies 4.1)
Tidal barforms Facies (3.2)
Barrier island and Wash-over fan
Migrating back barrier tidal sands (facies 3.3)
Coastal Plain

Figure 13 – Facies 3.2 - Inclined heterolithic strata – A-C) Inclined heterolithic strata with sigmoidal shaped sands; D) *Bergauria* along mud-sand contact; E) Sand-filled *Thalassinoides* burrows; F) *Rosselia* burrows in tidal sand; G) Gravel lag at the top of tidal bar facies, overlain by distal lower shoreface deposits; H) *Gastrochaenolites* borings into firmground mudstones, overlain by distal lower shoreface deposits.

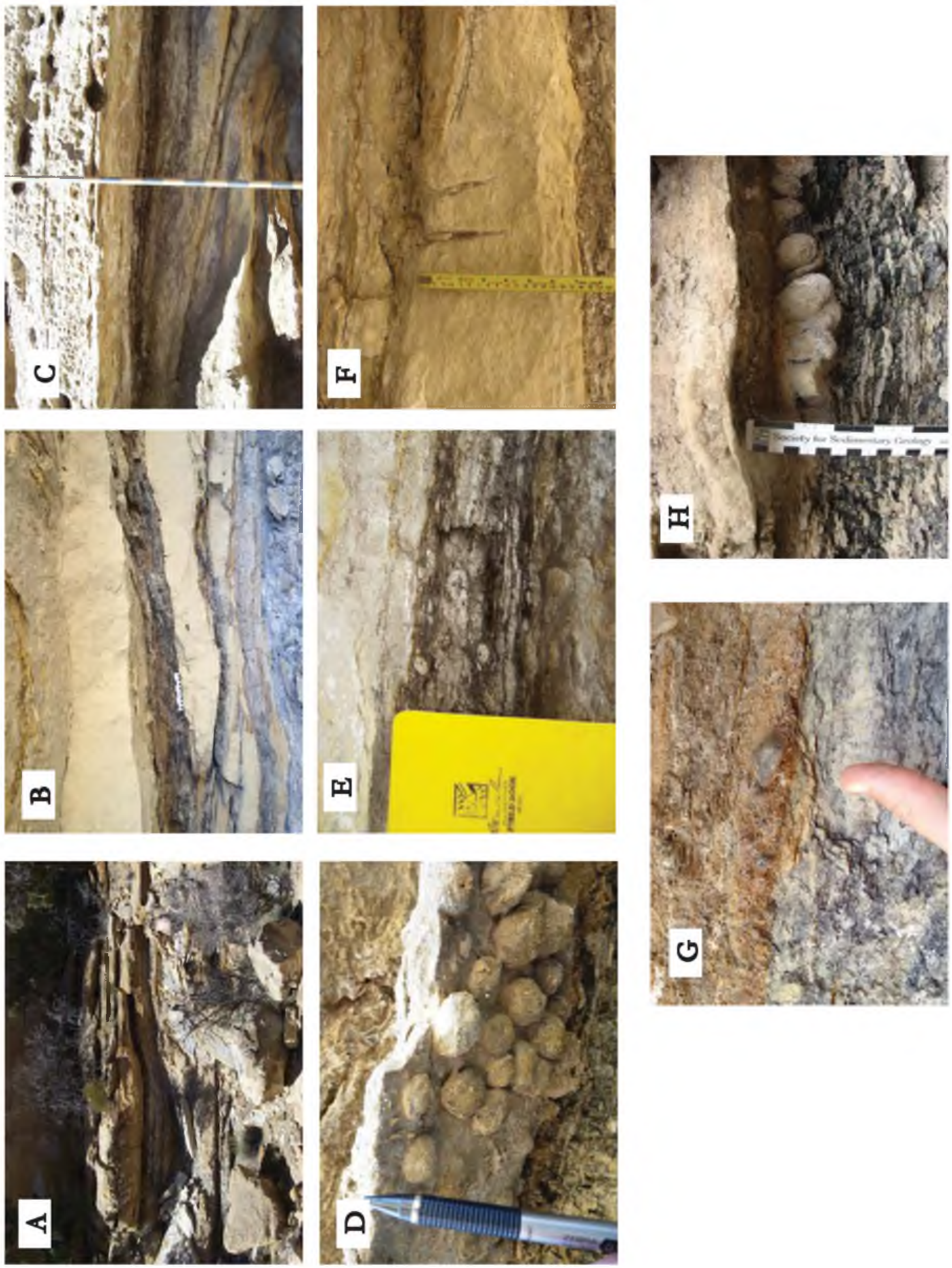
A
B
C
D
E
F
G
H

Figure 14 – Facies 3.3 – Non-channelized, bidirectional cross-stratified sandstone. A) Herringbone cross-stratification in a medium-grained sand; B) 15 m thick fine to medium-grained sandstone with abundant herringbone and tabular cross-stratification; C) Clay rip-up clasts near the base of facies 3.3 in the G interval; D) Landward pinchout of tidal sheet into lagoonal mudstones in the B interval.

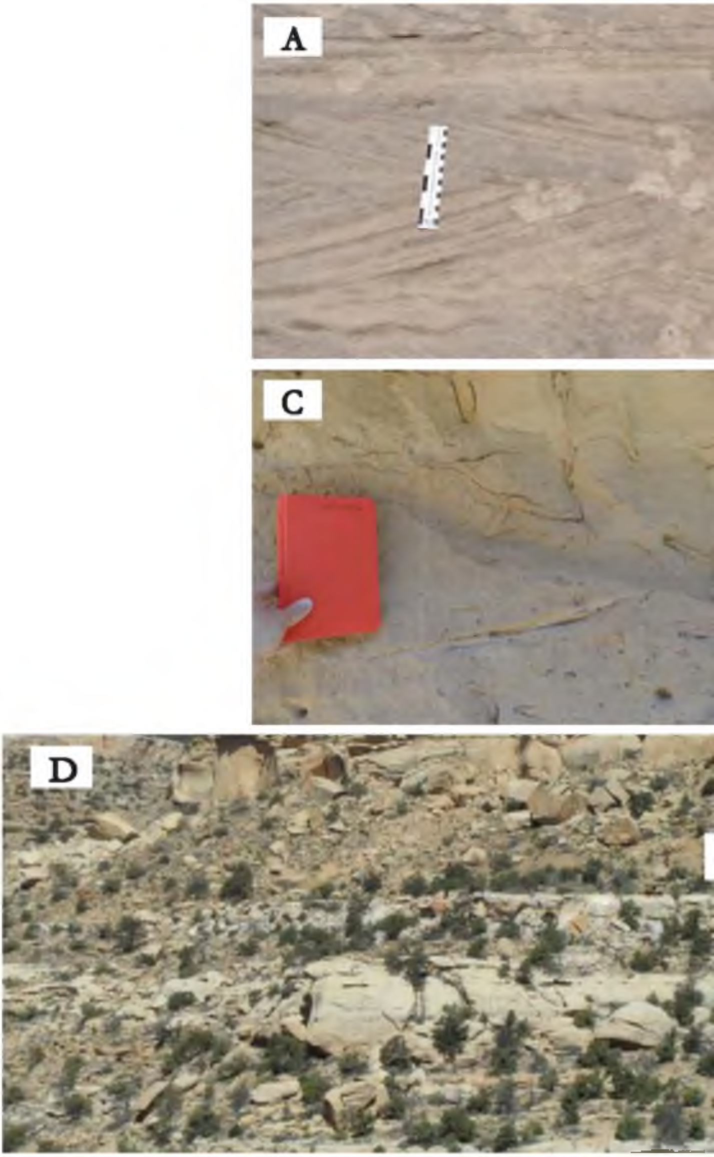
A
C
D


B

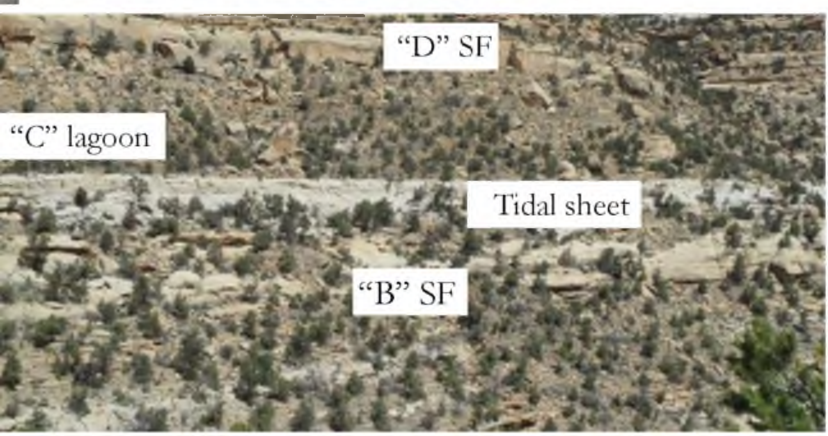
"D" SF
"C" lagoon
Tidal sheet
"B" SF

Figure 15 –Facies Association 4 – A) Christensen Coal Zone, which contains back-barrier deposits behind the C shoreface; B) Cerithid gastropods on top of a thin sand; C) Thin oyster lag; D) Large oyster lag, with shells as large as 15 cm in length; E) ~1 m thick washover fan deposit; F) Shell lag at the base of washover fan; G) *Skotlithos and Arenicolites* at top of washover fan deposit. The section at the top represents a typical lagoonal facies association behind a shoreface pinchout (Allen and Johnson, 2011). Paleocurrents from washover fans are taken from planar laminations dipping ~1° to the southwest.

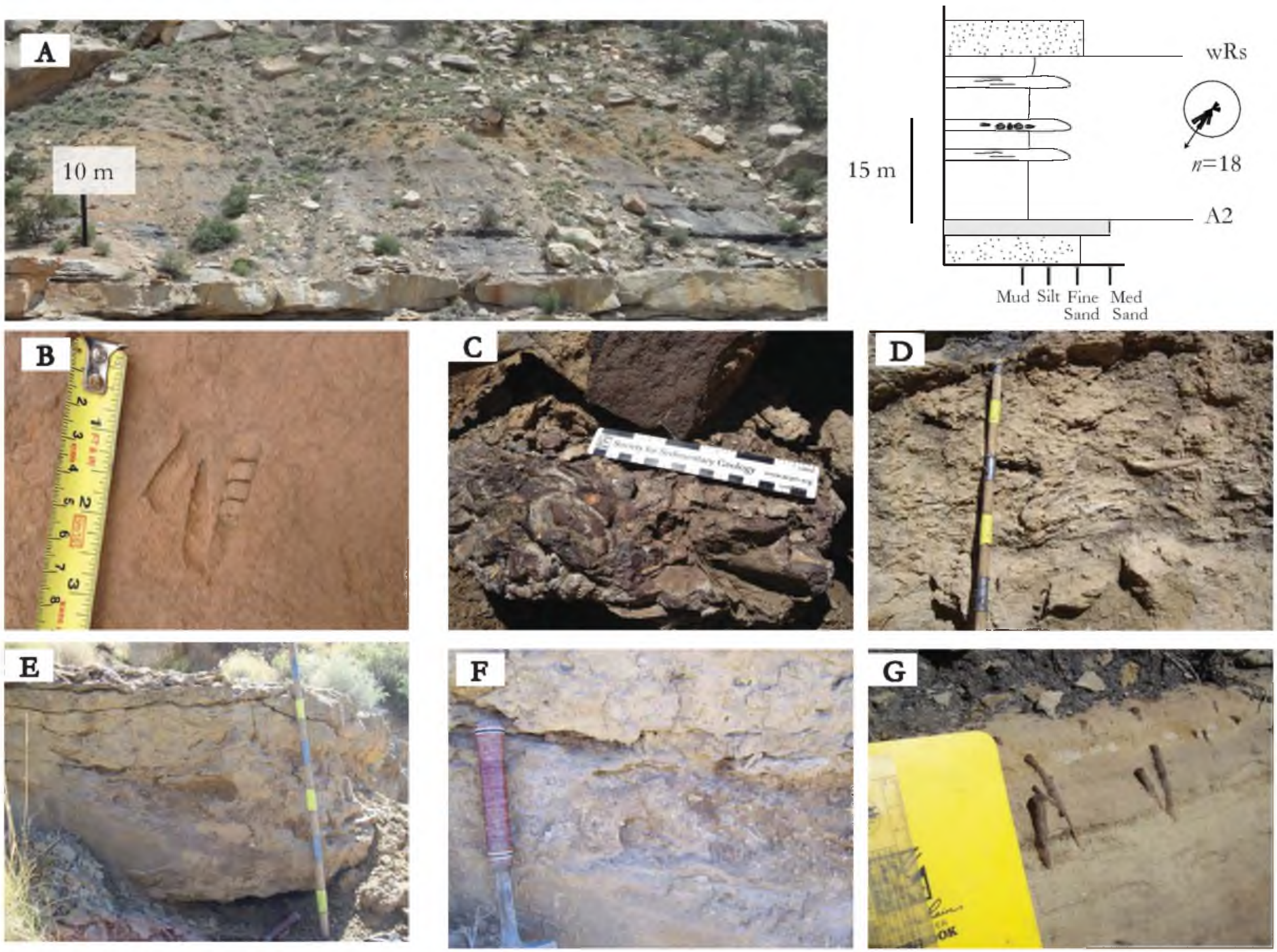
A
10 m
wRs
15 m
n=18
A2
Mud
Silt
Fine Sand
Med Sand
B
C
D
E
F
G

Figure 16 – Dip cross-section of the John Henry Member at Left Hand Collet showing the development of R-T cycles. Locations of sections are shown in Figure 2. Detailed sections are in Appendix A. Letters denote the shoreface package described by Peterson (1969a). R-T cycles are typically bounded by maximum transgressive surfaces at the top and bottom (wRs, solid red line). The onset of transgression is marked by a tidal ravinement or process change surface. R-T cycles 0-1 are dominated by regressive shoreface that are progradationally stacked. This progradation continues up through the middle John Henry in R-T cycle 2, where the shoreline is at its basinward most position. The pinchout of the C sandstone and parasequences therein are only observed at the mouth of the canyon. Rather, R-T cycle 2 is characterized by lagoonal mudstones and coals of the Christensen coal zone. Shell lags possibly indicate a A2 surface (Allen and Johnson, 2011) where there is an implied regressive interval basinward. Based on Allen and Johnson (2011) the middle John Henry Member exhibits net retrogradationally stacking cycles. This retrogradational pattern continues through R-T cycles 3 and 4. Here, the upper John Henry Member contains extensive tidal ravinement into shorefaces marking the onset of transgression. The tRs is overlain by sandstone-dominated tidal facies that thicken paleolandward. R-T cycle 5 is progradationally stacked with respect to the underlying cycles, as the shoreface is eroded by tidal channels and pinches out into lagoonal mudstones. R-T cycle 6 is again retrogradationally stacked with respect to R-T 5, and contains a thick succession of amalgamated tidal inlet fill and sheets.

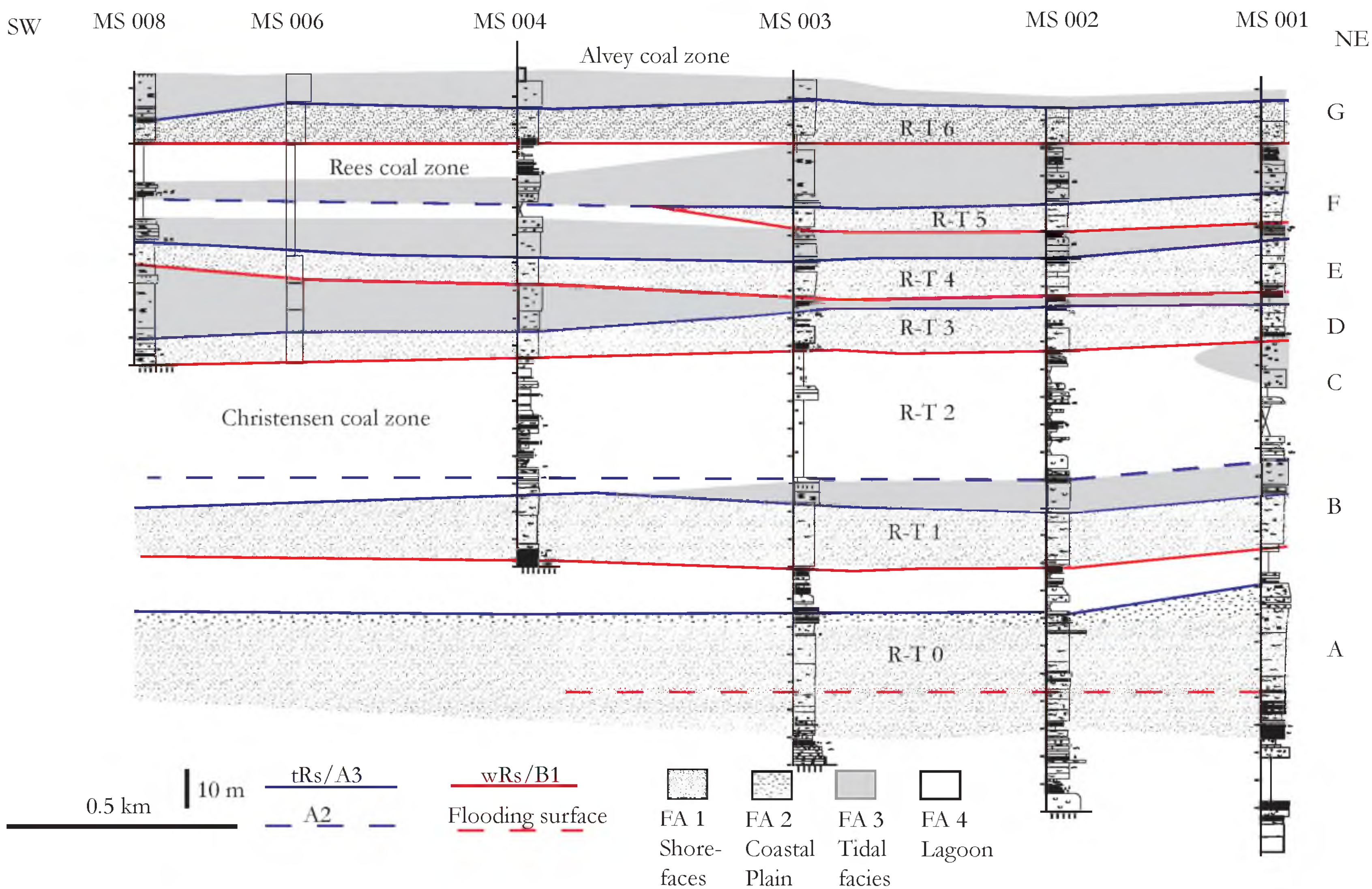
SW
MS 008
MS 006
MS 004
MS 003
MS 002
MS 001
NE
Alvey coal zone
Rees coal zone
Christensen coal zone
R-T 6
R-T 5
R-T 4
R-T 3
R-T 2
R-T 1
R-T 0
G
F
E
D
C
B
A
0.5 km
10 m
tRs/A3
A2
wRs/B1
Flooding surface
FA 1 Shore-faces
FA 2 Coastal Plain
FA 3 Tidal facies
FA 4 Lagoon

Figure 17 - Paleogeographic reconstructions of the John Henry shorelines at Left Hand Collet and Rogers Canyon for the C, D, and F intervals. (A) and (B) Two R-T cycles in the C interval show the retrogradational stacking pattern beginning in the middle John Henry. The regressive shoreface erodes and pinches out into the transgressive deposits from the underlying R-T cycle. The first pinchout shown in (A) is not observed at Left Hand Collet but inferred based on the pinchout trend at Rogers Canyon. (C) Regressive shoreface interval of the D sandstone, with coastal plain lying behind the shoreface. Note the location of the shoreline landward of the C pinchouts, implying net transgression. This pinchout is not observed at Left Hand Collet, but inferred from core studies. (D) Transgressive interval of the D sandstone showing tidal ravinement into the underlying shoreface and deposition of tidal inlet fill. (E) Pinchout of the F shoreface and arcuate trend of the shoreline between Left Hand Collet and Rogers Canyon. This pinchout is progradational with respect to the D and E intervals. Inset: Red star – Escalante; Gray star – Left Hand Collet Canyon; Blue star – Rogers Canyon.

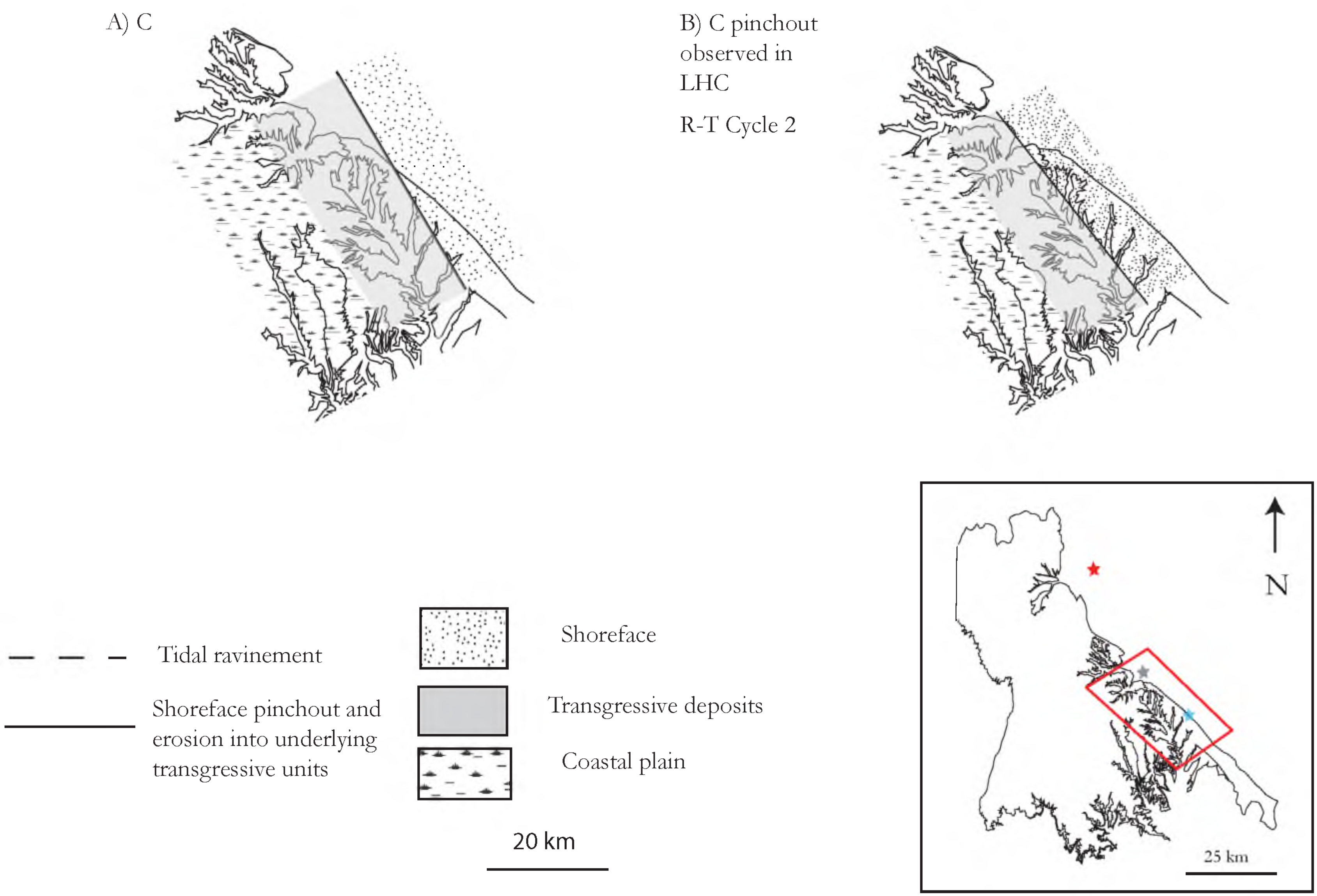
A) C
B) C pinchout observed in LHC
R-T Cycle 2
Tidal ravinement
Shoreface pinchout and erosion into underlying transgressive units
Shoreface
Transgressive deposits
Coastal plain
20 km
N
25 km

C) D Regressive shoreface

R-T Cycle 3

E) F pinchout and onset of T

R-T Cycle 5

D) D onset of T

R-T Cycle 3

Figure 17 - continued

Table 3

Summary of Regressive-Transgressive cycles observed in the John Henry Member at Left Hand Collet.

R-T Cycle	Primary R Units	Bounding surfaces (R deposits)	Paleolandward Expression (in LHC)	Primary Tr Units	Tidal Range	Bounding surfaces (T deposits)	Overall shoreline migration	Max thickness
R-T 0	LF 1.1-1.2; LF 2.1	Basal – B2 Upper – A1	Tabular	LF 4.1	Micro	Basal – A1 Upper - B1	Pro	R – 60 m T – 15 m
R-T 1	LF 1.1-1.2	Basal – B1 Upper – A3	Tabular	LF 3.3, 3.2	Meso	Basal – A3 Upper – A2	Pro	R – 25 m T – 20 m
R-T 2	LF 1.2	Basal – B1 Upper – A3	Pinches out into LF 2.1	LF 4.1, 4.2	Micro	Basal – A3 Upper – B1	Pro to Retro	R – 10 m T – 30 m
R-T 3	LF 1.2	Basal – B1 Upper – A3	Thins on B1; erosion by A3	LF 3.1, 3.2	Meso	Basal – A3 Upper – B1	Retro	R – 10 m T – 15 m
R-T 4	LF 1.2	Basal – B1 Upper - A3	Thins on B1; erosion by A3	LF 3.1	Meso	Basal – A3 B1	Retro	R – 12 m T – 10 m
R-T 5	LF 1.2	Basal – B1 Upper – A3	Pinches out into LF 2.1; erosion by A3	LF 4.1, 4.2, 3.3	Micro	Basal – A3 Upper – B1	Pro	R – 8 m T – 25 m
R-T 6	LF 1.2	Basal – B1 Upper – A3	Thins on B1; erosion by A3	LF 3.1, 3.3	Meso	Basal – A3 Upper – Gradational with Alvey Coal zone	Retro	R – 15 m T – 15 m

Maximum thicknesses of transgressive and regressive units are measured at its landward and basinward most extents, respectively. Lithofacies and surface codes are summarized in Tables 1 and 2. T = Transgressive; R = Regressive; Pro = Progradational; Retro = Retrogradational; See Table 1 for lithofacies codes; See Table 2 for bounding surface codes

DISCUSSION

The John Henry Member at Left Hand Collet is primarily composed of wave and tide-dominated facies with a stratigraphic architecture that reflects deposition in regressive and transgressive intervals, respectively. Tide-dominated facies are under-recognized in previous studies of the marginal marine John Henry Member, but comprise significant proportions of facies preserved. This discussion focuses on four key topics: (i) developing a conceptual model for transgressive, high energy, tide-dominated facies; (ii) hypothesizing paleogeography and regional correlations in marginal marine strata; (iii) interpreting controls on preservation of R-T cycles; and (iv) understanding implications for petroleum systems.

Tidal Facies Model

The Coniacian-Santonian shoreline in the Kaiparowits Plateau is generally considered a wave-dominated coast that passes landward into lagoonal, coal bearing paralic and fluvial strata (Peterson, 1969a; Shanley and McCabe, 1991; Hettinger, 2000). However, tidal facies form significant depositional units that are key to understanding the temporal and spatial variations in the shoreline. Tidal inlets, sheets, and bars form up to 20 m thick successions of sandstone rich units directly on top lower shoreface deposits. Back barrier tidal facies can be divided into sandstone or mudstone rich deposits, and tidal ranges are estimated based on facies assemblages and comparisons with modern analogs.

Tide-dominated back barrier facies

Vertical and lateral stacking patterns of tide-dominated successions vary significantly, but can be classified as either mudstone or sandstone rich. Sandstone-dominated successions are composed primarily of units of facies association 3 and generally exhibit bidirectional paleocurrents (Figure 9). In these successions, ravinement surface and an erosional channel system (facies 3.1) incises into proximal lower to middle shoreface facies (facies 1.2) (cf., Figure 11). Tidal inlet fill is overlain by tidal sandstone sheets forming behind the barrier island (facies 3.3) or tidal bar forms (facies 3.2), which are also found adjacent to inlet facies. Trends in the inlet fill successions may reflect lateral migration of tidal inlets with littoral drift (*sensu* Kumar and Sander, 1974). Tidal inlet fill sequences are found most prominently in the D, E, and G intervals where shorefaces are being eroded, but are not observed pinching out (Figures 10 and 16).

Tidal sandstone sheets represent back barrier accumulations of sand fed to the lagoon by wave and flood tidal currents (Figure 12). Littoral drift and flood currents transport large quantities of sediment into lagoons, and channel migration causes sheet like geometries in the rock record. Similar nonchannelized tidal sandstones occur in the Hosta Sandstone (Cretaceous, New Mexico) and are interpreted to record migration of barforms and dunes landward of the barrier island (Sixsmith et al., 2008). At Left Hand Collet, Shanley (1991) originally interpreted this unit as upper shoreface deposits. However, the tidal sheet interpretation is preferred according to its bidirectional cross-stratification and tidal indicators as well as the sand sheets' relationships with other tidal facies. Some sandstone sheet exposures contain tabular to trough cross-stratification with no herringbone stratification, which could lead to an upper shoreface interpretation. However, the evidence for bidirectional flow and additional tidal indicators such as mud draping and clay rip-ups is pervasive in other sandstone sheet exposures. Furthermore, this facies lies above tidal inlet facies (R-T cycle 6, Figures 9 and 16) and adjacent to tidal bars (R-T cycle 1), indicating deposition closely associated with barrier islands and protected lagoons (Figure 12). This facies represents transgressive tidal sandstones rather than regressive upper shorefaces.

Mudstone rich back barrier deposits are extensive in R-T cycles 2 and 5 up dip from the shoreface pinchout. These deposits extend at least 5 km landward and transition into coastal plain coal mires on the basis of the core study by Hettinger (2000). Thin washover fan deposits are surrounded by lagoonal mudstones and form during storm events when sediment is pushed landward (Figure 15E). Variations in back barrier facies likely reflect periodic changes in wave versus tide dominance. Muddy lagoons may reflect a lower energy, wave-dominated environment. Sand dominated back barriers may form under higher tidal energies with efficient longshore drift and lower wave dominance. Therefore, tidal range is an important controlling factor in composition of transgressive deposits.

Tidal range estimates

Tidal range (micro, meso, macro, or megatidal) of a coastline greatly affects the facies preserved in a depositional system. For example, tidal flats, sand ridges, and estuaries are common in macrotidal depositional systems where tidal currents are the dominant mechanism of sediment transport (Prandle, 2009; Dalrymple, 2010, Longhitano et al., 2012). The tidal range of a depositional system is key to recognizing facies variations and paleogeographic reconstructions of a coastline. Temporal and spatial variations in the tidal deposits of the John Henry Member at Left Hand Collet provide important insight to the processes dominating erosion and deposition of sediments.

Model-based estimates of tidal ranges for the Western Interior Basin generally suggest microtidal conditions for most of the seaway (Eriksen and Slingerland, 1990).

However, recent studies suggest that a number of regional and local changes in the shoreline can result in changes in tidal range (Steel et al., 2012; Longhitano et al., 2012). Comparing morphologies of modern tidal depositional systems with those in the rock record can provide an estimate for tidal range.

Wave and tide-dominated inlets exhibit distinct differences in coastal morphology that are observable in the rock record (Hayes, 1975; Hubbard et al. 1979; Davis and Hayes, 1984; Fitzgerald, 1996). Wave-dominated inlets are characterized by lobate flood tidal deltas with shallow channels emptying into a large, open lagoonal system. Microtidal inlets tend to have well developed flood tidal deltas characterized by a coarsening upward trend from bayfill mudstones at the base and by tidal delta and marsh deposits at the top (Hayes, 1980; Israel et al., 1987). R-T cycles 0, 2 (Christensen coal zone), and 5 (Rees coal zone) at Left Hand Collet are characterized by mudstone dominated lagoonal fill with thin washover fans, consistent with a microtidal, wave-dominated regime (Figure 16). Similar deposits were observed by Allen and Johnson (2011) in the Christensen coal zone John Henry Member at southwest Rogers Canyon (see discussion below).

In contrast to wave-dominated inlets, tide-dominated inlets contain a deep, ebb-dominated main channel flanked by channel margin bars and large sand shoals (Hubbard et al., 1979). Back barrier sediments tend to be muds forming in marshes or mudflats supplied by tidally influenced creeks. Channels are generally confined to one inlet with little migration along strike. However, wave and tide-dominated inlets are end member scenarios; in reality, a mixed wave and tide influenced environment is perhaps the more likely case.

The sandstone rich tidal channels in R-T cycles 1, 3, 4, and 6 (B, D, E, and G intervals) at Left Hand Collet exhibit characteristics of both wave and tide energies. Bases of channels contain lateral accretion surfaces downlapping onto a ravinement surface, reflecting migration of inlets with longshore currents. These channels may be flanked by heterolithic bars. Unlike strictly tide-dominated inlets, the majority of the inlet fill in these cycles are sandstones with bidirectional current indicators. Paleocurrents are variable, but tend to show an ebb-dominant flow towards the east-southeast, with a strong subordinate flood current (Figure 9). Sand is supplied to the system via longshore transport while wave action transports sand through inlets in the flood direction. Based on modern analogs, frequent migratory inlet sequences and the sandy nature of the back barrier deposits suggests a mesotidal inlet with wave input and longshore currents playing key roles in controlling inlet morphology and character of the back barrier as well (Hubbard et al., 1979; Uhlir et al., 1988; Kamola and Van Wagoner, 1994; Longhitano et al., 2012).

Based on architectural relationships, R-T cycles 0, 2, and 5 appear to be more wave-dominated with a microtidal range, while R-T cycles 1, 3, 4, and 6 appear to reflect mesotidal conditions at Left Hand Collet (Table 3). However, it is important to take caution in assigning distinct tidal ranges to coastlines, especially in the rock record, as the relative effects of waves and tides is perhaps more important than exact tidal range (Davis and Hayes, 1984; Anthony and Orford, 2003). For example, a coast can be wave-dominated even at large tidal ranges if the wave energy is also high. Similarly, a coast can be tide-dominated even at low tidal ranges if the wave action is also low.

Modern analogs – Friesian Islands

The Friesian Islands in the North Sea contains analogous facies and processes to those of the John Henry Member at Left Hand Collet, most notably the sandy back barrier deposits that form in response to longshore sediment transport (Figure 18). The Friesian Islands are a mesotidal barrier island system with moderate wave energy (Sixsmith et al., 2008). In the 4-12 km wide back barrier complex, numerous tidal inlets form breaks in the barrier island chain, while tidal creeks drain the tidal flats (Fitzgerald and Penland, 1987). There is a strong east-directed longshore wave current that transports sand and causes migration and tidal inlet scouring (Nummedal and Penland, 2009). The sediment in the back barrier region is sand dominated due to the influx of sediment from the basinward side of the barrier via flood tidal delta lobes. Over time, these sand dunes and bars will migrate to form a sheet like geometry with tidal indicators throughout. The Friesian coastline also lacks significant sediment input from the mainland, as no major fluvial systems empty to the North Sea at this locale. This analog is also used by Sixsmith et al. (2008) to describe the Santonian-aged Hosta sandstone which shows similar barrier island facies during transgressions.

There are a few notable differences between this proposed modern analog to the John Henry Member at Left Hand Collet. The Friesian Islands are interpreted to be a regressive barrier system (Fitzgerald and Penland, 1987), whereas the John Henry Member barrier systems appear to form during transgressions. Moreover, the Friesian Islands span larger distances (~250 km) along strike than the observable John Henry Member (<100 km). Nevertheless, the facies and tidal processes that occur along the North Sea appear to be analogous to the Cretaceous of the Kaiparowits Plateau.

Modern analog – Texas Gulf Coast

The Texas Gulf Coast is an interesting modern environment that exhibits similarities to the John Henry Member. Barrier islands, tidal inlets, and washover fans are common components of this largely wave and storm dominated shoreface (Figure 19). The San Luis Pass at the southern tip of Galveston Island is a classic tidal inlet and flood tidal delta complex in a microtidal, wave-dominated regime (Israel et al., 1987). Storms also create large washover fan complexes (Hayes, 1967) that can be exploited by tidal forces and transition to a tidal inlet (Davis et al., 1989). However, at different locations along the coast, barrier islands can be either regressive, aggradational, or transgressive (Morton, 1979; Galloway and Hobday, 1983, Simms et al., 2006).

Tidal range is not the only contributing factor to barrier island morphology and evolution. Studies have noted along strike variations along the modern Texas Gulf Coast related to sediment supply, erosion, and accommodation space that have important implications for shoreline evolution (Siringhan and Anderson, 1994; Wallace et al., 2010). Mustang Island in central Texas is an example of an aggradational barrier island system with more than 20 m of well-sorted quartz sands deposited since 9.5 ka (Simms et al., 2006). This succession is attributed to the highly aggradational nature of the barrier island due to the high sediment supply to the shoreline from three river deltas that kept pace with rising sea levels. Galveston Island, on the other hand, shows a net progradation of the shoreline through time, as older barrier island deposits are found landward of the modern barrier island (Rodriguez et al., 2004). Along the same coastline presumably experiencing similar eustatic sea level fluctuations, individual barrier island complexes exhibit unique stacking geometries via autocyclic controls, which can create difficulties in stratigraphic studies. Thus in addition to illuminating depositional environment interpretations, tidal facies contain useful information for paleogeographic reconstructions and details about the stratigraphic evolution of coastlines.

Paleogeography

Wave and tide-dominated facies reflect changes in the dominant mechanisms controlling deposition and coastline morphology. These temporal and spatial variations are key to characterizing the development of the shoreline. Paleogeographic reconstructions provide useful tools for displaying trends in the coastline through time. In particular, mapping shoreface pinchouts and onset of tidal ravinement helps elucidate shoreline movements. Generally the facies belts in Left Hand Collet have a NW-SE trend consistent with the overall strike of the shoreline and are slightly oblique to the orientation of Fifty Mile Mountain (Figure 17).

Two shorefaces pinch out in outcrops in Left Hand Collet, the C and the F (Figure 17). The pinchouts of the other shorefaces occur further landward and can only be inferred from core studies (Hettinger, 2000). The shorefaces erode into the underlying transgressive deposits, and are in turn overlain by lagoonal mudstones of the next transgression (Figure 10, R-T cycle 5). The R-T cycle extends from the base of the shoreface (wRs) to the top of the following transgressive interval (Figure 16). The C sandstone is the most basinward shoreface, pinching out within 1 km of the mouth of Left Hand Collet (Figure 2). The landward expression of the C interval is the Christensen coal zone which is up to 40 m thick, reflecting multiple generations of sea level rise with an associated regressive interval pinching out basinward.

The F sandstone is overlain by a tidal sheet and pinches out into lagoonal mudstones and coals of the Rees coal zone. However, the pinchout of the "F" sandstone at Left Hand Collet has an east-west trend, oblique to the northwest-southeast trend observed for shorelines at Rogers Canyon and elsewhere in the Straight Cliffs, suggesting slight variations in paleogeographic orientations of shorelines (Figure 17). Moreover, the modern expression of Left and Right Hand Collet along Fifty Mile Mountain (Figure 1) may reflect depositional differences. The two canyons have wide mouths that are set back from the rest of Fifty Mile Mountain (Figure 1), which may reflect preferential erosion of a depositional feature such as an embayment. This embayment may lead to more localized topographic restrictions that funnel and amplify tidal waves.

In the D-G intervals in particular, tidal ravinement is diachronous and represents gradual sea level rise. Figure 17 (C, D) shows the two parts of the R-T cycle 3. The D regressive shoreface pinches out into lagoonal mudstones and coastal plain (C), while the dashed line in Figure 17D represents the onset of tidal ravinement during the following transgression. Tidal ravinement surfaces occur less than 1 km from the mouth of Left Hand Collet. This is in contrast to Rogers Canyon, where there is considerably less tidal ravinement into shorefaces in the upper John Henry Member.

Correlation to Rogers Canyon

Allen and Johnson (2010; 2011) conducted comprehensive studies of the John Henry Member at Rogers Canyon, ~20-30 km to the south of Left Hand Collet. The overall trend of most shorelines between Monday and North Basin Canyon is NW-SE (Figure 17). Therefore, Left Hand Collet is slightly paleolandward with respect to Rogers Canyon and offers the opportunity to characterize the John Henry Member up depositional dip in addition to along strike (Figure 1).

There are discrepancies between the naming conventions of Peterson (1969a) and Allen and Johnson (2011) (Figure 3). Four R-T cycles pinch out into what were originally interpreted as the C-F sandstones by Allen and Johnson (2011). These sandstones are here reinterpreted as multiple parasequences in the C sandstone interval that pinch out into Christensen coal zone, according to the original lithostratigraphic study of Peterson (1969a (Figure 16). This package is overlain by three R-T cycles assigned to the G sandstone by Allen and Johnson (2011). Further to the west (paleolandward) of Rogers Canyon, the D-G sandstones pinch out into the Rees coal zone (Peterson 1969a). Thus the top of the section in Rogers Canyon, interpreted as multiple parasequences in the G sandstone by Allen and Johnson (2011), is here placed into the D-G sandstones according to Peterson (1969a). In

Left Hand Collet, this interval, the upper John Henry Member, is characterized by shorefaces and sandstone dominated tidal facies (Figures 10 and 20).

The overall trends in the John Henry Member are fairly consistent between Left Hand Collet and Rogers Canyon with a few notable exceptions (Figure 21). The base of the John Henry contains three progradationally stacked R-T cycles, corresponding to the A, B, and first parasequence of the C interval. These are R-T cycles 0-2 in Left Hand Collet and Rogers Canyon. In Rogers Canyon, the C interval, as discussed above, contains 4 R-T cycles stacked retrogradationally. In Left Hand Collet, there is only one R-T cycle observed. This is attributed to the position of Left Hand Collet paleolandward of Rogers Canyon, so it is believed that multiple shoreface pinchouts occur paleoseaward of Left Hand Collet (Figure 17). Thus, the thick Christensen coal zone is an amalgamation of transgressive lagoonal fill from multiple generations of sea level rise and fall without preservation of the regressive portion (Figure 16).

Above the first parasequence of the C interval, the R-T cycles are retrogradationally stacked at both Left Hand Collet and Rogers Canyon. This net transgressive movement of the shoreline through time at Left Hand Collet continues above the pinchouts of the C sandstones in the Christensen coal zone up through the D and E sandstone. The F sandstone represents a basinward step, before the G sandstone steps landward again (Figure 21). The approximate distance between the C and F shoreface pinchout points is roughly 4 km (Figure 3), so the shoreline migrates at least 4 km landward during the middle-upper John Henry Member.

The main differences between the John Henry Member at Left Hand Collet and Rogers Canyon appear in the D-G sandstones. The upper John Henry Member at Left Hand Collet contains prominent tidal ravinement surfaces and transgressive deposits not observed at Rogers Canyon (Figure 20). At Rogers Canyon, the D-G interval contains proximal lower shoreface down-dip, with more upper shoreface present up-dip. These deposits represent lenticular R-T cycles (Allen and Johnson, 2011) with tabular regressive units only. Lenticular R-T cycles are bounded by wave ravinement or flooding surfaces, and represent the basinward expression of wedge R-T cycles. At Left Hand Collet, this interval is characterized by tidal ravinement into proximal lower shoreface deposits. Though some channelization into shoreface deposits occurs at Rogers Canyon (Allen, personal communication), tidal incision is more prominent at Left Hand Collet.

Moreover, the transgressive deposits in the D, E, and G intervals at Left Hand Collet are more sandstone rich with amalgamated channels, tidal bars, and back barrier tidal sheets, while few transgressive deposits are found in this interval in Rogers Canyon. The D, E, and G transgressive sandstones do not pinch out into lagoonal mudstones but appear to transition to coastal plain deposits up-dip based on core studies (Hettinger, 2000). The F shoreface pinches out into lagoonal mudstones in the Rees coal zone, though there is significant erosion by tidal channels and a tidal sheet as well. This suggests the transgressive, back barrier portions of the upper John Henry Member at Left Hand Collet are higher energy and/or more sand dominated than other locations in the John Henry Member. These along strike variations are partially due to the position of Left Hand Collet paleolandward of Rogers Canyon, where the strata at Left Hand Collet represent the landward expression of lenticular R-T cycles (*sensu* Allen and Johnson, 2011). However, the lack of upper shoreface facies at Left Hand Collet suggests additional fundamental differences between the two locations.

The high energy tidal facies in the upper John Henry Member at Left Hand Collet appears to be a localized feature, as tidal ravinement is not extensive elsewhere along strike

(Allen and Johnson, 2011) (Figure 20). It is also a long term feature, since multiple generations of sea level rise and fall produce similar stratigraphic signatures at Left Hand Collet. These trends are not readily explained in conventional sequence stratigraphic models but represent important depositional features key to understanding shoreface evolution (Yoshida et al., 2007; Ponten and Plink-Bjorklund, 2009). The process changes in the John Henry Member (e.g., increased tidal erosion and high energy tidal inlets at Left Hand Collet) may be explained by variations in sediment supply and proximity to the source.

The upper John Henry Member at Left Hand Collet appears to have higher sediment influx than Rogers Canyon in the D-G intervals, as indicated by repeated ravinement and erosion of shoreface deposits and relatively coarse grained tidal sands. This could be a function of proximity to the sediment source. South-directed longshore transport, inferred from tabular cross-stratification at the base of tidal inlets (Figure 9), southward deflected mouth bars at Rogers Canyon (Allen and Johnson, 2010), and the regional transport direction in the Western Interior Seaway (Ericksen and Slingerland, 1990), carries sediment from a delta to the north along the John Henry Member shoreline (Figure 22). Areas more proximal to the sediment source (Left Hand Collet) would experience greater sediment input than distal locations (Rogers Canyon). Proximal locations experience erosion of upper shoreface and foreshore facies by laterally migrating inlet channels. Ebb-currents shed sediment basinward and flood tidal currents move sand into protected back barrier lagoons (Figure 12). Since Rogers Canyon is located further from the source, the majority of the sediment is trapped in lagoons closer to the source. Therefore, large sand dominated channels are not as frequent and do not erode as drastically into the upper shoreface and foreshore at Rogers Canyon (Figure 20). This interpretation relies on the existence of a theoretical delta to the north that supplies sediment to the marginal marine environments via longshore drift.

Regional Correlation across the Kaiparowits Plateau

The John Henry Member to the southwest in the Kaiparowits Plateau is composed of over 200 m thick successions of fluvial strata, with paleocurrents generally trending to the east (Shanley and McCabe, 1991; Gooley, 2010; Pettinga, 2013). However, fluvial outlets to the shoreline are sparse in the marginal marine successions (e.g., this study, Allen and Johnson, 2011). The lack of significant fluvial input along the marginal marine John Henry Member between Left Hand Collet and Rogers Canyon suggests the fluvial systems are being truncated or deflected to regions of higher accommodation space. Large fluvial fans, such as those observed in the John Henry Member to the southwest, are controlled by available horizontal accommodation space and will thus carry sediment towards areas with higher subsidence rates and accommodation space (Hartley et al., 2010; Gooley, 2010; Pettinga, in prep). Peterson (1969a) notes irregular thickening of the John Henry Member in the northeast, where deposits are up to 330 m thick. Thus, higher rates of sedimentation, accommodation, or subsidence can be inferred to the north. This seems the most likely location for a delta system, although very likely it would represent a wave modified delta as opposed to a river-dominated delta.

Furthermore, coal studies conducted in the Kaiparowits Plateau may support this hypothesis. Isopach maps of coal thickness from core in the John Henry Member reveal coal deposits over 120 ft (36.5 m) thick in the southeastern portions of the Kaiparowits Plateau (Figure 22) (Hettinger, 2000). Previous studies by Shanley and McCabe (1991) and McCabe and Shanley (1992) postulate that large coal mires prohibit fluvial input to the marginal marine environments, whereas high stand shorefaces are pinching out into coal bearing strata on the basinward side of the mires. The production of prolific coal mires prohibits deltaic deposition in the southeastern portion of the plateau and results in wave and tide-dominated strata basinward of the mires. The raised mires likely trap sediment on their landward edges or force fluvial systems to the northeast, where there is the greatest thickness of strata in the John Henry Member, but the coal seams are not as thick (Peterson, 1969a; Hettinger et al., 1996).

Initial reconnaissance of the John Henry Member in the northernmost portion of the Kaiparowits Plateau near Main Canyon (Figure 1) shows large, northeast dipping clinoforms in the lower interval of the John Henry Member. Further detailed research will determine whether this represents a fluvial outlet to the shoreline, which would be the main sediment source for the John Henry shoreline as postulated here.

Extensive erosion of shoreface strata and deposition of sandstone dominated tidal deposits reflects the combination of rising sea level, increased tidal energy, and proximity to the sediment source. Tidal inlet scouring during transgressions results in a tidal ravinement and formation of barrier islands with lagoons filled with relatively coarse grained sediments delivered via longshore transport from a deltaic source to the north. However, deposition and preservation of transgressive deposits require specific configurations of shoreline trajectory and sediment supply.

Controls on Preservation of R-T Cycles

Deposition and preservation of transgressive deposits are aided by shoreline trajectory, which is defined as the cross-sectional shoreline migration path along the depositional dip (Helland-Hansen and Gjelberg, 1994). Accretionary transgressions occur when the shoreline trajectory is steeper than the transgressed topography (Helland-Hansen and Gjelberg, 1994; Cattaneo and Steel, 2003). Accretionary transgressions are common when sediment supply is abundant, often in association with efficient longshore sediment transport (Helland-Hansen and Martinsen, 1996). During sea level rise, barrier islands build up, which creates accommodation space behind the barrier in lagoons. Sediment is shed landward into the lagoon from tidal inlets and washover fans. A wave ravinement surface occurs with the maximum transgression, along with a coal or shell lag. This ravinement erodes into the tidal deposits, but does not completely erode all underlying transgressive facies. As sea level falls, regressive shorefaces again build out into the basin (Figure 14 of Allen and Johnson, 2011). During the subsequent transgression, tidal inlets erode considerably into the shoreface, removing upper shoreface/foreshore deposits.

An important component of accretionary transgressions is that sediment accumulation rates are high and sediment supply actively participates in defining the shoreline trajectory (Helland-Hansen and Martinsen, 1996). Minimum sedimentation rates (not accounting for compaction) for the John Henry Member are between 53.5 and 59 m/Ma based on biostratigraphic dates of the middle Coniacian to late Santonian (Eaton, 1987, 1991; Eaton and Nations, 1991; Allen, 2009). At Left Hand Collet, minimum sedimentation rate for the John Henry Member is 56.2 m/Ma, based on the updated time scale of Gradstein et al. (2012). Shanley and McCabe (1995) report subsidence rates of 35.3 m/Ma, which do account for compaction via backstripping. These rates suggest moderately high sedimentation and accommodation space for the entire John Henry Member, which appears to be conducive to transgressive deposition.

In order to deposit and preserve both the tidal ravinement surface and the transgressive strata below the wave ravinement surface, there must be a high tidal energy and high sediment supply and subsidence rate (Catuneanu, 2006). In order to erode strata of the foreshore and upper shoreface, the shoreline must experience a high energy during transgression and sea level rise must have been gradual (Bruun, 1962; Sanders and Kumar, 1975; Helland-Hansen and Martinsen, 1996). This erosion and cannibalization of underlying shoreface deposits provides sediment and accommodation space for tidal deposits to fill in during relative sea level rise. High rates of sediment supply, deposition, and subsidence protects the transgressive deposits from further erosion during the maximum transgression (Bruun, 1962; Allen and Johnson, 2010). If eustatic sea level rise occurred rapidly, the result would be drowning of the barrier system, little to no transgressive deposition, and a significant landward shift in the shoreline (Sanders and Kumar, 1975; Cattaneo and Steel, 2003).

Global, regional, and local sea level fluctuations are important to understanding controlling factors in marginal marine deposition. Eustatic sea level curves (Haq et al., 1987, 1988; Miller et al., 2005) provide estimates of sea level on the global scale, which can be correlated with regional and local sea level curves to determine whether autogenic or allogenic factors control basin evolution. Figure 21 shows the comparison between eustatic, regional (Kauffman, 1977) and local coastal onlap (this study). There is considerable disagreement between the curves, which is interpreted reflect temporal resolution and autogenic processes. The temporal resolution in the John Henry Member does not currently allow for definitive ties to global or regional sea level curves. However, even if the temporal resolution was well constrained, the sea level curves would not necessarily agree. In addition to the eustatic fluctuations in sea level, rates of accretion and erosion along an individual coastline and its barrier islands are subject to more localized changes in sediment supply and subsidence, coastal morphology, and process changes within a shoreline (Yang et al., 1988; Yoshida et al., 2007). The Texas Gulf Coast is a prime example of these potential variations, as adjacent shorelines can be either progradational, aggradational, or retrogradational

(Morton, 1979). Thus, the marginal marine successions of the John Henry Member are controlled by autogenic processes as well as eustatic sea level rise.

Implications for Hydrocarbon Exploration

The John Henry Member contains impressive accumulations of sandstones along Fifty Mile Mountain over 250 m thick with shoreface parasequences over 30 m thick. While these sandstones may appear to be continuous, tabular bodies, high resolution sequence stratigraphic studies reveal many complexities in the marginal marine strata and stratigraphic architecture along strike and dip that have important implications for hydrocarbon exploration. For example, understanding sandstone body geometries along strike and dip are critical for reservoir characterization and connectivity.

Estimates of facies proportions can provide insight into the dominant processes active in an environment (e.g., wave, tide, or river energy) and improve predictive models for clastic shorelines (Ainsworth et al., 2011). Facies proportions for the John Henry Member at Left Hand Collet are estimated from measured sections averaged throughout and are not decompacted. Tidal facies comprise 48% of the facies at Left Hand Collet, wave-dominated facies comprise 47% and coastal plain deposits account for 5% of the total. This implies a mixed tide and wave-dominated environment with little fluvial influence. However, these percentages do not account for sections with loss to cover, which particularly affects the lower John Henry Member that contains thick shoreface parasequences. Thus, these percentages have a preservation bias, but the approach could be useful on a smaller scale. For example, this method could compare percentages of facies along dip of an R-T cycle, quantifying the landward partitioning of sediment during transgression.

Transgressive deposits have significant internal heterogeneity, which is problematic for correlation and connectivity in reservoirs (Cattaneo and Steel, 2003). However, these heterogeneities may increase the likelihood of stratigraphic trapping (Devine, 1991; Hendricks, 1994). A prominent example of transgressive reservoirs is the Tarbert Formation in the Viking Graben in the North Sea (Marjanac and Steel, 1997). The reservoirs in this field are channelized sandstones in landward-thickening transgressive deposits above a tidal ravinement surface and below a wave ravinement surface, similar to the John Henry Member at Left Hand Collet (Ravnas and Steel, 1998). Thus, transgressive deposits have potential to be significant reservoirs.

Two major sand rich units are observed at Left Hand Collet: wave-dominated shorefaces and tide-dominated back barrier deposits. At the most basinward extents of the John Henry Member at Left Hand Collet, shoreface sandstones stack to thicknesses in excess of 300 m. Individual shoreface packages can be as thick as 50 m thick at the base of the section (A sandstone). However, these shorefaces appear to be separated by thin mudstones deposits and begin pinching out into mudstone rich lagoonal successions as little as 1 km into Left Hand Collet.

The mudstone rich back barrier deposits are sand poor with only laterally discontinuous, likely disconnected sand bodies. Washover fans are typically less than 2 m thick and 200 m wide. The mudstone rich deposits can be as much as 40+ m thick and may prove to be efficient seals. Shoreface pinchouts into lagoonal mudstones represent potential stratigraphic traps.

Sandstone rich back barrier deposits amalgamate to form thick sheets of fine-medium grained sandstones. Reservoir potential is greatest in these facies in R-T cycles 3, 4, and 6, all cases where amalgamated tidal sand bodies lie between two shoreface sand bodies. This geometry results in sandstone packages in excess of 20 m thick. In the landward extents of R-T cycles 3-4 (D-E sandstones), sandstone-rich cycles are bound on either side by mudstones and coals of the Christensen and Rees coal zones. Although heterogeneities abound in transgressive deposits, several trends can be recognized that aide in reservoir characterization studies. The landward thickening of transgressive tidal deposits provides a predictable trend in correlation of this facies. These potential reservoirs include more thick packages of amalgamated tidal sands with good preservation potential during accretionary transgressions. Finally, their relationship with less permeable mudstones and limited lateral extents may prove to be effective seals or stratigraphic traps.

Figure 18 - Plan view Google Earth image of The West Friesian Islands, Netherlands, a barrier island complex along the coast of the North Sea. Barrier islands are roughly 25 km wide by 3 km long and separated by tidal inlets. Tidal inlets migrate laterally with longshore transport and wave and flood-tidal currents deliver sand to the lagoon (Fitzgerald and Penland, 1987). Tidal channels and creeks drain the back barrier platform, which range from 5-30 km wide. Sand is reworked by tidal and longshore currents into dunes and barforms that migrate and form large sheetforms (Sixsmith et al., 2008).

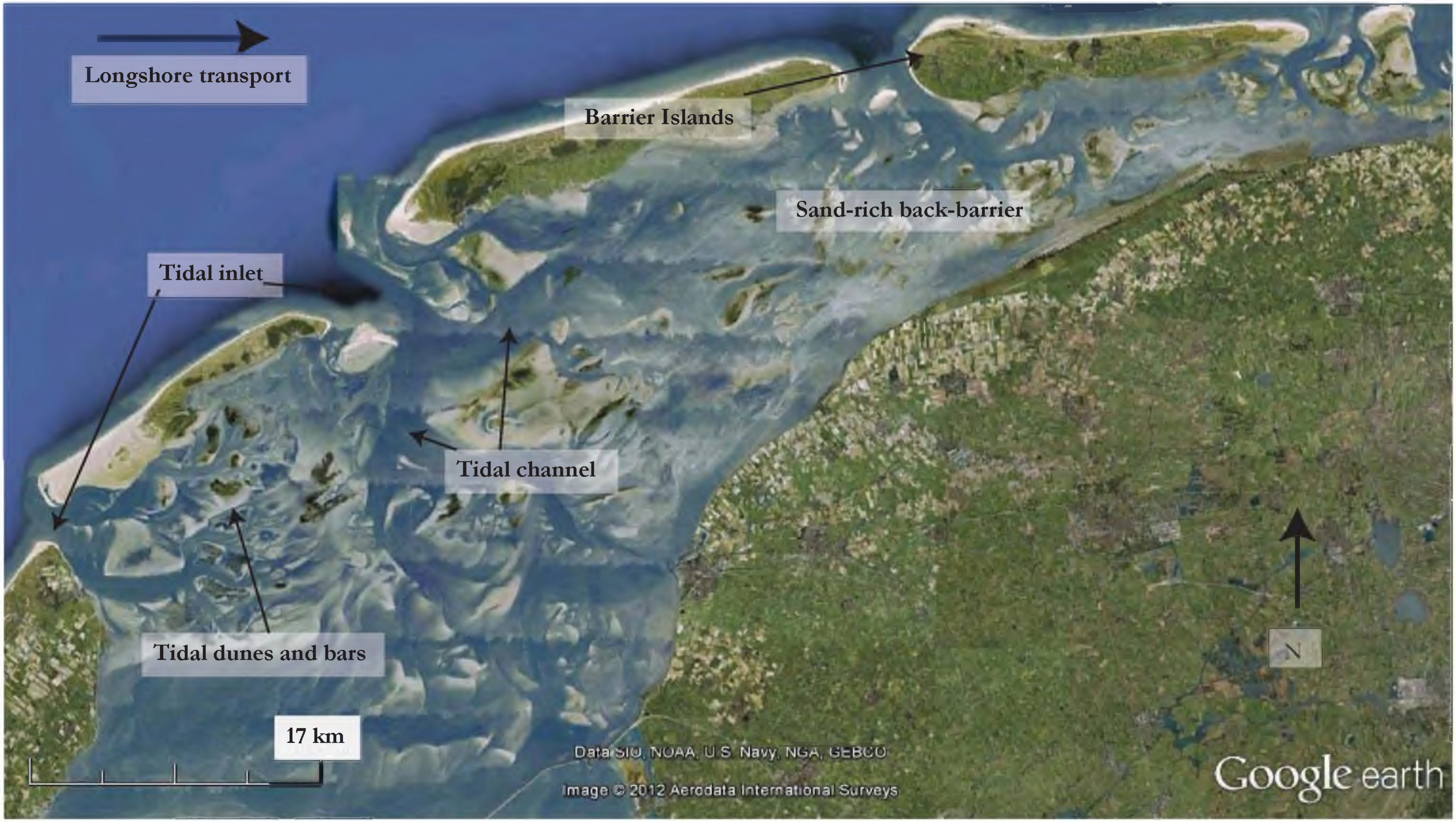
Longshore transport
Barrier Islands
Sand-rich back-barrier
Tidal inlet
Tidal channel
Tidal dunes and bars
17 km
N
Data SIO, NOAA, U.S. Navy, NGA, GEBCO
Image © 2012 Aerodata International Surveys
Google earth

Figure 19 - Plan view Google Earth image of Galveston Island, TX, a wave-dominated, microtidal barrier island. Galveston Island is ~40 km long and less than a km wide at its narrowest. The San Luis pass flood tidal inlet/delta separates Galveston Island to the north and Follets Island to the South. The inlet is ~1.5 km wide at the mouth. Tidal bars form along the edges of flood-tidal channels.


Galveston Bay
Galveston Island
Flood tidal delta
Tidal bars
Longshore transport
N
Accreting bars
Tidal inlet
Christmas Bay
5 km
Data SIO, NOAA, U.S. Navy, NGA, GEBCO
Google earth

Figure 20 - Schematic regional correlation for a given R-T cycle in the upper John Henry Member from Monday Canyon (MC) in the southeast to North Basin Canyon (NBC) to Left Hand Collet (LHC) in the northwest (see inset). The cross section shows regressive parasequences with proximal lower and upper shoreface in Monday Canyon with occasional channelization into upper shoreface. At Left Hand Collet, tidal erosion scours down into proximal lower/middle shoreface and is overlain by sand-rich tidal facies (facies 3.1 -3.3). The result is thicker transgressive deposits to the northwest and a thicker regressive interval to the southeast. A wave ravinement surface separates the R-T cycle below from the base of the overlying, younger R-T cycle. Inset: Gray star – Left Hand Collet; Blue star – North Basin Canyon; Purple star – Monday Canyon

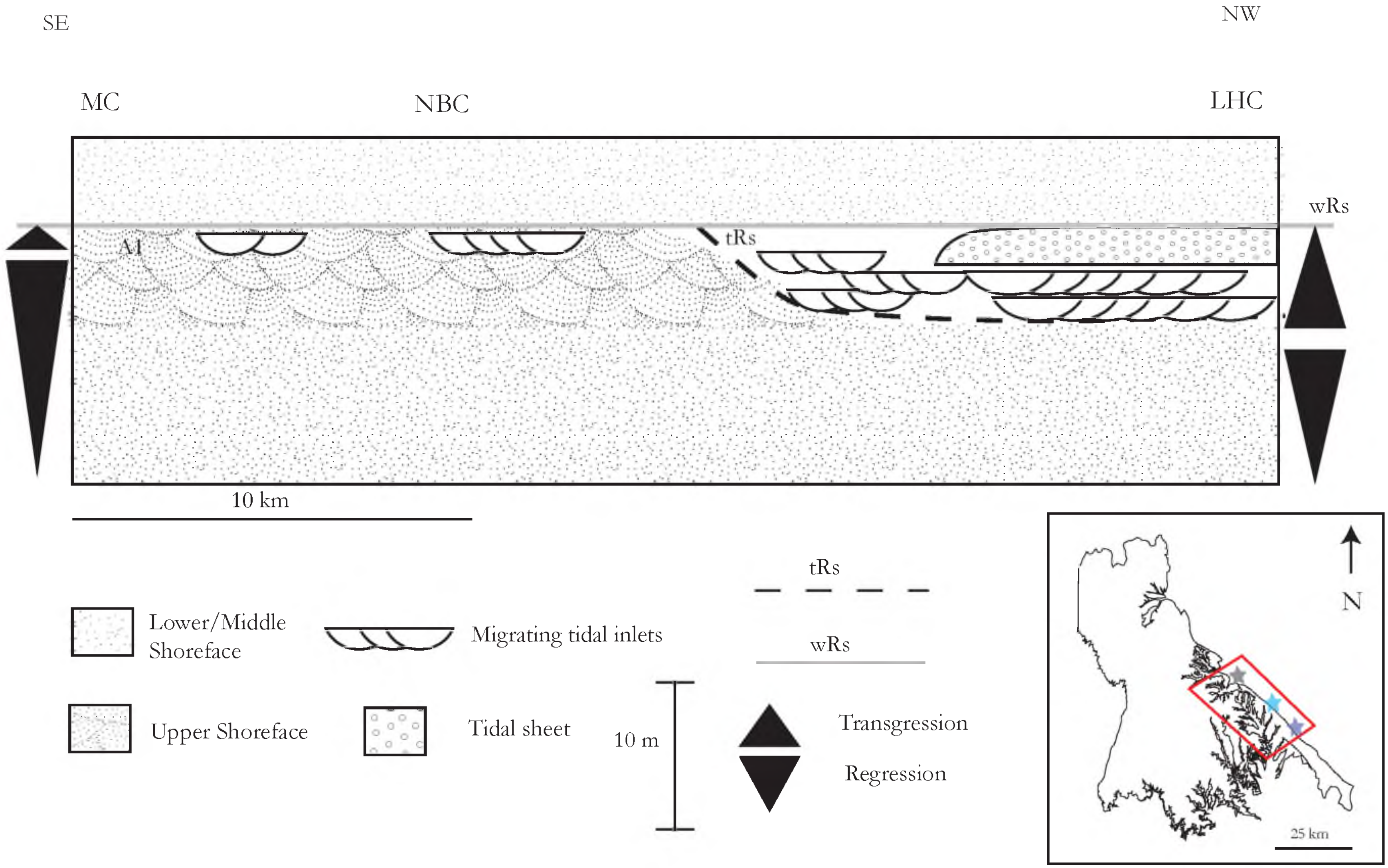
SE
NW
MC
NBC
LHC
A1
tRs
wRs
10 km
tRs
wRs
Lower/Middle Shoreface
Migrating tidal inlets
Upper Shoreface
Tidal sheet
10 m
Transgression
Regression
N
25 km

Figure 21 - Sea level curves for the Coniacian to Santonian. Eustatic sea level curves (Miller et al. (2005) and Haq et al. (1987)) provide estimates for global sea level changes. The relative sea level curve by Kauffman (1977) documents transgressive-regressive cycles across the Western Interior Seaway. The relative sea level curve at Left Hand Collet is based on coastal onlap and shows three major trends - sea level fall and progradation through R-T cycles 0-2; retrogradational stacking of R -T cycles 2-4; and slight progradation between cycles 4-5 before the final transgression at R-T 6. Open circles note shoreface pinchout locations. Ages based on timescale of Gradstein et al. (2012).

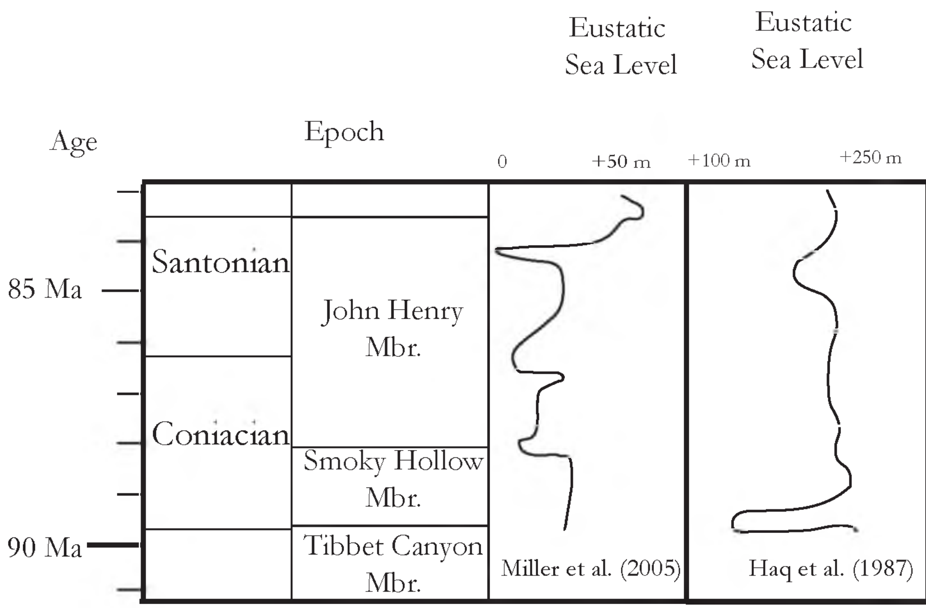
Eustatic
Sea Level
Eustatic
Sea Level
Age
Epoch
0
+50 m
+100 m
+250 m
85 Ma
90 Ma
Santonian
Coniacian
John Henry
Mbr.
Smoky Hollow
Mbr.
Tibbet Canyon
Mbr.
Miller et al. (2005)
Haq et al. (1987)

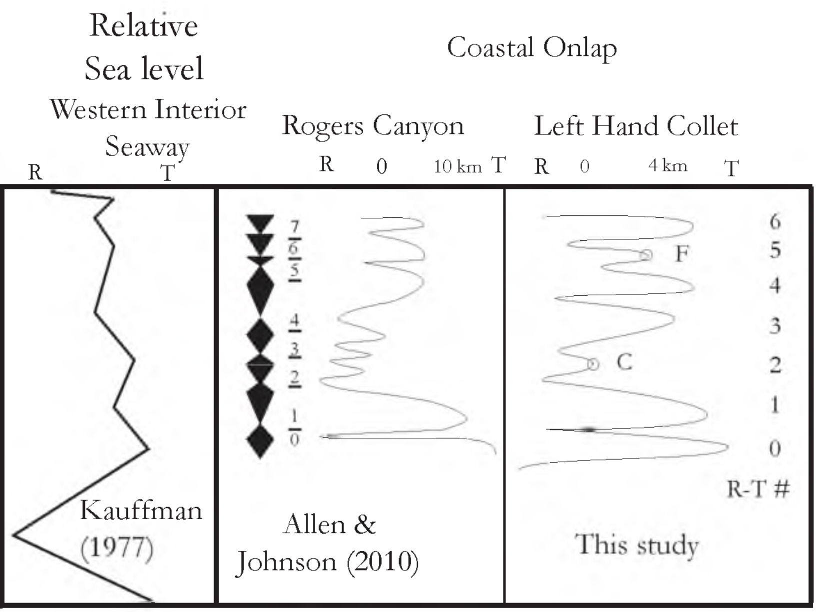
Relative
Sea level
Western Interior
Seaway
R
T
Coastal Onlap
Rogers Canyon
R
0
10 km
T
Left Hand Collet
R
0
4 km
T
7
6
5
4
3
2
1
0
6
5
4
3
2
1
0
F
C
R-T #
Kauffman
(1977)
Allen &
Johnson (2010)
This study

Figure 22 - Isopach map of net coal thickness (in feet) for the John Henry Member in Kaiparowits Plateau (Hettinger, 2000). The isopach map shows maximum thickness of coals landward of the marginal marine strata at Left Hand Collet and Rogers Canyon. These coals were likely deposited in raised mires (McCabe and Shanley, 1992) that had an important influence on the depositional system. Coal mires prohibited the movement of fluvial systems to the marginal marine regions of Left Hand Collet and Rogers Canyon. These mires may have truncated the rivers or deflected them to the northeast, where rates of accommodation appear to be greater (Peterson, 1969a). A delta to the northeast would supply sediment to the coastline via longshore drift. Solid arrows show direction of sediment transport based on paleocurrent measurements (Gooley, 2010; Gallin, 2010; Allen, 2009; Pettinga, 2013), while the dashed arrow represents predicted direction where measurements are lacking in the middle-upper John Henry Member.

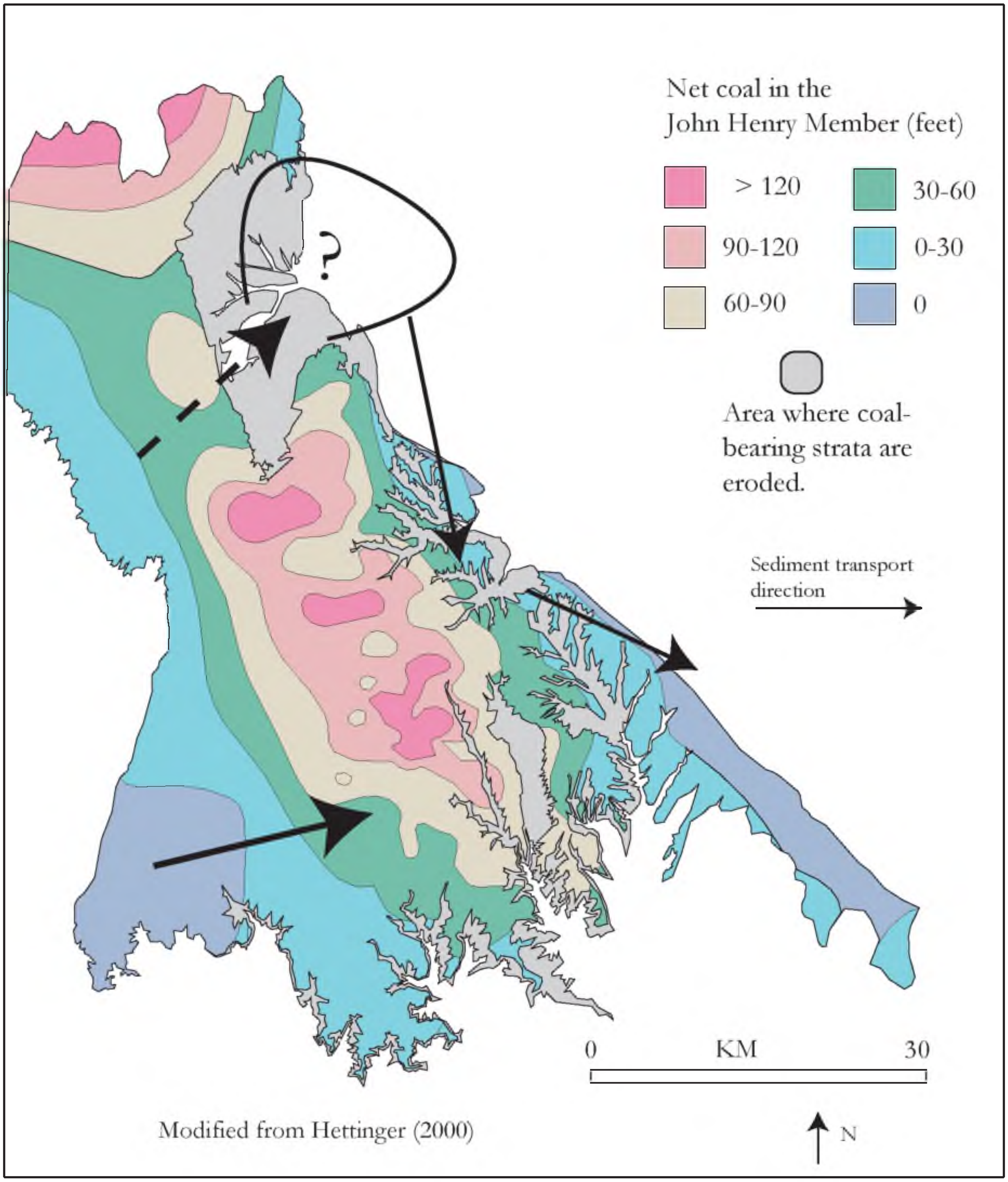
Net coal in the
John Henry Member (feet)
> 120
90-120
60-90
30-60
0-30
0
Area where coal-bearing strata are eroded.
?
Sediment transport direction
0
KM
30
N
Modified from Hettinger (2000)

CONCLUSIONS

The John Henry Member at Left Hand Collet is composed of four main facies associations: wave-dominated shorefaces, coastal plain facies, sandstone rich tide-dominated deposits, and low energy lagoonal facies. Wave-dominated and coastal plain facies reflect deposition of a regressive shoreface, whereas tide-dominated and lagoonal facies reflect deposition in a barrier island setting during transgression. The overall geometry of the facies can be described via Regressive-Transgressive cycles. Cycles are bound at the top and bottom by a maximum transgressive surface (wave ravinement or flooding surface), with the onset of transgression marked by a tidal ravinement surface. Regressive intervals thin landward onto a wave ravinement surface at the base and tidal ravinement at the top. Tidal deposits thicken landward and are truncated at the top by a wave ravinement surface marking the beginning of a younger R-T cycle.

Sandstone-dominated, landward thickening successions of tidal inlets, tidal bars, and tidal sheets form significant facies that stack to thicknesses over 20 m. These facies have a highly erosive base that scour into proximal lower to middle shorefaces. Erosion of the underlying shoreface occurs at the onset of transgression with migration of a mesotidal barrier island system with high sediment supply from efficient longshore drift. This setting is analogous to the modern day Friesian Islands, a sand-rich mesotidal barrier island complex in the North Sea. Mudstone-dominated lagoons are also prevalent in the marginal marine John Henry Member and represent a microtidal, wave-dominated barrier island system comparable to the modern day Galveston Island. The overall retrogradational stacking patterns of the shorefaces at Left Hand Collet suggest that rising relative sea level led to the deposition of tidal facies. Tidal resonance increases due to the increased shelf width and transgression across the landward-shallowing shelf. Tidal prism increases in localized embayments with barrier islands and tidal inlets, consistent with observations at Left Hand Collet.

Regional correlations suggest three separate influences on marginal marine deposition in the John Henry Member: waves, tides, and rivers. Wave-dominated shorefaces develop basinward of raised coal mires, which prohibit significant fluvial influx to the shoreface. Highly tidally-influenced shorelines with effective longshore currents occur in the central region of the shoreline, where southward migrating tidal channels erode as far down as the lower shoreface. To the southeast at Rogers Canyon, shorefaces in the upper John Henry Member contain less ravinement than Left Hand Collet, suggesting more localized erosion to the northwest, possibly due to its proximity to the sediment source. Sediment is likely being shed from a delta to the north of Left Hand Collet, as fluvial systems are deflected or truncated by thick coal mires landward of the Fifty Mile Mountain shorelines.

Shoreline trajectory is an important controlling factor that leads to preservation of transgressive deposits. Accretionary shoreline trajectories with a high sediment supply and subsidence rates allow for the deposition of transgressive deposits and their protection from transgressive erosion. Tidal ravinement at the onset of transgression requires high basinal energy, possibly due to increased tidal prism along an embayed coast.

While there are significant inherent heterogeneities, tide-dominated transgressive deposits are known to form prolific reservoirs. Landward thickening amalgamations of tidal channels and sheets could form significant transgressive reservoirs. Mudstone dominated barrier island successions encapsulate shoreface pinchouts and tidal sandstones, which may prove to be effective seals or stratigraphic traps.

APPENDIX A

GEOLOGIC ROAD GUIDE TO LEFT HAND COLLET CANYON

Turn off Highway 12 onto Hole-in-the-Rock road. Zero odometers.

14 mi - turn right/west onto Collet Top road towards Left Hand Collet Canyon.

16.4 mi – The turnoff to the right leads to dinosaur tracks in the Entrada sandstone. Stay on the main road to the left. Drive through the Dakota Formation into the blue shaley slopes of the Tropic Formation.

17.6 mi – Stop at the mouth of canyon for overview of previous work on the John Henry Member at Left Hand Collet Canyon.

19.8 mi – Pull off on side of road to view the Tibbet Canyon Member and possible sequence boundary. Overlying the sequence boundary is another fluvial incision into the Smoky Hollow Member.

20.4 mi – Two thick parasequences within the A sandstone, with fluvial incision at the top of the second parasequence

21.0 mi – Park along the side of the road. This stop begins at the top of the A interval. At road level, there are several meters of inclined heterolithic strata with mud draping and trace fossils including *Thalassinoides* and *Rosselia*. This is interpreted to represent a tidal bar.

At the top of this succession, there is a gravel lag overlain by interbedded mudstones and sandstones with hummocky cross-stratification. This surface is interpreted to be a transgressive lag. This coarsens upward into ~30 m fine-grained sandstone with abundant hummocky-swaley cross-stratification indicative of lower shoreface in the B sandstone. The shoreface is capped by a ravinement surface and 10 m of inclined heterolithic strata.

Head into Willard Canyon to examine the Christensen coal zone (the C lagoonal succession). Paleobasinward to the northeast, this interval contains multiple shoreface parasequences that pinchout into mudstones and coal. Thin, laterally discontinuous siltstones-sandstones with brackish fauna and trace fossils are scattered throughout the mudstones. These are interpreted as washover fans. There are tidally-influenced channels at the top of the mudstone succession, with large oyster lags adjacent to channels.

Head back to the cars and continue along Collet Top road, the road will turn to the left. The road climbs through the Christensen coal zone. The first sandstone along the road is the D shoreface.

22.4 mi – The D sandstone here contains swaley cross-stratification with erosion at the top. The tidal ravinement surface marks the onset of transgressive portion of the R-T cycle. This ravinement surface is overlain by sandstones with south-directed planar-tabular laminations. This is interpreted to represent migration of a tidal inlet with longshore currents. Continue along the road, where the tidal successions are exposed along the road. These sandstones contain bi-directional current indicators and slight mud-draping. Continue up the road, where the section transitions to inclined heterolithic strata, interpreted as a tidal bar adjacent to inlet channels. At the top of the IHS-section, there is a firmground lag represented by *Gatrochaenolites* borings. This is a wave-ravinement surface marking the maximum transgression and beginning of the regressive portion of the R-T cycle. The sandstone above is the E distal to proximal lower shoreface.

Continue up the road. There are channelized sandstones within the Rees coal zone, landward of the F shoreface pinchout.

23.6 mi – Pull off on side of the road and hike up shaley slope to thick sandstone succession of the G sandstone. The base of the interval contains bi-directional current indicators and some clay rip-ups, with abundant scour surfaces and channelization. This represents tidal inlet fill deposits. Above this lies a massive sandstone sheet with tidal indicators, but lacking internal channelization. The G interval is overlain by the Alvey coal zone.

23.9 mi – The road climbs steeply through the Alvey coal zone into the Drip Tank Member. Continue up the road to the top of the plateau and turn-around where possible.

Two options from here to get back to Escalante - Head back down the canyon towards Hole-in-the-Rock road; or continue northwest up to Smoky Mountain Road and to the east down Alvey Wash.

APPENDIX B

MEASURED STRATIGRAPHIC SECTIONS

Appendix B contains eight detailed measured sections from Left Hand Collet Canyon. A legend of symbols is provided. See Figure 2 for a detailed map of sections at Left Hand Collet Canyon.

Legend of stratigraphic symbols

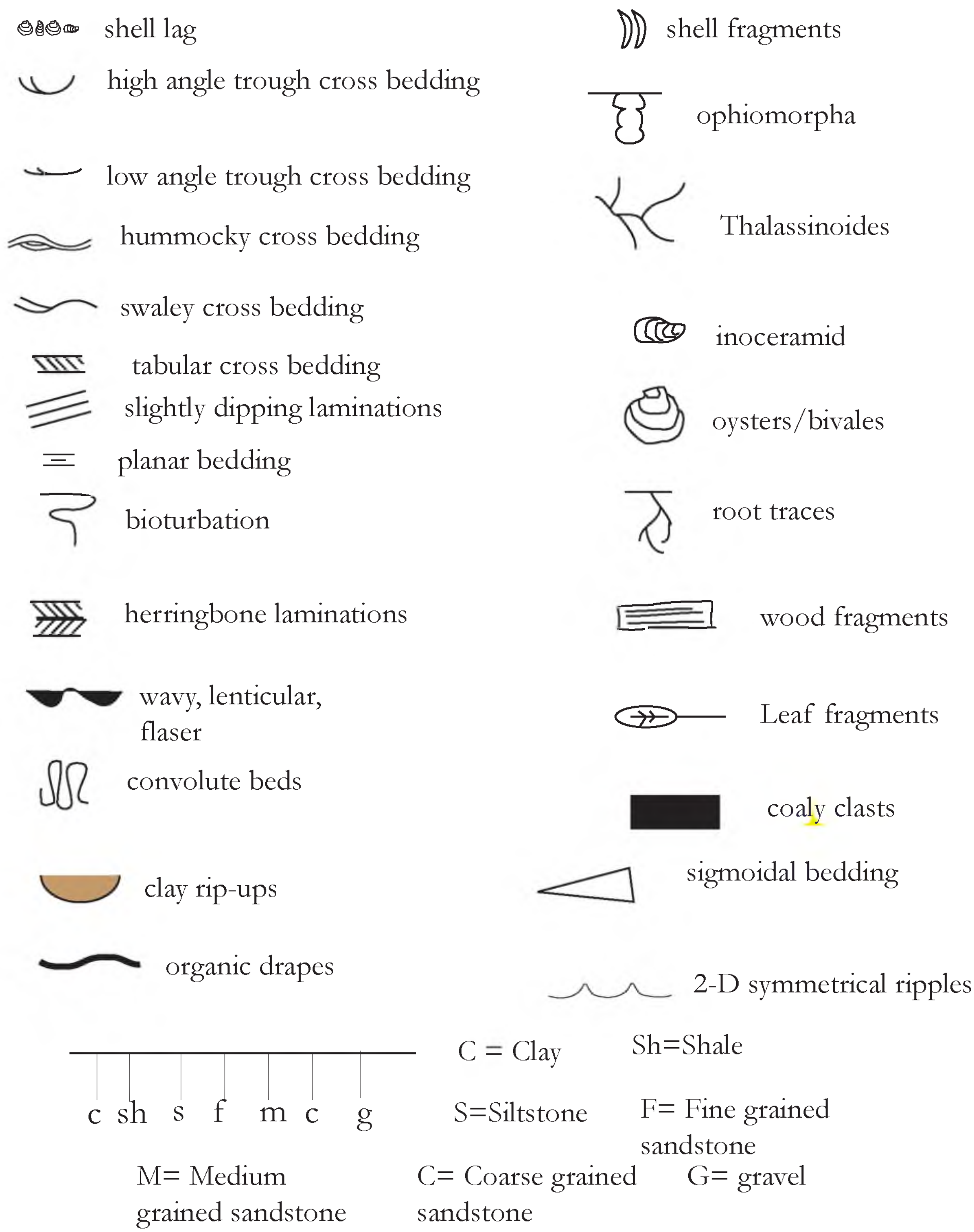

LHC MS 001

Measured section 001 starts in the Tibbet Canyon Member and ends at the top of the G shoreface in the John Henry Member.

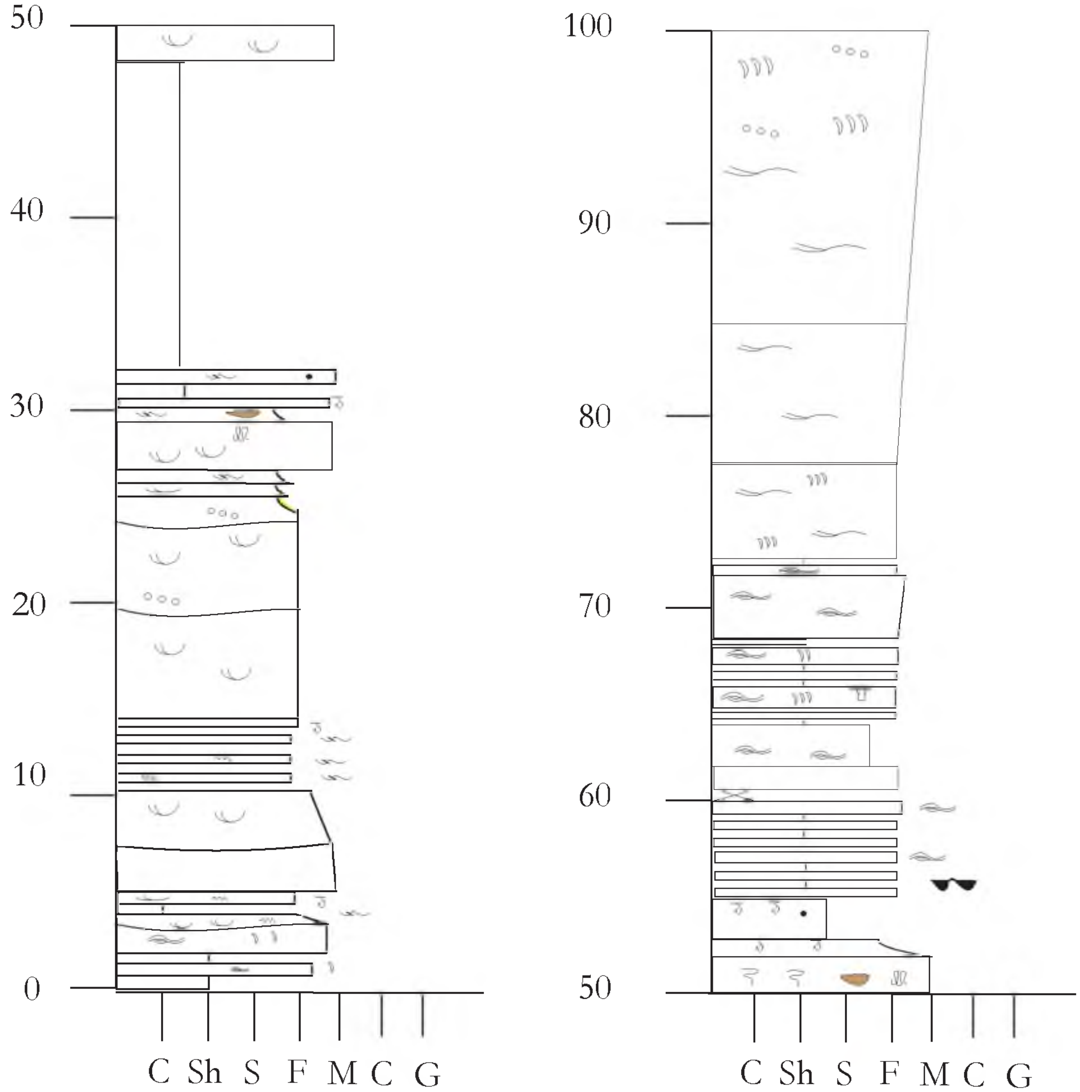
50
40
30
20
10
0
C Sh S F M C G
100
90
80
70
60
50
C Sh S F M C G

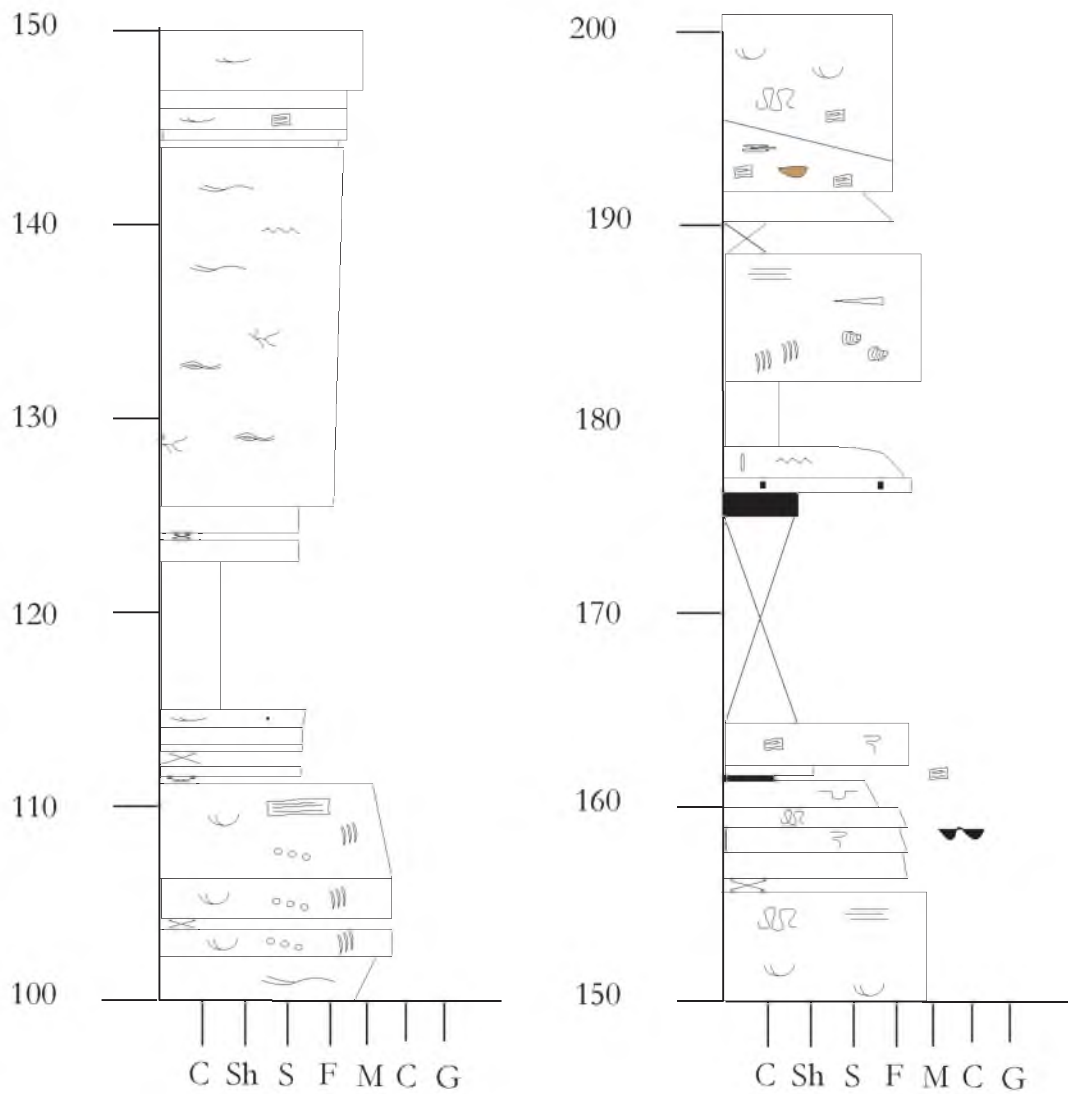
150
140
130
120
110
100
C Sh S F M C G
200
190
180
170
160
150
C Sh S F M C G

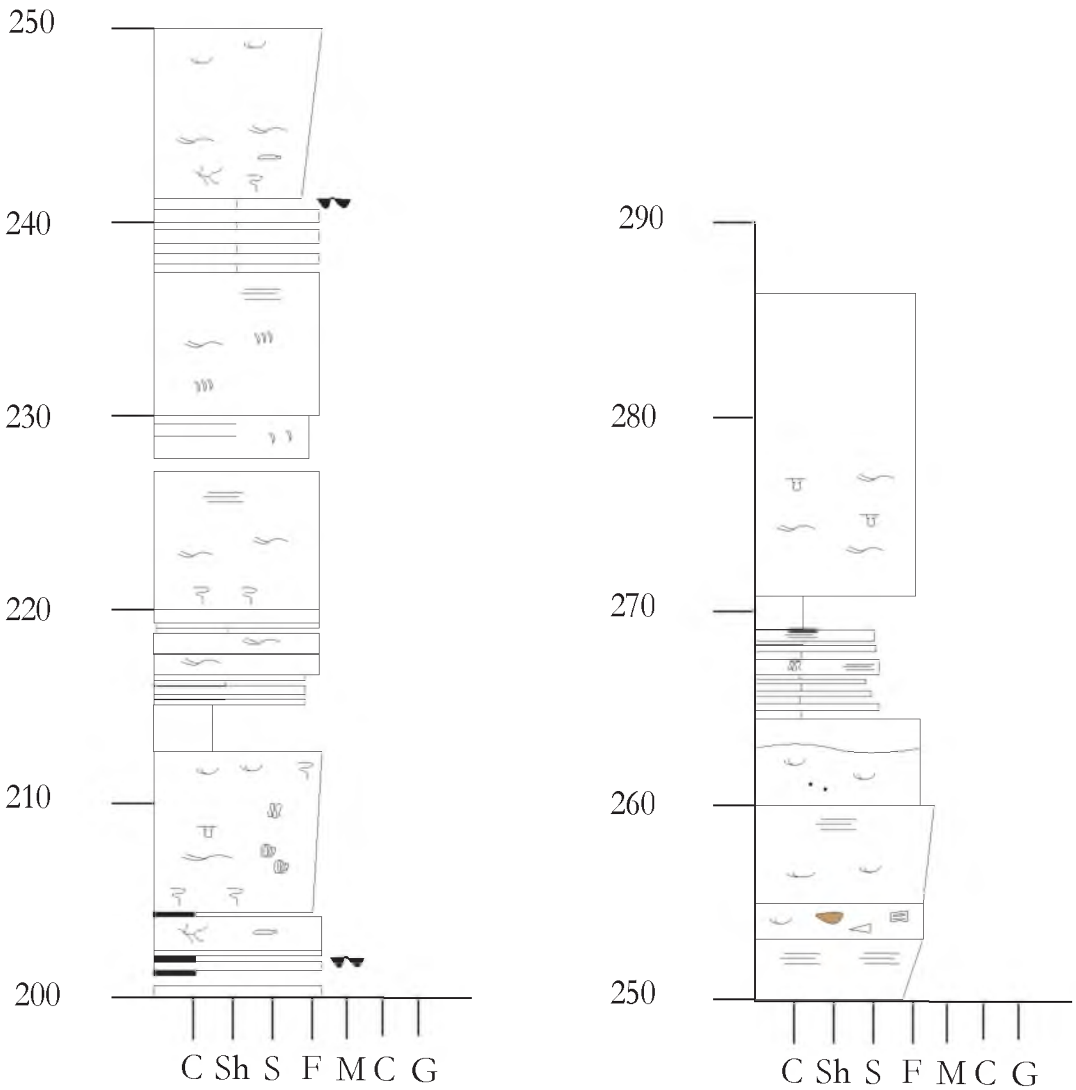
250
240
230
220
210
200
C Sh S F M C G
290
280
270
260
250
C Sh S F M C G

LHC MS 002

Measured section 002 starts in the Smoky Hollow Member and ends at the top of the G shoreface in the John Henry Member.

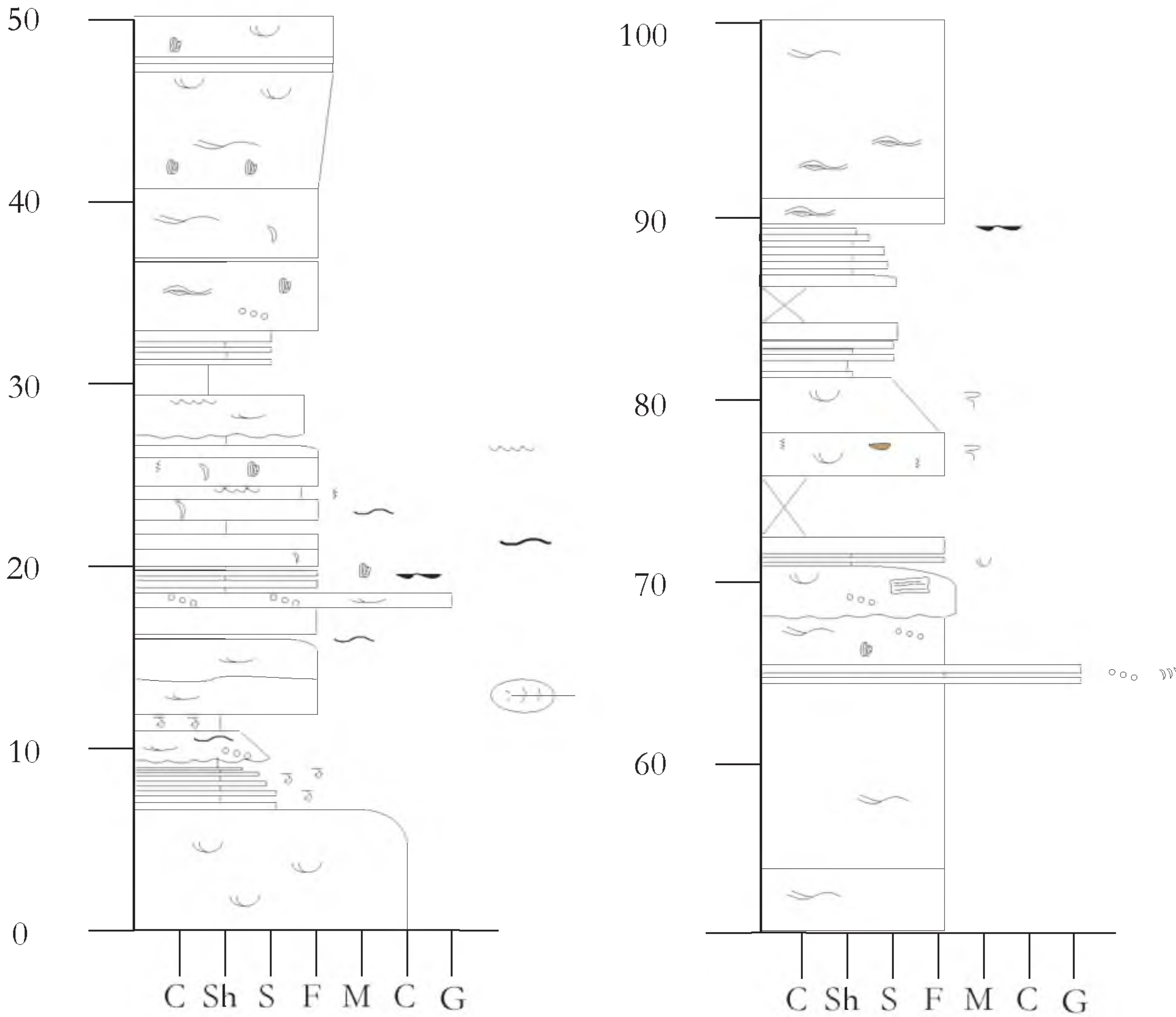
50
40
30
20
10
0
C Sh S F M C G
100
90
80
70
60
C Sh S F M C G

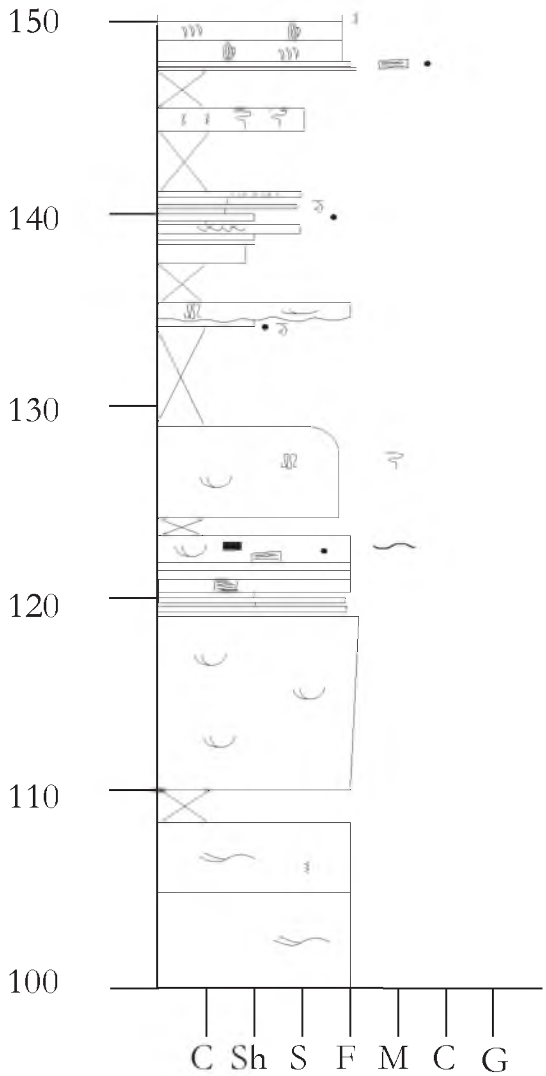
150
140
130
120
110
100
C Sh S F M C G

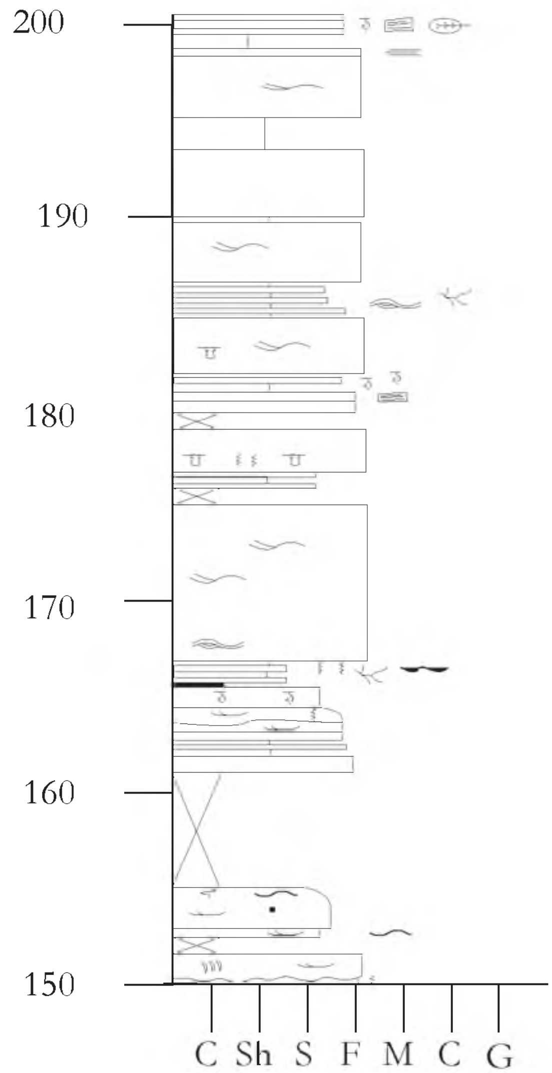
200
190
180
170
160
150
C Sh S F M C G

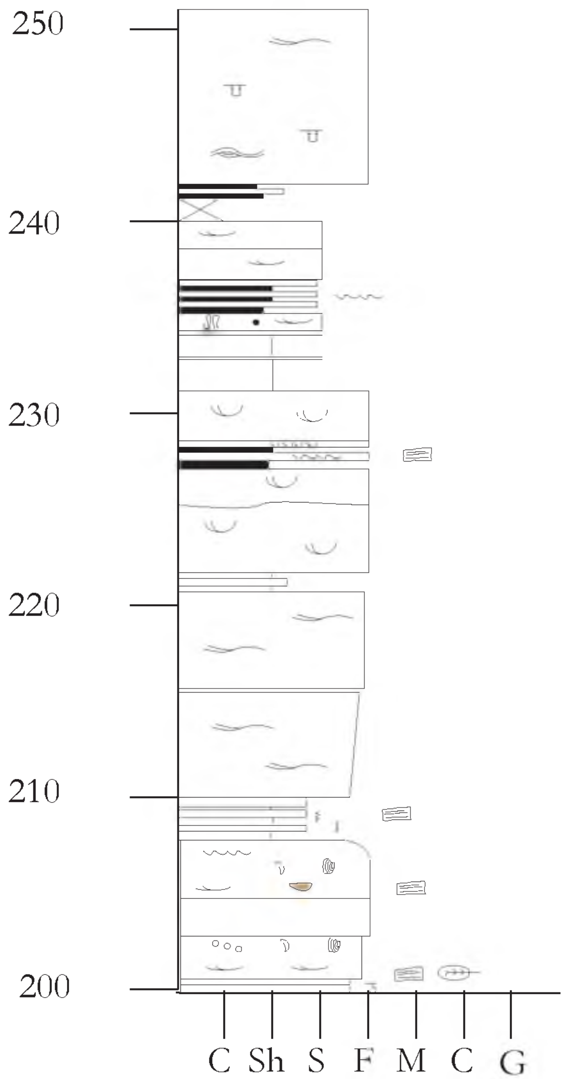
250
240
230
220
210
200
C Sh S F M C G

LHC MS 003

Measured section 003 starts in the Smoky Hollow Member and ends at the top of the G shoreface in the John Henry Member.

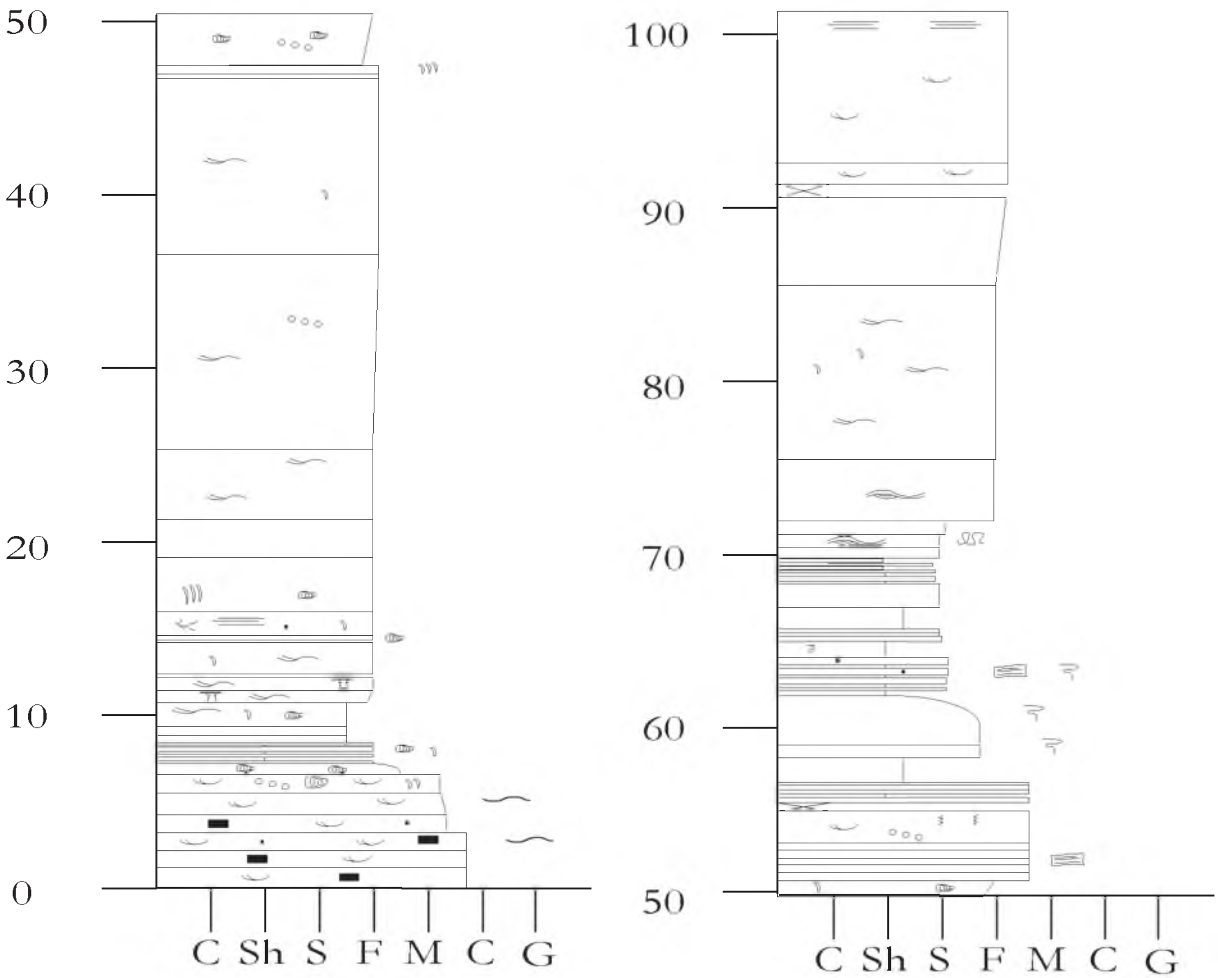
50
40
30
20
10
0
C Sh S F M C G
100
90
80
70
60
50
C Sh S F M C G

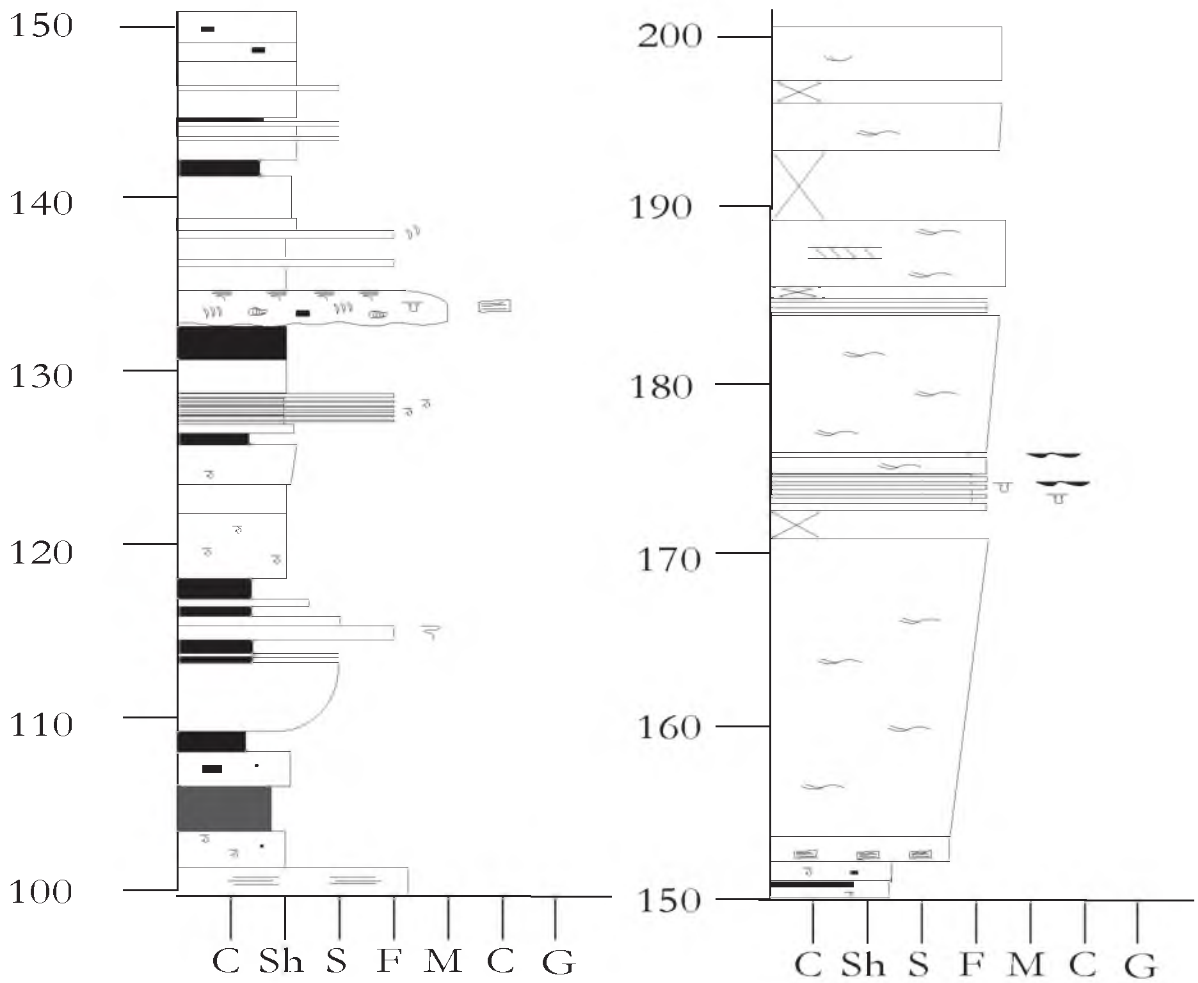
150
140
130
120
110
100
C Sh S F M C G
200
190
180
170
160
150
C Sh S F M C G

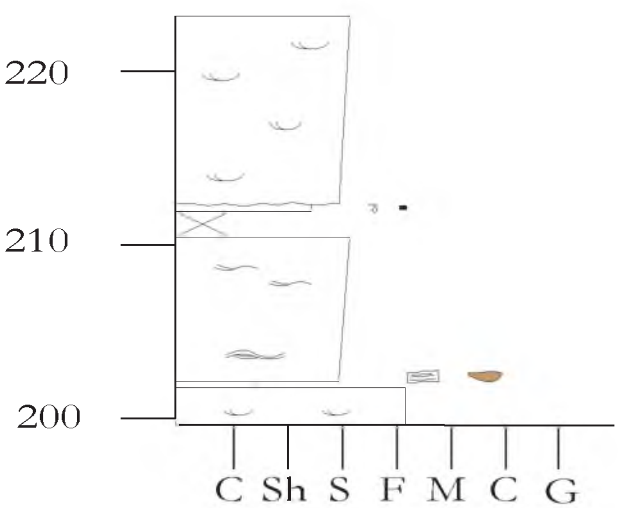
220
210
200
C Sh S F M C G

LHC MS 004

Measured section 004 starts at the top of the A sandstone of the John Henry Member and ends at the top of the G shoreface of the John Henry Member.

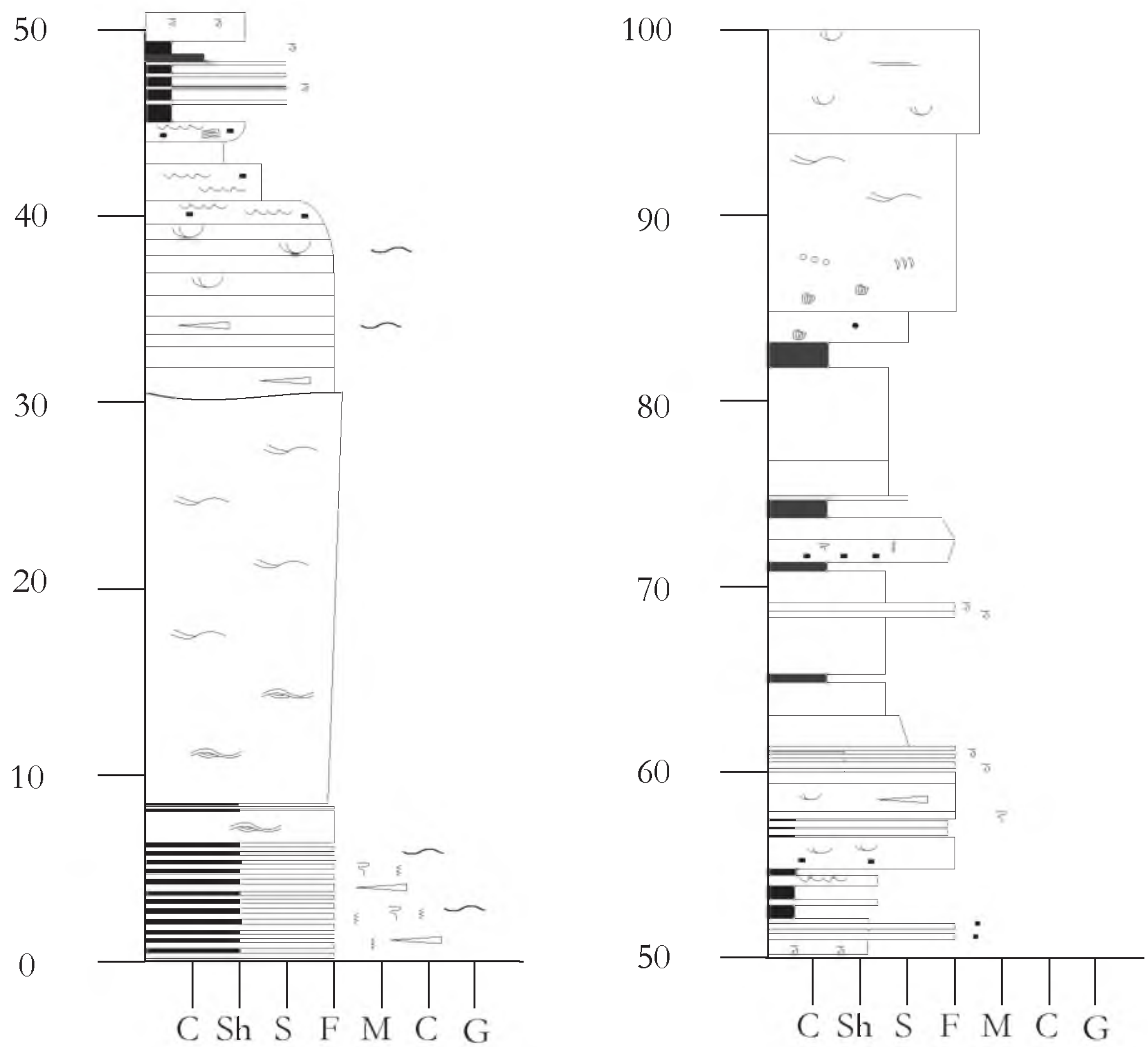

50
40
30
20
10
0
C Sh S F M C G
100
90
80
70
60
50
C Sh S F M C G

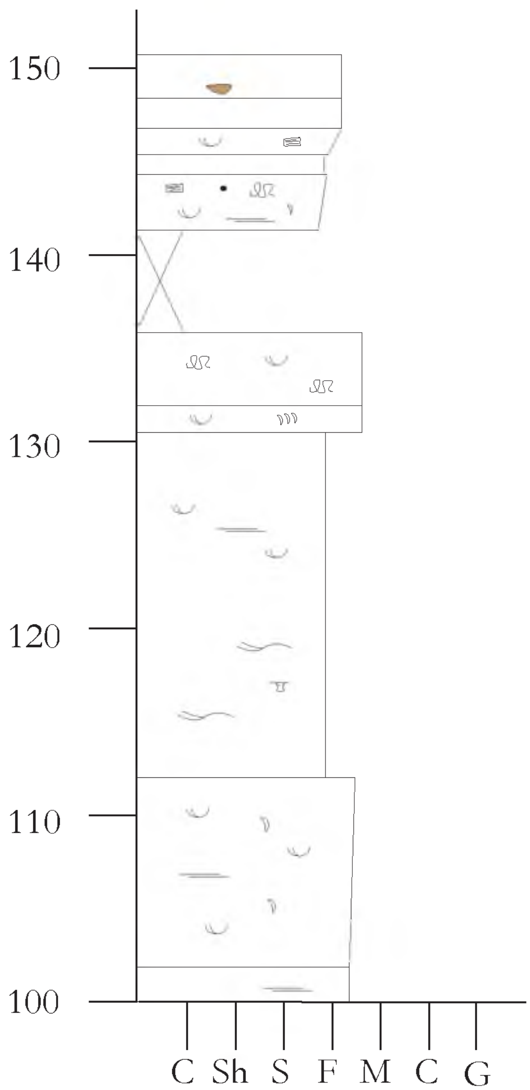
150
140
130
120
110
100
C Sh S F M C G

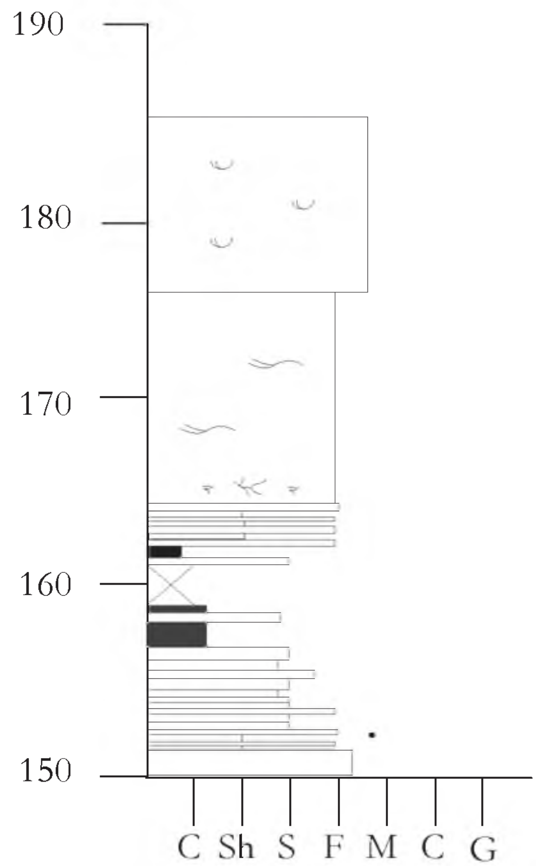
190
180
170
160
150
C Sh S F M C G

LHC MS 005

Measured section 005 starts at the top of the B sandstone of the John Henry Member and ends at the top of the G shoreface of the John Henry Member.

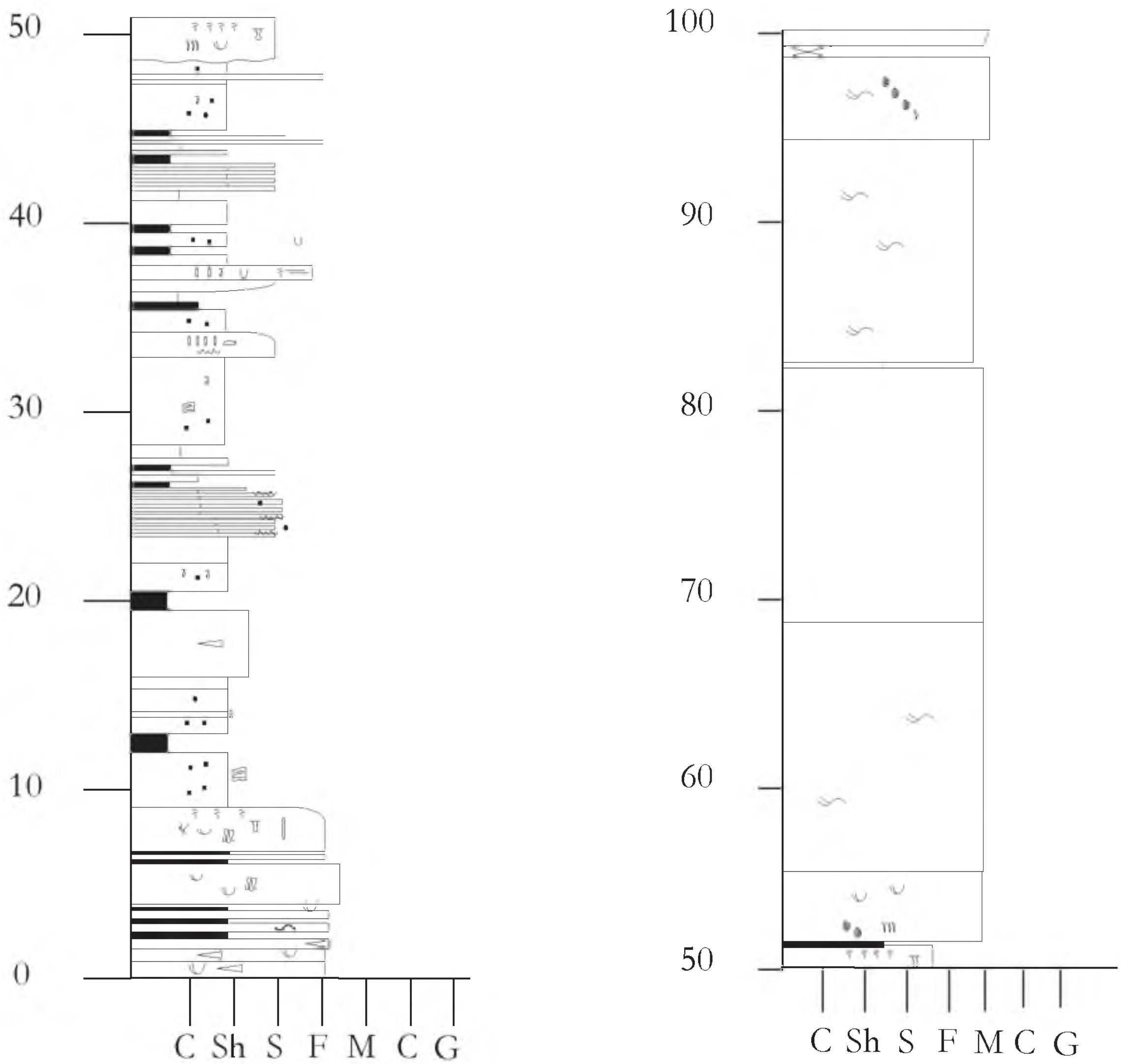
50
40
30
20
10
0
C Sh S F M C G
100
90
80
70
60
50
C Sh S F M C G

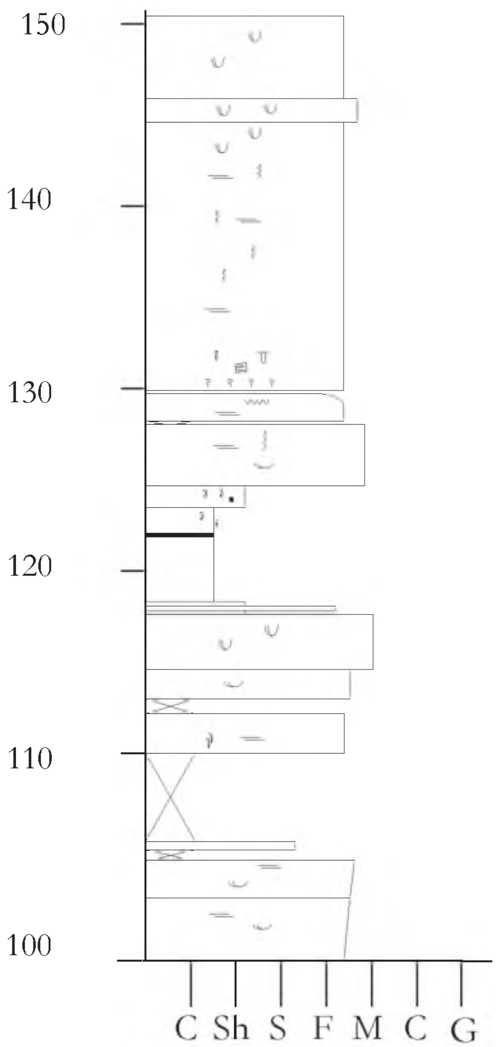

150
140
130
120
110
100
C Sh S F M C G

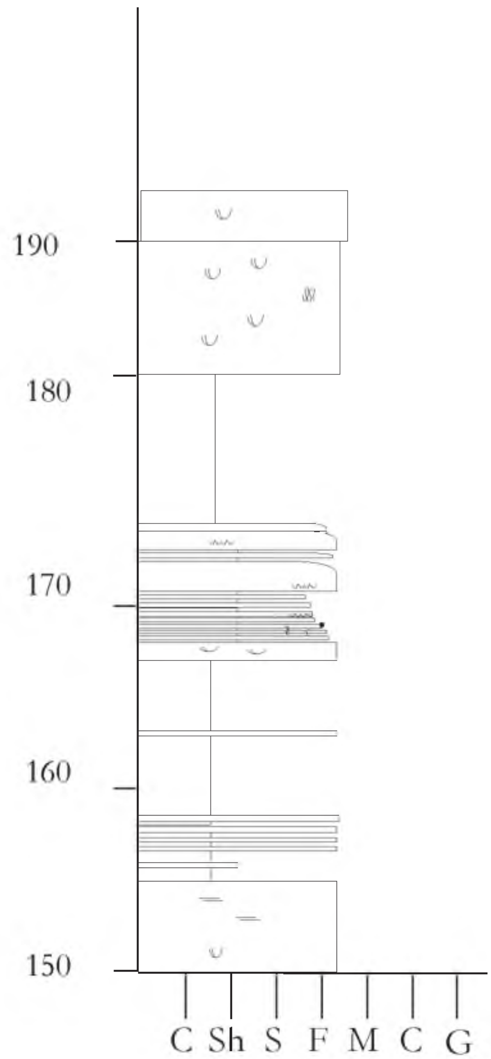

190
180
170
160
150
C Sh S F M C G

LHC MS 006

Measured section 005 starts at the base of the D sandstone of the John Henry Member and ends at the top of the G shoreface of the John Henry Member.

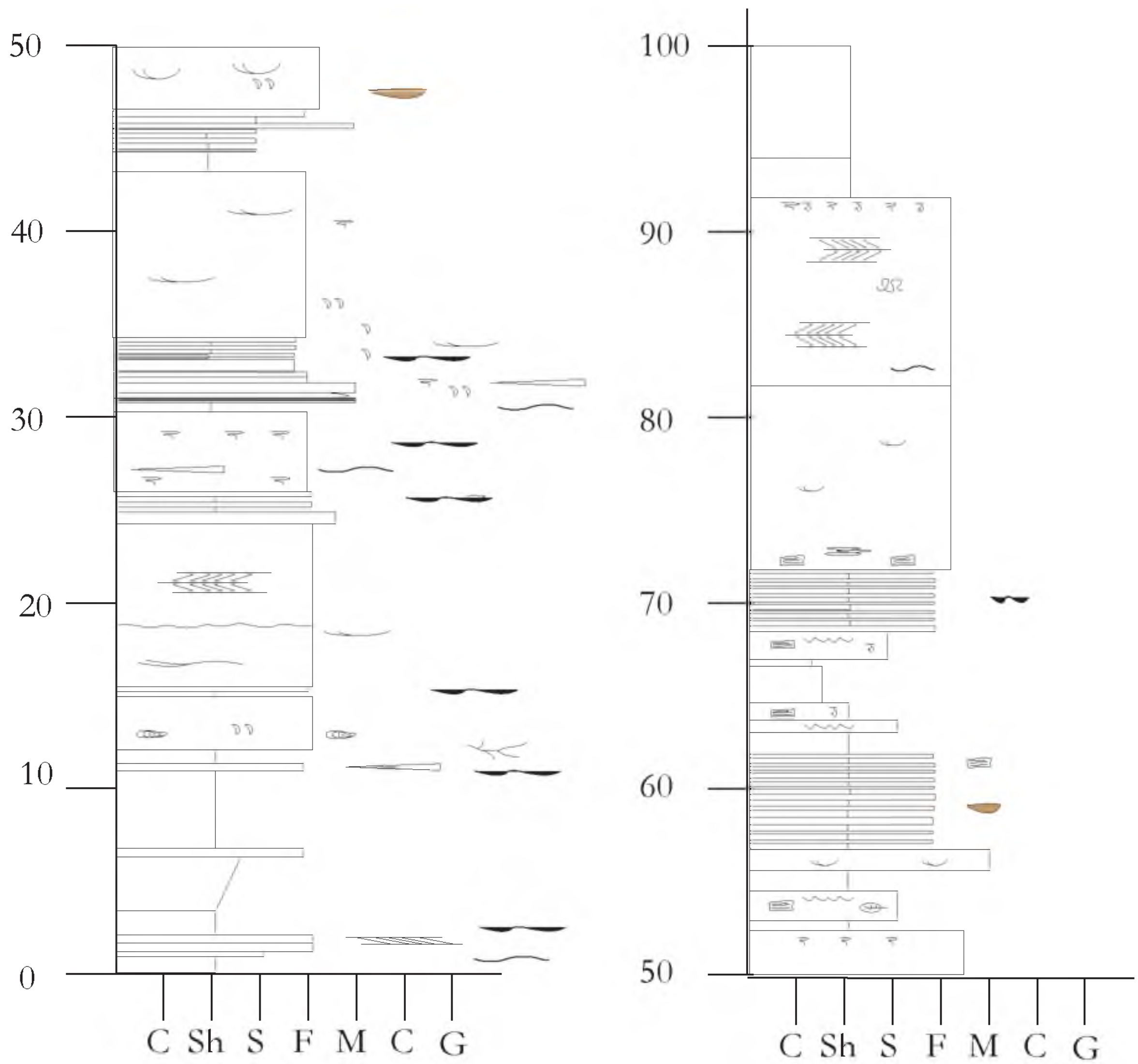
50
40
30
20
10
0
C Sh S F M C G
100
90
80
70
60
50
C Sh S F M C G

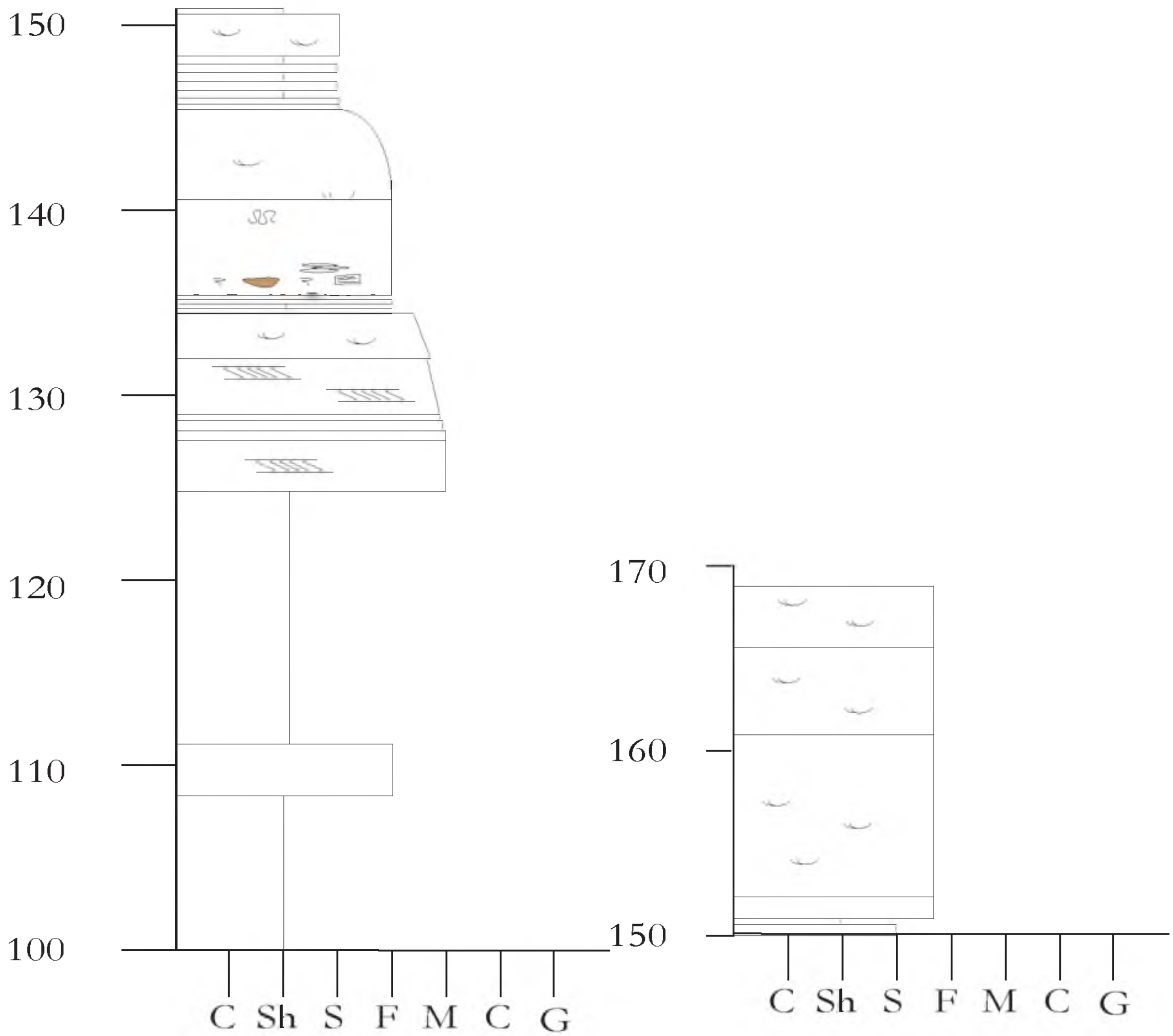
150
140
130
120
110
100
C Sh S F M C G
170
160
150
C Sh S F M C G

LHC MS 007

Measured section 005 starts at the base of the B sandstone of the John Henry Member and ends at the top of the G shoreface of the John Henry Member.

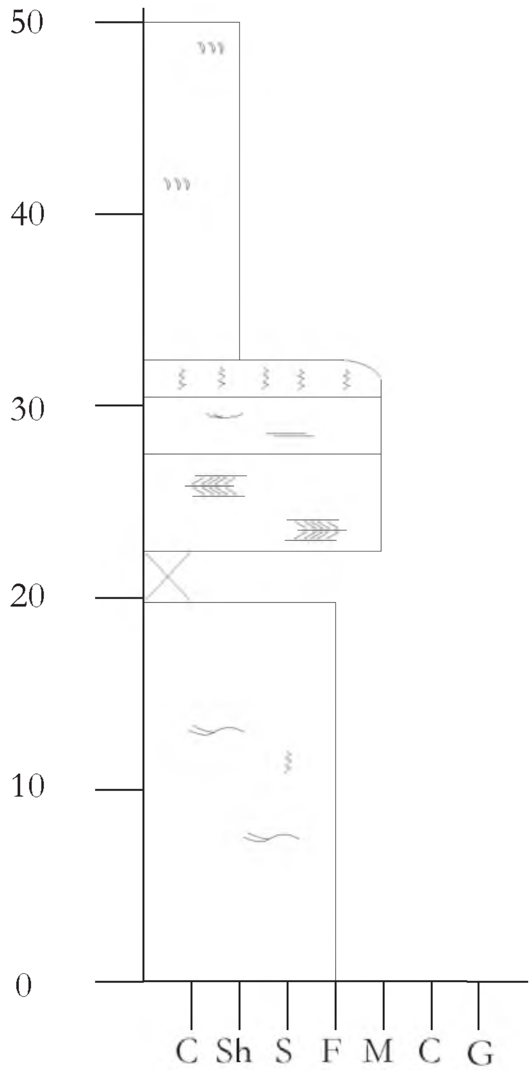
50
40
30
20
10
0
C Sh S F M C G

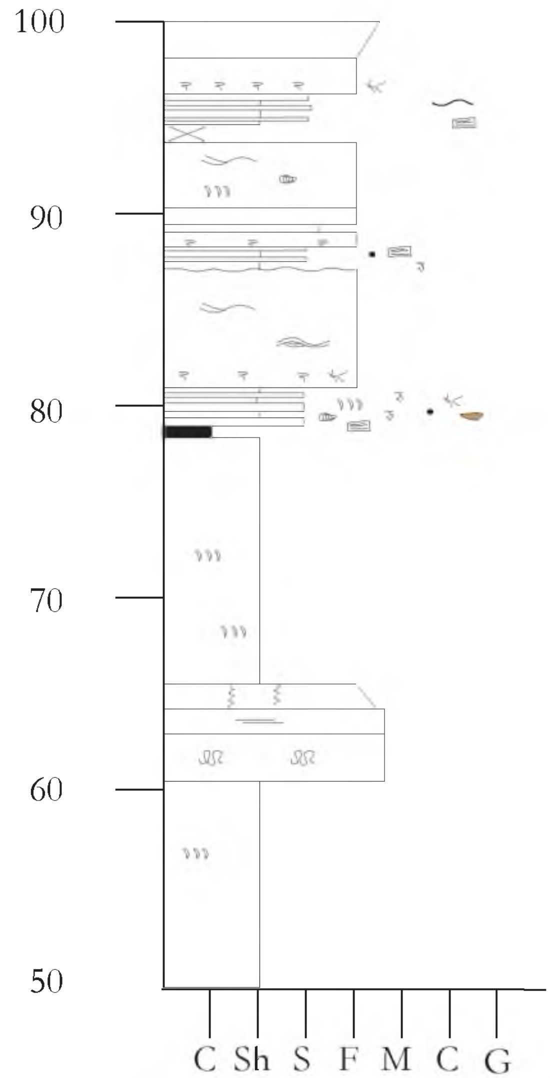
100
90
80
70
60
50
C Sh S F M C G

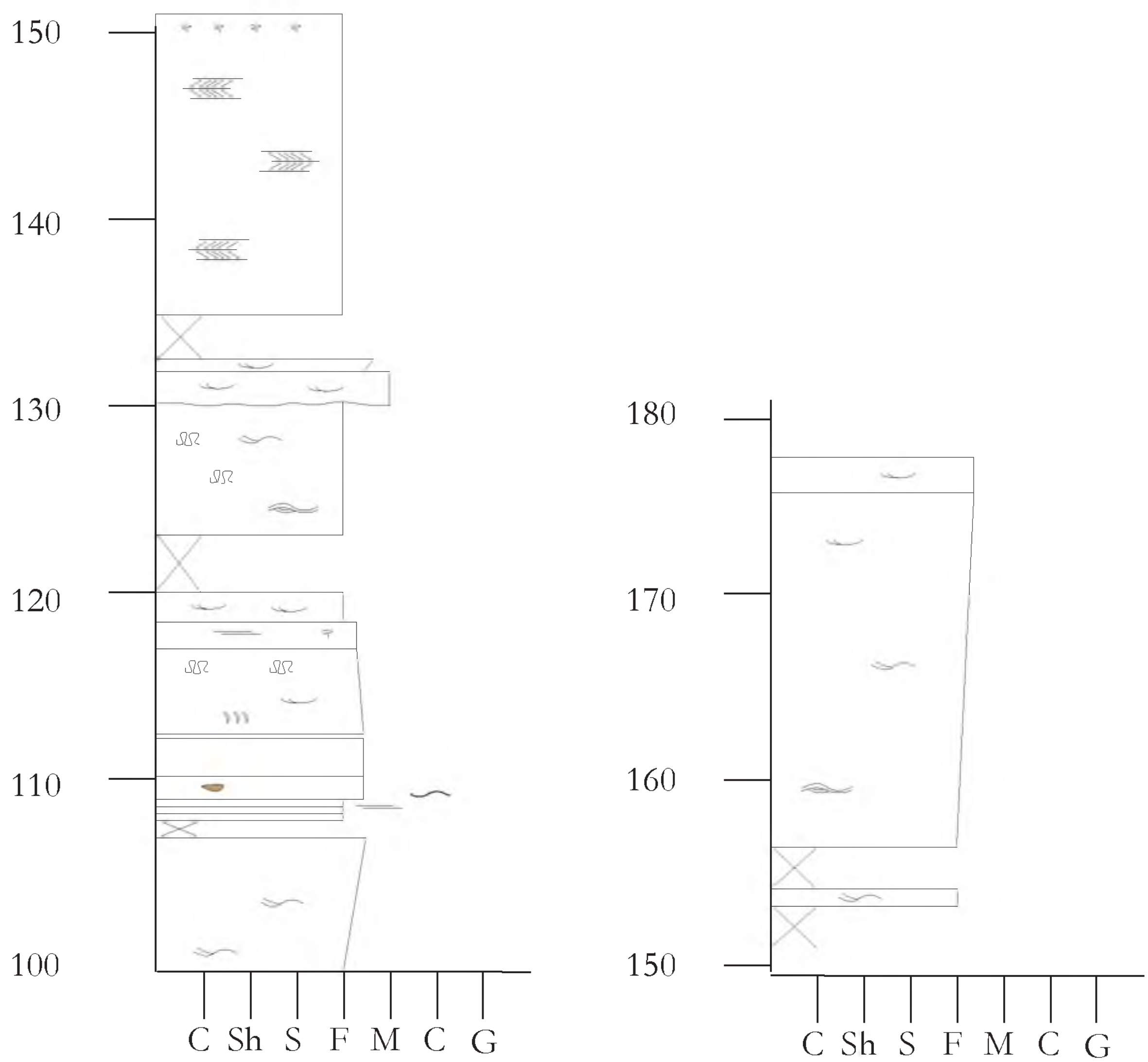
150
140
130
120
110
100
C Sh S F M C G
180
170
160
150
C Sh S F M C G

LHC MS 008

Measured section 005 starts at the base of the D sandstone of the John Henry Member and ends at the top of the G shoreface of the John Henry Member.

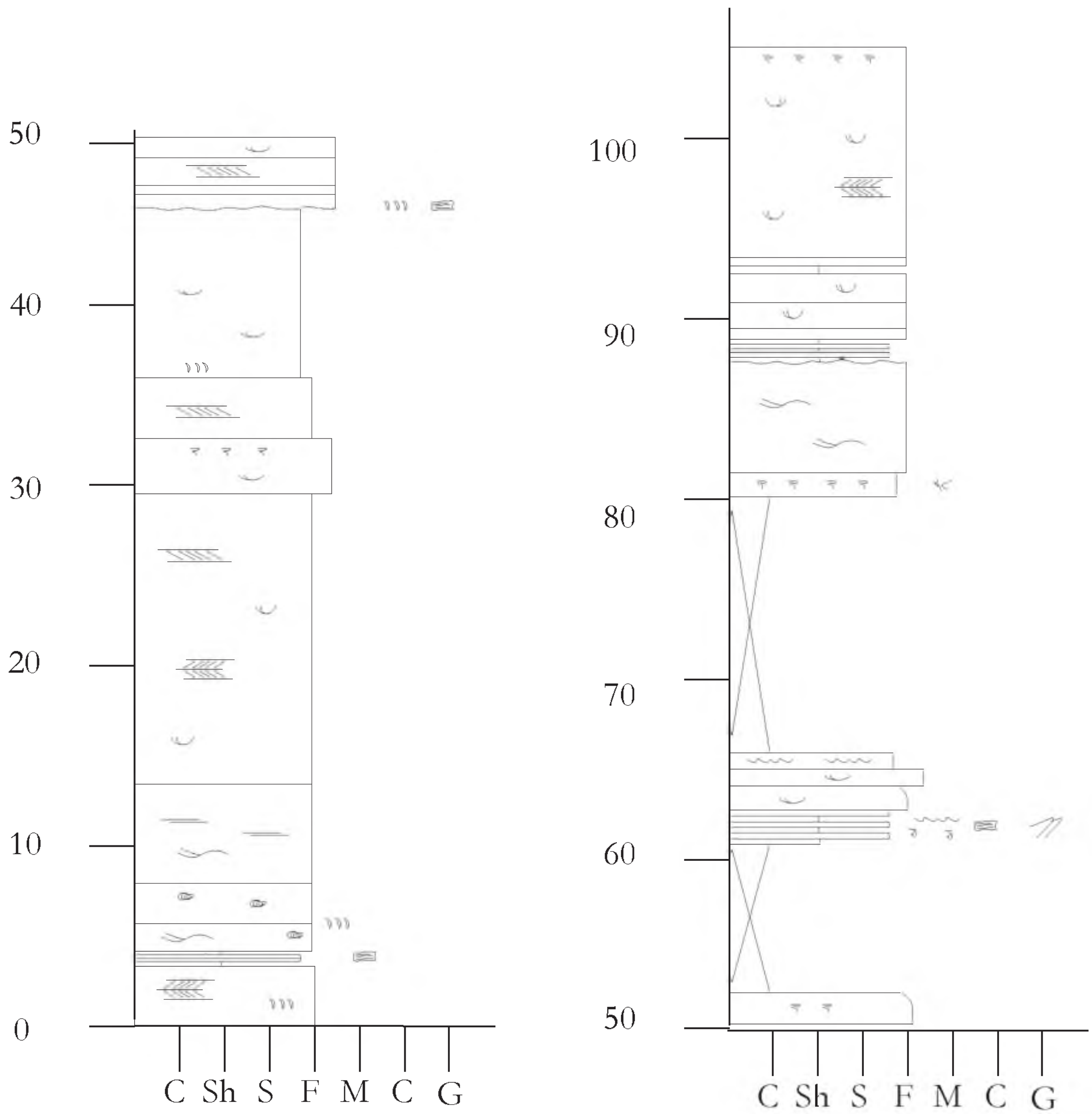
50
40
30
20
10
0
C Sh S F M C G
100
90
80
70
60
50
C Sh S F M C G

REFERENCES

Ainsworth, R. B., Vakarelov, B. K., and Nanson, R. A., 2011, Dynamic spatial and temporal prediction of changes in depositional processes on clastic shorelines: Toward improved subsurface uncertainty reduction and management: AAPG Bulletin, v. 95, no. 2, p. 267-297.

Allen, J. L., 2009, Transgressive-Regressive Cycles in the John Henry Member, Straight Cliffs Formation, Souther Utah, USA [Ph.D]: University of Utah, 188 p.

Allen, J. L., and Johnson, C. L., 2010, Facies control on sandstone composition (and influence of statistical methods on interpretations) in the John Henry Member, Straight Cliffs Formation, Southern Utah, USA: Sedimentary Geology, v. 230, no. 1-2, p. 60-76.

-, 2011, Architecture and formation of transgressive-regressive cycles in marginal marine strata of the John Henry Member, Straight Cliffs Formation, Upper Cretaceous of Southern Utah, USA: Sedimentology, v. 58, no. 6, p. 1486-1513.

Ambrose, W. A., and Ayers, W. B., 2007, Geologic controls on transgressive-regressive cycles in the upper Pictured Cliffs Sandstone and coal geometry in the lower Fruitland Formation, northern San Juan Basin, New Mexico and Colorado: AAPG Bulletin, v. 91, no. 8, p. 1099-1122.

Anthony, E. J., and Orford, J. D., 2002, Between wave- and tide-dominated coasts: the middle round revisited: Journal of Coastal Research, v. Special Issue 36, p. 8-15.

Bhattacharya, J. P., and Giosan, L., 2003, Wave-influenced deltas: geomorphological implications for facies reconstruction: Sedimentology, v. 50, no. 1, p. 187-210.

Boyd, R., 2010, Transgressive wave-dominated coasts, *in* Dalrymple, R. W., and James, N. P., eds., Facies Models 4: St. John's, Geological Association of Canada, p. 265-294.

Bruun, P., 1962, Sea-level rise as a cause of shore erosion: Journal of Waterways and Harbours Division, American Soceity of Civil Engineers, v. 88, p. 117-130.

Bullimore, S. A., Helland-Hansen, W., Henriksen, S., and Steel, R. J., 2008, Shoreline trajectory and its ipact on coastal depositional environments: an example from the Upper Cretaceous Mesaverde Group, northwestern Colorado, U.S.A, *in* Hampson,

G. J., Steel, R. J., Burgess, P. M., and Dalrymple, R. W. eds., Recent Advances in models of siliciclastic shallow-marine stratigraphy, SEPM special publications, Volume 90: Tulsa, p. 209-236.

Cantuneanu, O., 2006, Principles of sequence stratigraphy, Amsterdam, Elsevier, 375 p.

Cattaneo, A., and Steel, R. J., 2003, Transgressive deposits: a review of their variability: Earth-Science Reviews, v. 62, no. 3-4, p. 187-228.

Curray, J. R., 1964, Transgressions and regressions: Papers in Marine Geology: New York, Macmillan, p. 175-203.

Dalrymple, R. W., 2010, Tidal depositional systems, *in* James, N. P., and Dalrymple, R. W., eds., Facies Models 4, Geological Association of Canada, p. 201-232.

Dashtgard, S. E., MacEachern, J. A., Frey, S. E., and Gingras, M. K., 2012, Tidal effects on the shoreface: towards a conceptual framework: Sedimentary Geology, v. 279, p. 42-61.

Davis, R. A., 1994, The evolving coast, New York, Scientific American Library, 231 p.:

Davis, R. A., and Hayes, M. O., 1984, What is a wave-dominated coast?: Marine Geology, v. 60, no. 1, p. 313-329.

Devine, P. E., 1991, Transgressive origin of channeled estuarine deposits in the Point Lookout Sandstone, northwestern New Mexico: A model for Upper Cretaceous, cyclic regressive parasequences of the U.S. western interior: AAPG Bulletin, v. 75, no. 6, p. 1039-1063.

Duke, W. L., 1985, Hummocky cross-stratification, tropical hurricanes, and intense winter storms: Sedimentology, v. 32, no. 2, p. 167-194.

Dumas, S., and Arnott, R. W. C., 2006, Origin of hummocky and swaley cross-stratification— The controlling influence of unidirectional current strength and aggradation rate: Geology, v. 34, no. 12, p. 1073.

Eaton, J. G., 1987, The Campanian-Maastrichtian boundary in the Western Interior of North America: Newsletters on Stratigraphy, v. 18, p. 31-39.

Eaton, J. G., 1989, Stratigraphic revision of Campanian (Upper Cretaceous) rocks in the Henry Basin, Utah: The Mountain Geologist, v. 27, no. 1, p. 27-38.

-, 1991, Biostratigraphic framework for the Upper Cretaceous rocks of the Kaiparowits Plateau, southern Utah, *in* Nations, J. D., and Eaton, J. G., eds., Stratigraphy, depositional environments, and sedimentary tectonics of the western margin, Cretaceous Western Interior Seaway: Geological Society of America Special Paper 260, p. 47-63.

Eaton, J. G., and Nations, J. D., 1991, Introduction; Tectonic setting along the margin of the Cretaceous Western Interior Seaway, southwestern Utah and northern Arizona: GSA Special Paper, v. 260, p. 1-8.

Embry, A. F., 2002, Transgressive-regressive (TR) sequence stratigraphy: sequence stratigraphic models for exploration and production: Evolving Methodology, Emerging Models and Application Histories, v. 22, p. 151-172.

Embry, A. F., and Johannessen, E. P., 1993, T-R sequence stratigraphy, facies analysis and reservoir distribution in the uppermost Triassic-Lower Jurassic succession, western Sverdrup Basin, Arctic Canada, *in* Vorren, T. O., Bergsager, E., Dahl-Stamnes, O. A., Holter, E., Johansen, B., Lie, E., and Lund, T. B., eds., Arctic geology and petroleum potential, Volume 2, Special Publication-Norwegian Petroleum Soceity, p. 121-146.

Ericksen, M. C., and Slingerland, R., 1990, Numerical simulations of tidal and wind-driven circulation in the Cretaceous Interior Seaway of North America: Geological Society of America Bulletin, v. 102, no. 11, p. 1499-1516.

FitzGerald, D., Buynevich, I., and Hein, C., 2012, Morphodynamics and facies architecture of tidal inlets and tidal deltas, *in* Davis Jr, R. A., and Dalrymple, R. W., eds., Principles of Tidal Sedimentology: New York, Springer, p. 301-333.

FitzGerald, D. M., 1996, Geomorphic variability and morphologic and sedimentologic controls on tidal inlets: Journal of Coastal Research, p. 47-71.

Fitzgerald, D. M., and Penland, S., 1987, Backbarrier dynamics of the East Friesian Islands: Journal of Sedimentary Research, v. 57, no. 4, p. 746-754.

Folkestad, A., and Satur, N., 2008, Regressive and transgressive cycles in a rift-basin: Depositional model and sedimentary partitioning of the Middle Jurassic Hugin Formation, southern Viking Graben, North Sea: Sedimentary Geology, v. 207, no. 1, p. 1-21.

Frey, R. W., and Howard, J. D., 1986, Mesotidal estuarine sequences; a perspective from the Georgia Bight: Journal of Sedimentary Research, v. 56, no. 6, p. 911-924.

Gallin, W. N., 2010, Fluvial stratigraphic architecture of the John Henry Member of the Straight Cliffs Formation, Kaiparowits Plateau, Utah, USA [M.Sc].: University of Utah, 255 p.

Galloway, W. E., 1989, Genetic stratigraphic sequences in basin analysis I: architecture and genesis of flooding-surface bounded depositional units: AAPG Bulletin, v. 73, no. 2, p. 125-142.

Galloway, W. E., and Hobday, D. K., 1983, Terrigenous clastic depositional systems: applications to petroleum, coal and uranium exploration, New York, Springer-Verlag, 420 p.:

Gooley, J., 2010, Alluvial architecture and predictive modeling of the late Cretaceous John Henry Member, Straight Cliffs Formation, southern Utah [M.Sc].: University of Utah, 376 p.

Gradstein, F. M., Ogg, J. G., Schmitz, M., and Ogg, G., 2012, The geologic time scale 2012, Elsevier, 1176 p.

Haq, B. U., Hardenbol, J., and Vail, P. R., 1987, Chronology of fluctuating sea levels since the Triassic: Science, v. 235, no. 4793, p. 1156-1167.

Haq, B. U., Hardenbol, J., and Vail, P. R., 1988, Mesozoic and Cenozoic chronostratigraphy and cycles of sea-level change, *in* Wilgus, C. K., Hastings, B. S., Kendall, C. G. S. C., Posamentier, H. G., Poss, C. A., and Van Wagoner, J. C., eds., Sea-level changes: an integrated approach, Volume 42, SEPM Special Publication, p. 72-108.

Hartley, A. J., Weissmann, G. S., Nichols, G. J., and Warwick, G. L., 2010, Large distributive fluvial systems: characteristics, distribution, and controls on development: Journal of Sedimentary Research, v. 80, no. 2, p. 167-183.

Hayes, M. O., 1967, Hurricanes as geological agents, south Texas coast: Geological Notes: AAPG Bulletin, v. 51, no. 6, p. 937-942.

-, 1975, Morphology of sand accumulation in estuaries: an introduction to the symposium: Estuarine research, v. 2, p. 3-22.

-, 1980, General morphology and sediment patterns in tidal inlets: Sedimentary Geology, v. 26, no. 1, p. 139-156.

Helland-Hansen, W., and Gjelberg, J. G., 1994, Conceptual basis and variability in sequence stratigraphy: a different perspective: Sedimentary Geology, v. 92, no. 1–2, p. 31-52.

Helland-Hansen, W., and Martinsen, O. J., 1996, Shoreline trajectories and sequences: description of variable depositional-dip scenarios: Journal of Sedimentary Research, v. 66, no. 4, p. 670-688.

Hendricks, M. L., 1994, Ravinement surface control on hydrocarbon accumulation in transgressive systems tracts: Almond Formation, Green River Basin, Wyoming: RMAG, Unconformity Controls Symposium, p. 209-218.

Hettinger, R. D., 1995, Sedimentological descriptions and depositional interpretation, in sequence stratigraphic context, of two 300-meter cores fom the Upper Cretaceous Straight Cliffs Formation, Kaiparowits Plateau, Kane County, Utah, *in* Survery, U. S. G., ed., Volume Bulletin 2115-A.

Hettinger, R. D. (2000). A summary of coal distribuiton and geology in the Kaiparowits Plateau, Utah. Geologic Assesment of Coal in the Colorado Plateau: Arizona, Colorado, New Mexico, and Utah. M. A. Kirschbaum, L. R. Roberts and L. H. Biewick, U.S. Geological Survey. 1625-B.

Hettinger, R. D., McCabe, P. J., and Shanley, K. W., 1993, Detailed facies anatomy of transgressive and highstand systems tracts from the Upper Cretaceous of southern Utah, U.S.A., Siliciclastic Sequence Stratigraphy: Recent Developments and Applications, Volume AAPG Memoir 58, p. 235-357.

Hettinger, R.D., Roberts, L.N.R., Biewick, L.R.H., and Kirschbaum, M.A., 1996, Preliminary investigations of the distribution and resources of coal in the Kaiparowits Plateau, southern Utah: U.S. Geological Survey Open-File Report 96-539, 72 p.

Horn, B. W., Cross, T. A., Hornbeck, J., Vielma, M., and Zavala, M., Stratigraphic controls on reservoir strata: a comparison of fluvial and tidal reservoirs in the Almond Formation, Coal Gulch, Wamsutter, Echo Springs and Table Rock Fields, Washakie Basin, Wyoming, *in* Proceedings Wyoming Gas Resrouces and Technology: Rocky Mountain Section Meeting Technical Program2002, p. 149-161.

Hubbard, D. K., Oertel, G., and Nummedal, D., 1979, The role of waves and tidal currents in the development of tidal-inlet sedimentary structures and sand body geometry; examples from North Carolina, South Carolina, and Georgia: Journal of Sedimentary Research, v. 49, no. 4, p. 1073-1091.

Hwang, I.-G., and Heller, P. L., 2002, Anatomy of a transgressive lag: Panther Tongue Sandstone, Star Point Formation, central Utah: Sedimentology, v. 49, p. 977-999.

Ichaso, A. A., and Dalrymple, R. W., 2009, Tide- and wave-generated fluid mud deposits in the Tilje Formation (Jurassic), offshore Norway: Geology, v. 37, no. 6, p. 539-542.

Israel, A. M., Ethridge, F. G., and Estes, E. L., 1987, A sedimentologic description of a microtidal, flood-tidal delta, San Luis Pass, Texas: Journal of Sedimentary Research, v. 57, no. 2, p. 288-300.

Kamola, D. L., and Van Wagoner, J. C., 1995, Stratigraphy and facies architecture of parasequences with examples from the Spring Canyon Member, Blackhawk Formation, Utah, *in* Van Wagoner, J. C., and Bertram, G. T., eds., Sequence stratigraphy of foreland basin deposits; outcrop and subsurface examples from the Cretaceous of North America, Volume 64: Tulsa, OK, American Association of Petroleum Geologists, p. 27-54.

Kauffman, E. G., 1977, Geological and biological overview: Western Interior Cretaceous Basin: The Mountain Geologist, v. 14, p. 75-99.

Kieft, R. L., Hampson, G. J., Jackson, C. A.-L., and Larsen, E., 2011, Stratigraphic architecture of a net-transgressive marginal- to shallow-marine succession: Upper Almond Formation, Rock Springs Uplift, Wyoming, U.S.A: Journal of Sedimentary Research, v. 81, no. 7, p. 513-533.

Kumar, N., and Sanders, J. E., 1974, Inlet sequence: a vertical succession of sedimentary structures and textures created by the lateral migration of tidal inlets: Sedimentology, v. 21, no. 4, p. 491-532.

Leckie, D. A., and Walker, R. G., 1982, Storm- and tide-dominated shorelines in Cretaceous Moosebar-Lower Gates interval - outcrop equivalents of deep gas trap in western Canada: AAPG Bulletin, v. 66, p. 138-157.

Little, W. W., 1995, The influence of tectonics and eustasy on alluvial architecture, Middle Coniacian through Campanian strata of the Kaiparowits Basin [PhD]: University of Colorado.

Longhitano, S. G., Mellere, D., Steel, R. J., and Ainsworth, R. B., 2012, Tidal depositional systems in the rock record: A review and new insights: Sedimentary Geology, v. 279, p. 2-22.

Marjanac, T., and Steel, R. J., 1997, Dunlin Group sequence stratigraphy in the northern North Sea: A model for Cook Sandstone deposition: AAPG Bulletin, v. 81, no. 2, p. 276-292.

McCabe, P. J., and Shanley, K. W., 1992, Organic control on shoreface stacking patterns: Bogged down in the mire: Geology, v. 20, no. 8, p. 741-744.

Mellere, D., and Steel, R., 1995, Variability of lowstand wedges and their distinction from forced-regressive wedges in the Mesaverde Group, southeast Wyoming: Geology, v. 23, no. 9, p. 803-806.

Miller, K. G., Kominz, M. A., Browning, J. V., Wright, J. D., Mountain, G. S., Katz, M. E., Sugarman, P. J., Cramer, B. S., Christie-Blick, N., and Pekar, S. F., 2005, The Phanerozoic record of global sea-level change: Science, v. 310, no. 5752, p. 1293-1298.

Morton, R. A., 1979, Temporal and spatial variations in shoreline changes and their implications, examples from the Texas Gulf Coast: Journal of Sedimentary Research, v. 49, no. 4.

Nio, S.-D., and Yang, C.-S., 1991, Diagnostic attributes of clastic tidal deposits, *in* Smith, D. G., Reinson, G. E., Zaitlin, B. A., and Rahmani, R. A., eds., Clastic Tidal Sedimentology, Volume Memoir 16, Canadian Society of Petroleum Geologists, p. 3-28.

Nummedal, D., and Penland, S., 2009, Sediment dispersal in Norderneyer Seegat, West Germany, Holocene marine sedimentation in the North Sea Basin, Blackwell Publishing Ltd., p. 187-210.

Olsen, T. R., Mellere, D., and Olsen, T., 1999, Facies architecture and geometry of landward-stepping shoreface tongues: the Upper Cretaceous Cliff House Sandstone (Mancos Canyon, south-west Colorado): Sedimentology, v. 46, p. 603-625.

Pemberton, S. G., MacEachern, J. A., and Frey, R. W., 1992, Trace fossil facies models: their environmental and allostratigraphicsignificance, *in* Walker, R. G., and James, N. P., eds., Facies Models: A Response to Sea-Level Changes, Geological Association of Canada, p. 47-72.

Peterson, F., 1969a, Cretaceous sedimentation and tectonism in the southeastern Kaiparowits region, Utah, Volume 69-202: Reston, VA, USGS Open File Report, p. 259.

-, 1969b, Four new members of the upper cretaceous straight cliffs formation in the southeastern kaiparowits region, kane county, Volume 1274-J: Reston, VA, USGS Bulletin, p. j1-j28.

Pettinga, L., 2013, Alluvial architecture and paleomorphodynamics of the upper Cretaceous John Henry Member, Straight Cliffs Formation, Kaiparowits Plateau, Utah [M.Sc].:University of Utah.

Plink-Björklund, P., 2011, Effects of tides on deltaic deposition: Causes and responses: Sedimentary Geology, v. 279, p. 107-133.

Pontén, A., and Plink-Björklund, P., 2009, Regressive to transgressive transits reflected in tidal bars, Middle Devonian Baltic Basin: Sedimentary Geology, v. 218, no. 1-4, p. 48-60.

Prandle, D., 2009, Estuaries: dynamics, mixing, sedimentation and morphology: Oceanography, v. 22, no. 4, p. 252.

Ravnas, R., and Steel, R. J., 1998, Architecture of marine rift-basin successions: AAPG Bulletin, v. 82, no. 1, p. 110-146.

Rodriguez, A. B., Anderson, J. B., Siringan, F. P., and Taviani, M., 2004, Holocene evolution of the East Texas coast and inner continental shelf: Along-strike variability in coastal retreat rates: Journal of Sedimentary Research, v. 74, no. 3, p. 405-421.

Sanders, J. E., and Kumar, N., 1975, Evidence of shoreface retreat and in-place “drowning” during Holocene submergence of barriers, shelf off Fire Island, New York: GSA Bulletin, v. 86, p. 65-76.

Seidler, L., and Steel, R., 2001, Pinch-out style and position of tidally influenced strata in a regressive–transgressive wave-dominated deltaic sandbody, Twentymile Sandstone, Mesaverde Group, NW Colorado: Sedimentology, v. 48, no. 2, p. 399-414.

Shanley, K. W., 1991, Sequence stratigraphic relationships and facies architecture of Turonian-Cenomanian Strata, Kaiparowits Plateau, south central Utah [PhD]: Colorado School of Mines, 390 p.

Shanley, K. W., and McCabe, P. J., 1991, Predicting facies architecture through sequence stratigraphy - an example from the Kaiparowits Plateau, Utah: Geology, v. 19, p. 742-745.

Shanley, K. W., and McCabe, P. J., 1995, Sequence stratigraphy of Turonian-Santonian strata, Kaiparowits Plateau, southern Utah, U.S.A.; implications for regional correlation and foreland basin evolution, *in* Van Wagoner, J. C., and Bertram, G. T., eds., Sequence stratigraphy of foreland basin deposits; outcrop and subsurface examples from the Cretaceous of North America, Volume 64: Tulsa, OK, American Association of Petroleum Geologists, p. 103-136.

Simms, A. R., Anderson, J. B., and Blum, M., 2006, Barrier-island aggradation via inlet migration: Mustang Island, Texas: Sedimentary Geology, v. 187, no. 1–2, p. 105-125.

Siringan, F. P., and Anderson, J. B., 1994, Modern shoreface and inner-shelf storm deposits off the east Texas coast, Gulf of Mexico: Journal of Sedimentary Research, v. 64, no. 2.

Sixsmith, P. J., Hampson, G. J., Gupta, S., Johnson, H. D., and Fofana, J. F., 2008, Facies architecture of a net transgressive sandstone reservoir analog: The Cretaceous Hosta Tongue, New Mexico: AAPG Bulletin, v. 92, no. 4, p. 513-547.

Steel, R. J., Plink-Bjorklund, P., and Aschoff, J., 2012, Tidal deposits of the Campanian Western Interior Seaway, Wyoming, Utah and Colorado, USA, p. 437-471.

Stutz, M. L., and Pilkey, O. H., 2011, Open-ocean barrier islands: Global influence of climatic, oceanographic, and depositional settings: Journal of Coastal Research, v. 27, no. 2, p. 207-222.

Swift, D. J. P., 1968, Coastal erosion and transgressive stratigraphy: The Journal of Geology, v. 76, no. 4, p. 444-456.

Uhlir, D. M., Akers, A., and Vondra, C. F., 1988, Tidal inlet sequence, Sundance Formation (Upper Jurassic), north-central Wyoming: Sedimentology, v. 35, no. 5, p. 739.

Van Wagoner, J. C., Posamentier, H. W., Mitchum, R. M., Vail, P. R., Sarg, J. F., Loutit, T. S., and Hardenbol, J., 1988, An overview of the fundamentals of sequence stratigraphy and key definitions, *in* Wilgus, C. K., Hastings, B. S., Ross, C. A., Posamentier, H. W., Van Wagoner, J., and Kendall, C. G. S. C., eds., Sea-level changes; an integrated approach, Volume 42: Tulsa, OK, SEPM (Society for Sedimentary Geology), p. 39-45.

Vaninetti, G. E., 1979, Coal stratigraphy of the John Henry Member of the Straight Cliffs Formation, Kaiparowits Plateau, Utah [M.Sc.]: University of Utah, 274 p.

Walker, R. G., and Plint, A. G., 1992, Wave- and storm-dominated shallow marine systems, St. Johns, NL, Geological Association of Canada, Facies models; response to sea level change, 219-238 p.:

Wallace, D. J., Anderson, J. B., and Fernández, R. A., 2010, Transgressive ravinement versus depth of closure: a geological perspective from the upper Texas coast: Journal of Coastal Research, v. 26, p. 1057-1067.

Yang, W., Kominz, M. A., and Major, R. P., 1998, Distinguishing the roles of autogenic versus allogenic processes in cyclic sedimentation, Cisco Group (Virgilian and Wolfcampian), north-central Texas: Geological Society of America Bulletin, v. 110, no. 10, p. 1333-1353.

Yoshida, S., Steel, R. J., and Dalrymple, R. W., 2007, Changes in depositional processes--An ingredient in a new generation of sequence-stratigraphic models: Journal of Sedimentary Research, v. 77, no. 6, p. 447-460.

Zonneveld, J., Gingras, M. K., and Pemberton, S. G., 2001, Trace fossil assemblages in a Middle Triassic mixed siliclastic-carbonate marginal marine depositional system, British Columbia: Palaeogeography, Palaeoclimatology, Palaeoecology, v. 166, p. 249-276.